

Mining method selection based on cost modelling and stability analysis for Mine 2 of the Stjernøy Mine in Norway.

by

J. van Duijn

to obtain the degree of Master of Science
at the Delft University of Technology,
to be defended publicly on 29 September 2020 at 16:00

Student number:	4292170	
Project duration:	November 2019 – September 2020	
Supervisors:	Dr. M.W.N. Buxton,	TU Delft
	Dr. A. Barnhoorn,	TU Delft
	Ir. M. Keerseemaker,	TU Delft
	Dr. ir. R.M. Schmitz CEng CGeol,	Sibelco

An electronic version of this thesis is available at <http://repository.tudelft.nl/>.

Abstract

To optimise mining in a safe, geotechnically controlled and economical most beneficial way in Mine 2 of the Stjernøy mine, a choice has been made to review the current mining method, sublevel open stoping, and a different mining method, vertical crater retreat. The Stjernøy mine is an open pit and underground mine for Nepheline Syenite and this thesis focuses on Mine 2, the underground mine which is partially completed. The stopes of Mine 2 are closely located to old stopes, which can cause stability issues. Between the new and old stopes is a barrier pillar which is a key element in the stability of the underground mine and the infrastructure for the open pit operation as well. This project consists of field work and laboratory testing to create a basis for the numerical stability analysis of the mine and the creation of a cost model for the two different mining methods.

The results of the cost modeling show that the use of sublevel open stoping will result in a cost per tonne of 9.86 NOK and the use of vertical crater retreat will result in a cost per tonne of 10.39 NOK. The use of sublevel open stoping as mining method is the most economically beneficial option for the mining operation. It is less expensive as a mining method and it is a proven method at this mine site. The vertical crater retreat method uses a more expensive blasting method, with the same burden and spacing parameters as the sublevel open stoping. The results of the field work and the laboratory testing provided important parameters for the numerical modelling, such as the strength of the material. Based on these results the numerical modelling also showed that it is beneficial for the stability of the pillar if some stopes near the barrier pillar are not extracted. The extraction of these stopes will decrease the factor of safety of certain areas of the barrier pillar to one or for some areas below one. The stope size has also been reviewed. To make sure that the stopes are well connected to drawpoints, it is important to keep them the same size, which is a stable stope size for the roof. Smaller stope sizes are found to be a bit more stable, however the effect of the increasing amount of pillars is not known on the overall stability.

Acknowledgements

First of all, I would like to thank everyone that participated in this project. I would like to thank Sibelco for providing the project and opportunity to work on this project. I would also like to thank all the people at Stjernøy, that provided information for my research, or helped me get familiar with the mine. A special thanks to Robrecht Schmitz, for helping me to find this project and for his support and guidance during my thesis. I would like to thank Mike Buxton, Auke Barnhoorn and Marco Keersemaker for their support, feedback and guidance during my research in Delft.

Jaap van Duijn

Contents

List of Figures	xi
List of Tables	xiii
1 Introduction	3
1.1 Stjernøy	3
1.1.1 Climate	5
1.1.2 Geology	5
1.1.3 Mining Method	7
1.2 Problem Statement	9
1.3 Goal and Objectives	9
1.4 Method	10
1.5 Scope	10
1.6 Thesis Outline	10
2 Mining Theory	13
2.1 Sublevel Open Stopping	13
2.2 Vertical Crater Retreat	15
2.3 Dilution	17
2.4 Sequencing	18
2.5 Rib Pillar	18
2.6 Stereonet Projection	19
2.7 Mine Stability	20
2.7.1 Case Study	23
2.8 RS2	24
2.9 Conclusion	25
3 Rock Mechanics	27
3.1 Stress-Strain Relation	27
3.2 Young's Modulus	28
3.3 Poisson Ratio	28
3.4 Rock Quality Designation Index	29
3.5 RMR	29
3.6 Q system	30
3.7 Geological Strength Index	32
3.8 Hoek-Brown Criterion	32
3.9 Disturbance Factor	34
3.10 Generalised Hoek & Diedrichs	34
3.11 Kirsch Equation	34
4 Field work & laboratory testing	39
4.1 Scanline Mapping	39
4.1.1 Stereonet Projection	40
4.2 Rock Mass Classification	41
4.3 Laboratory Testing	42
4.3.1 Samples	42
4.3.2 Density	43
4.3.3 UCS, Poisson Ratio and Young's Modulus	43
4.3.4 Sonic Velocity	43
4.3.5 Tensile Strength	44

5	Stability Analysis	45
5.1	Mathews Stability Graph	45
5.2	Numerical Model	46
5.2.1	Pre-Modelling	47
5.2.2	Model Generation	47
5.3	Data Used	49
6	Cost Model & Mine Planning	51
6.1	Approach	51
6.2	Sublevel Open Stoping Cost Model	52
6.2.1	Stopes.	52
6.2.2	Drifts & Top Slice	53
6.2.3	Working Hours	53
6.2.4	Consumables	53
6.3	Mine Planning	54
6.4	Mining Method	54
6.5	Data Used	54
7	Fieldwork & Laboratory testing	57
7.1	Fieldwork	57
7.2	Laboratory Testing	60
7.2.1	Historical Data Comparison	62
8	Stability Analysis	63
8.1	Stability Graph	63
8.2	Numerical Model	64
8.2.1	Stages.	65
8.2.2	Mesh	72
8.2.3	Stress Distribution	72
8.2.4	Stope Connections	74
8.2.5	Effect of Bolts	75
8.2.6	Strength Factor Evaluation.	77
8.3	Sensitivity Analysis	79
9	Cost model	81
9.1	Operations	81
9.2	Drifting & Production	81
9.3	Planning.	82
9.4	Capital Cost.	84
10	Discussion	85
10.1	Fieldwork and Laboratory Testing	85
10.2	Stability Analysis	86
10.3	Cost Model	87
11	Conclusion	91
11.1	Cost Model	91
11.2	Stability	91
11.3	Stope Size	92
12	Recommendations	93
12.1	Cost Modelling	93
12.2	Stress Modelling	93
12.3	New Mining Area	93

Bibliography	95
13 Appendix A	99
14 Appendix B	105
15 Appendix C	107
15.1 sublevel open stoping	107
15.2 Vertical Crater Retreat	114

List of Figures

1.1	Location of the Mine. Sibelco 2019.	4
1.2	The partly underground site layout. Sibelco 2019.	5
1.3	Map of Seiland Igneous Province and close up of Stjernøy. Xiaoyan Li 2013.	6
1.4	Geological map of alkaline complex on Stjernøy. Xiaoyan Li 2013.	6
1.5	Shape of the orebody. Direction of view is north west. Sibelco 2019.	7
1.6	Layout of the stopes of Mine 2, plan view. Visible are the footwall stopes (closest to the drift and the hangingwall stopes).	8
1.7	Side view of the stopes. Mine 1 is visible in green and Mine 2 is visible in blue.	8
2.1	Sublevel open stoping. SME Mining Engineering Handbook, 2011. Modified.	14
2.2	Cratering Dimensions. Liu et al 2018.	15
2.3	Volume/Charge weight ratio versus Depth of burial ratio/critical depth. Liu et al, 2018	16
2.4	Planned and unplanned dilution. SME mining engineering handbook, 2011.	17
2.5	Rib pillar stability graph, showing: stable, transition and failed zones. Villaescusa 2014.	19
2.6	Stereonet projection. Left part shows the imagined sphere on the plane. Right part shows the great circle and the pole on the lower hemisphere. Brady & Brown (2004)	19
2.7	Example of an equal angle stereonet used for plotting the planes. Terzaghi (1965)	20
2.8	The different factors for the stability graph. (a) Stress factor A. (b) Joint orientation factor B. (c) Mode of failure factor for gravity fall and slabbing. (d) Mode of failure factor for sliding. Suorineni 2010.	21
2.9	Dimensions of the stope that are used to calculate the hydraulic radius. McKinnon 2018.	22
2.10	Stability graph. Hutchinson & Diederichs 1996.	23
2.11	Analysis of 122 stope hangingwalls (left graph) and 101 stope back walls (right graph). Hudson 1995.	24
3.1	Top graph: Elastic constitutive model. Bottom graph: elastic-plastic constitutive model. McKinnon 2018.	28
3.2	Number of joint sets visible in a stereonet projection. McKinnon 2018.	31
3.3	Joint Roughness number. Hutchinson & Diederichs 1996.	31
3.4	The effect of lower and higher values for the parameter m in the Hoek-Brown Criterion. Eberhardt 2012.	33
3.5	Stresses around a 2D circular excavation with a biaxial stress field. McKinnon 2018	35
3.6	Influence of excavation shape and ratio of applied stresses on boundary stress. Hoek and Brown 1980	36
4.1	Example of the scanline survey in the underground mine. The measuring tape has been placed along the wall.	40
7.1	Four major joint sets that are present in the rock mass	60
7.2	Stress strain curves for the six cores that have been tested for UCS strength by Liege University.	61
8.1	The layout of the numerical model. With Mine 1, Mine 2, the primary processing and faults.	65
8.2	The different modelling materials that are used.	66
8.3	Stages 2 to 9 show the development of the model	67
8.4	Stages 10 to 17 show the development of the model	68
8.5	Stages 18 to 25 show the development of the model	69
8.6	Stages 26 to 33 show the development of the model. At stage 29 the first part of stope 2 is blasted. At stage 30, the first part of stope 1 is blasted, and at stage 31, the second part of stope 1 is blasted. This is modelled like this to recreate the current situation.	70

8.7 Stages 34 to 41 show the development of the model	71
8.8 Stage 42	72
8.9 Model with discretization and mesh.	72
8.10 Sigma 1 Stress distribution in the model before all excavation work.	73
8.11 Kirsch variation that was used to calculate the stress with a different tunnel shape.	74
8.12 The yielded elements in the pillar between stope 4 and stope 5 of Mine 2.	75
8.13 The effect of bolts on the stress distribution around the stopes.	76
8.14 The legend for figure 8.15 and figure 8.16	77
8.15	78
8.16 The effect of different UCS value on the factor of safety for the barrier pillar.	79
8.17 The effect of different UCS value on the factor of safety for the barrier pillar.	80
13.1 Rock Mass Rating (RMR) system rating table. Brady & Brown	100
13.2 Rock Mass Rating (RMR) system rating table. Brady & Brown	101
13.3 General chart for Geological Strength Index from geological observations. Marinos, Marinos & Hoek 2005	101
13.4 Geological Strength Index for heterogeneous rock masses. Marinos, Marinos & Hoek 2005	102
13.5 Guidelines for estimating disturbance factor D. Hoek & Brown 2019.	103
13.6 Guidelines for estimating Mi value if laboratory testing is not possible. Hoek 2007	104
14.1 Stresses at the point that was measured by SYNTEF.	105
15.1 Stope calculations	107
15.2 drift and vertical slot calculations	108
15.3 top slices calculations	109
15.4 Amount of explosives	109
15.5 Operations calculations	110
15.6 Personnel calculations	111
15.7 Equipment calculations	112
15.8 Finances calculations part 1	113
15.9 Finances calculations part 2	114
15.10 Costs for certain spare parts	114
15.11 Stope calculations for VCR	115
15.12 drift and vertical slot calculations for VCR	116
15.13 top slices calculations for VCR	116
15.14 Amount of explosives for VCR	117
15.15 Operations calculations for VCR	117
15.16 Finances calculations part 1 for VCR	118
15.17 Finances calculations part 2 for VCR	118

List of Tables

1.1	Research Scope	10
3.1	Determination of Rock Mass Rating	30
3.2	Joint alteration number (Ja). Hutchinson & Diederichs 1996.	32
4.1	Core samples location, length and width	43
5.1	Mesh parameters	47
5.2	Parameters used in the RS2 model	48
5.3	Stress field parameters	49
5.4	Stress testing historical values to be used to validate model.	50
6.1	Assumptions in Cost model	55
7.1	Results from the fieldwork for three locations	58
7.2	Results from joint analysis fieldwork for Mine 2 stope 1 classification	59
7.3	Results from joint analysis fieldwork for drift 460 level classification	59
7.4	Dip and dip direction of each joint set that has been found in the scanline mapping	60
7.5	Uniaxial compression tests results	61
7.6	Brazilian tests results	62
8.1	Results of the stability graph method for the mine 2 stope and for the new workshop	63
8.2	Results of the stability graph method for two variations of stope 5	64
8.3	Hydraulic radius calculations for the different stability graph versions that have been performed.	64
8.4	Stress testing historical values to be used to validate model.	73
9.1	Preparation times for the different operations for sublevel open stoping and vertical crater retreat.	81
9.2	Cost model results sublevel open stoping	82
9.3	Stopes to be mined in Mine 2 with costs for each stope and per level	82
9.4	Drifts to be mined with length, volumes and costs.	83
9.5	Top slice for each level to be mined.	83
9.6	Cost per level and the percentage of the total cost and volume is from the top slice and drift.	83
9.7	Costs of different drill rigs	84

Acronyms

SRF	Stress reduction factor
GSI	Geological Strength index
VCR	Vertical crater retreat
HR	hydraulic radius
UCS	Uniaxial Compressive Strength
RQD	Rock Quality Designation Index
RMR	Rock Mass Rating
D	Disturbance Factor
RS2	Numerical modelling software

Part I

Introduction

Introduction

Nepheline Syenite, an igneous rock, is used in various products, such as glass and paint. Sibelco Europe produces nepheline syenite in their Stjernøy operation, located in Norway. The site consists of three parts, an open pit mine, an underground mine and processing plant. The mine is located in the arctic which limits the months of operation to June till December for the open pit because of the amount of precipitation as snow. The processing plant is operating (almost) the whole year, which means that the ore must be mined in the underground mine or stockpiled from the open pit. This material is stockpiled in several stopes used as silos in the underground mine which are connected to the open pit by ore chutes. Which is part of the reason why the mine is operating an underground mine. The other reason is a higher ore recovery of the deposit. The underground mine produces part of the ore that is used for processing, with a focus on the underground part in the winter period. The other part of the ore is mined from the open pit and then stored in the stopes that were mined before. Other stopes are used for the storage of waste material.

The first part of this chapter is an introduction to the Stjernøy site, the site's location and layout will be discussed after which the climate is shortly reviewed. After the climate section, the mining method and the geology will be reviewed. With this background information clear, the problem statement is the next section. After which the goal and objectives, the method and the scope follow.

1.1. Stjernøy

The site is located on an island, approximately 20 kilometres north of the city Alta, in Norway. Figure 1.1 shows the location of the mine. The mining operation at Stjernøy, is partly an open pit and partly an underground operation. The mine has a production of 530.000 tonnes of raw material and 400.000 tonnes of waste rock. Of this, 90 percent is mined by the open pit operation and the other 10% by the underground operation. The waste rock is only produced in the open pit. In the underground mine, the development and the mining activities are all inside the orebody. The open pit is operational from June 20th till mid-December. For the rest of the year, the underground mine is operational to provide the processing plant with ore. The production from the underground mine is not sufficient to run the processing plant, so material from the open pit is stockpiled in stopes to use during the winter months. This is as well one of the reasons why the ore is mined underground. The other reason is that the orebody is extending into the mountain, which means that the use of underground mining methods increases the amount of ore that can be mined. During the months that the open pit is in operation, there is almost no production from the underground mine. This is because the open pit is cheaper to operate and has a higher production than the underground mine. The only work that happens during these months in the underground mine is development work.



Figure 1.1: Location of the Mine. Sibelco 2019.

The material that is mined is nepheline syenite, which is a combination of Nepheline and Syenite. Nepheline is a mineral that forms in alkaline complexes in igneous rocks and is most commonly found in the rock Nepheline Syenite (Feick 2019). Nepheline syenite is a material that is used in paint, filler and glass production. The nepheline syenite is mined in this area in Norway because it is of a high quality, with low degree of impurities.

The site consists of an open pit mine, underground mine, underground crusher, underground storage, plant, international port and silos. The exact layout is shown in figure 1.2. The open pit is located on the mountain, 700 meters higher than the processing plant. Mine 1, the grey stopes, is no longer in operation, it is only used for raw material from the open pit mine and waste rock storage. The stopes of Mine 1 and 2 have been mined with sublevel open stoping. The stopes of Mine 2 that have been mined already are visible at the right part of the figure. The new stopes for Mine 2 are planned to be above the stopes of Mine 2 that have been mined out already. The pillar between Mine 1 and the area above Mine 2 is a point of concern. This pillar is the barrier pillar between Mine 1 and Mine 2 and the stability of this pillar must be guaranteed. It needs to be strong enough to withstand all the stresses imposed by mining. However, if it is too thick, valuable ore is lost. The reserves of the mine are enough for production at the current level for approximately 65 years.

The material from the open pit is transported by truck into the underground mine, where it is dumped in the correct stope. The waste material is dumped in the grey stopes, and the ore is dumped into the orange stopes, the raw material storage. The material falls down from the top of the stopes to the level the stopes are filled now, this can be hundreds of meters. The waste rock filled stopes are starting to fill up, and it is planned that they are full before the open pit mine arrives at the top of the old stopes. The raw material in the raw material storage stopes is drawn from the bottom of the stopes with a front loader. The front loader feeds the raw material into the crusher hall, where primary crushing takes place. The mixing of the material is done by the front loader, it draws the material from different draw points from the raw material storage or the underground Mine 2 stopes.

From the primary crusher, the material is transported by a conveyor belt to a 3-day-storage facility, this facility provides a short-term stockpile capability, so that the operating plant has a constant inflow of material. From the 3-day-storage it is transported to the processing plant by conveyor belt. In the processing plant, the raw material is processed by drying, additional crushing stages and multiple separation stages to create different sizes products.

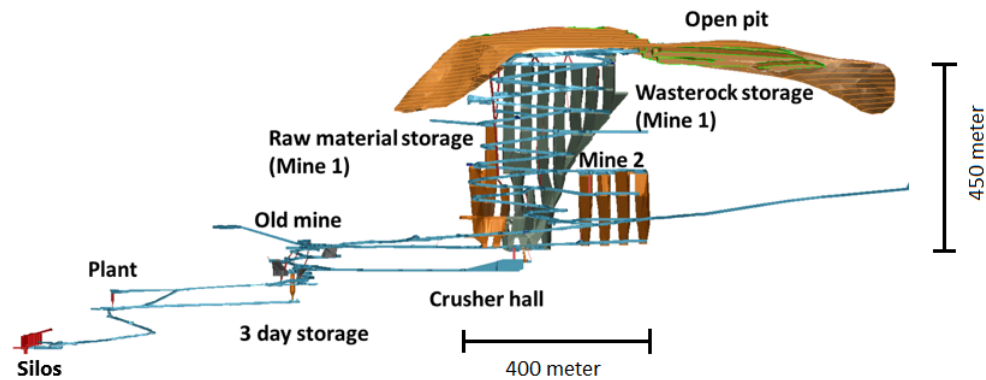


Figure 1.2: The partly underground site layout. Sibelco 2019.

1.1.1. Climate

The local climate is a continental subarctic climate, with average temperatures ranging from 12.1 Celsius in July to -3.7 Celsius in January. The average amount of precipitation is 830.6 mm, of which is mostly in the form of snow. The average monthly temperatures are below freezing for a six to eight months and snow on the ground for many months (*Oksfjord, Norway. The climate in Oksfjord Norway 2020*). The amount of precipitation causes water inflow in the mine, especially in thawing conditions.

1.1.2. Geology

The deposit on the island Stjernøy is part of the Seiland Igneous Province, in the Caledonian nappes of northern Norway (Roberts et al. 2010). It consists of 5.000 square kilometres on the islands of Seiland, Sørøy and Stjernøy and the northern part of the Finnmark province. The history of the Seiland Igneous Province is a complex magmatic evolution. It consists of an abundance of ultramafic rocks, layered gabbroic plutons and a final stage of calc-alkaline intrusions in the form of alkaline pyroxenite, syenite, nepheline syenite, and carbonite. The final stage happened approximately 574 ± 5 million years ago (Li 2013). A Pluton is a body of intrusive rock that crystallized from slowly cooling magma (Glazner et al. 2004). One of the characteristics of a pluton is that it is non-tabular shaped, which is also true for the Seiland Igneous Province. A map of the Seiland Igneous Province and a close up of Stjernøy is given in Figure 1.3.

The Nabberen orebody is a lens shaped orebody located just north of the summit of the mountain Nabberen, which is also shown in Figure 1.4. The location of the mining facilities that are on the surface is given with the small box at the bottom of the figure. Figure 1.5 shows the shape of the orebody relative to the mountain looking towards the north west. The top of the mountain is at a height of 700 meter above sea level. The orebody is approximately 1700 meter long, 300 meter wide and has a dip of 70 degrees.

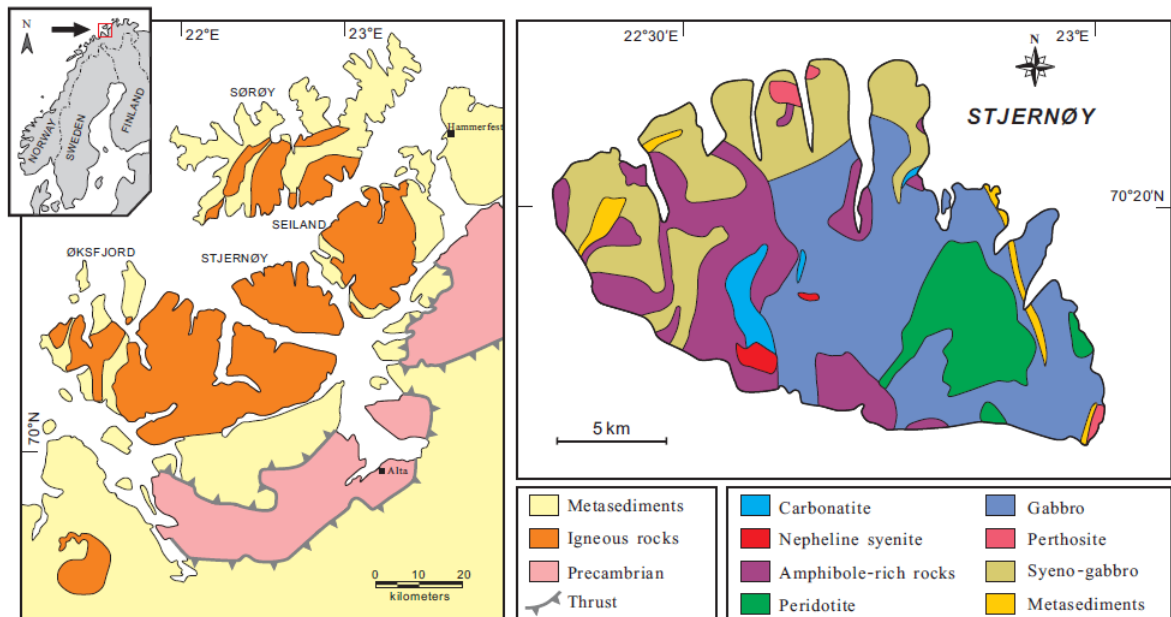


Figure 1.3: Map of Seiland Igneous Province and close up of Stjernøy. Xiaoyan Li 2013.

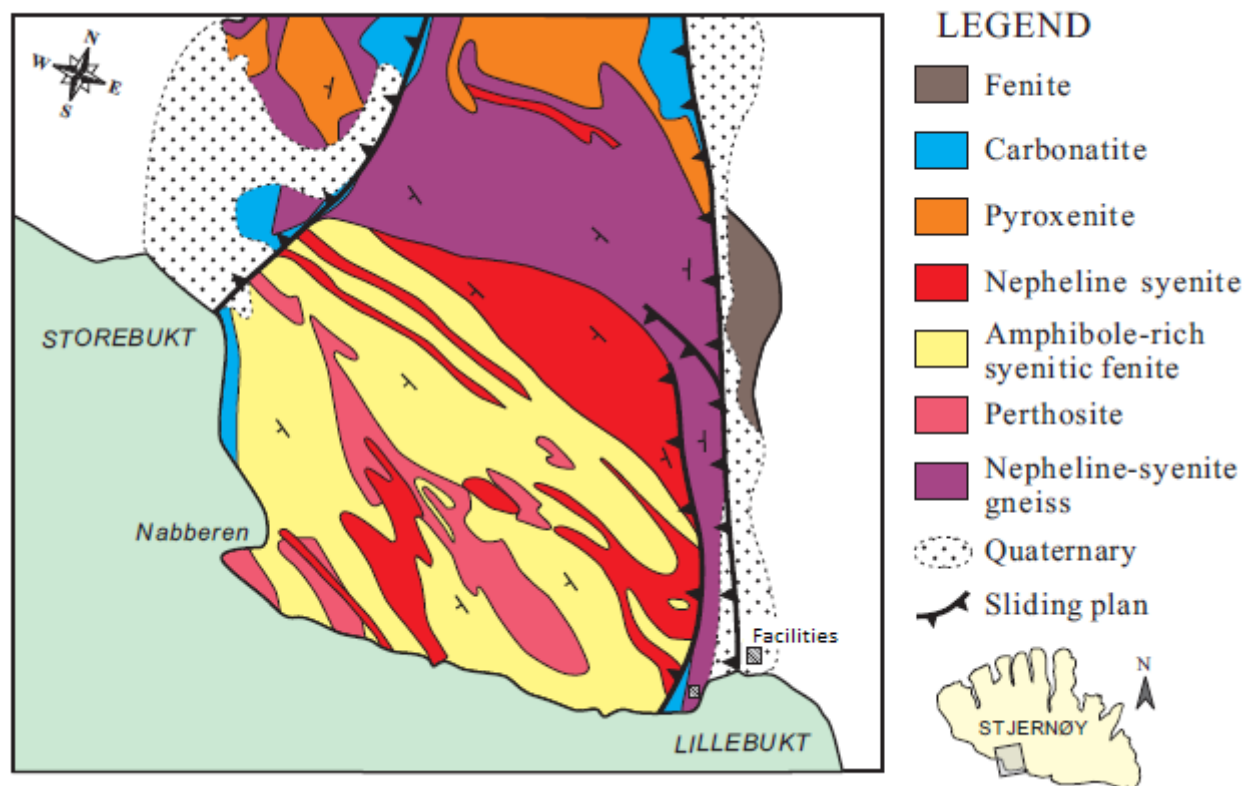


Figure 1.4: Geological map of alkaline complex on Stjernøy. Xiaoyan Li 2013.

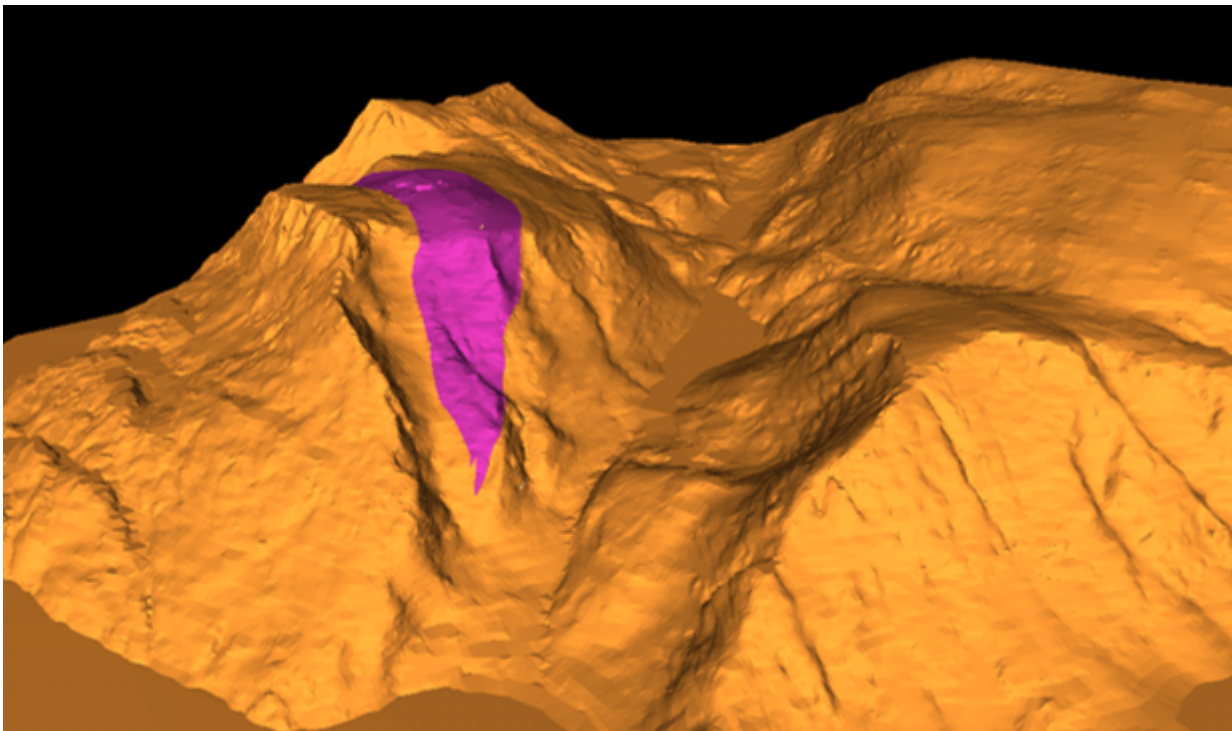


Figure 1.5: Shape of the orebody. Direction of view is north west. Sibelco 2019.

1.1.3. Mining Method

The mining method that is currently used is a variation of sublevel open stoping. The final open stopes that have been created in Mine 1 are 400 meters high and are being filled with waste material or raw material. The Mine 2 stopes are approximately 150 meters high. The first steps of the mining process for Mine 2 was creating the drift at the base of the planned stopes, see Figure 1.6. Drawpoints are created at this level, to remove the blasted material. 50 meters higher, at the planned top of the stopes, another drift was developed. This drift provides access to the stopes from the top. From this drift, new drifts towards the furthest stope from the original are created. In one of the corners of the stopes, a shaft is created that leads to the drawpoint of that stope. This shaft is used for dumping material from the development blasts to the drawpoints and to create a free face for blasting. A slice with the complete size of the stope is developed. In case of the southern stopes, a slice with the dimensions 6.5 meters high, 27 meters wide and 50 meters long is developed. The slice is used to drill the vertical production holes per blast. Each stope is divided into four or five slices that are blasted towards the free face.

The next stope that is developed is developed in the same way as the first stope, in addition that it is connected to an existing stope by a drift. This is done to dump the material of the development directly in the mined out stope to eliminate transport of the material. Before the stopes at a level are all mined out, a drift is developed 50 meters above that level, to provide access to the development of new stopes. The development of the new stopes follows the same steps as the stopes below, with the only difference that there is one more free face at the bottom of the stope. This process continues upwards, and results in stopes that can be hundreds of meters high. The stopes follow the dip of the orebody, which can be seen in Figure 1.7. In this figure, the green stopes are the stopes from Mine 1 and the blue stopes the stopes from Mine 2.

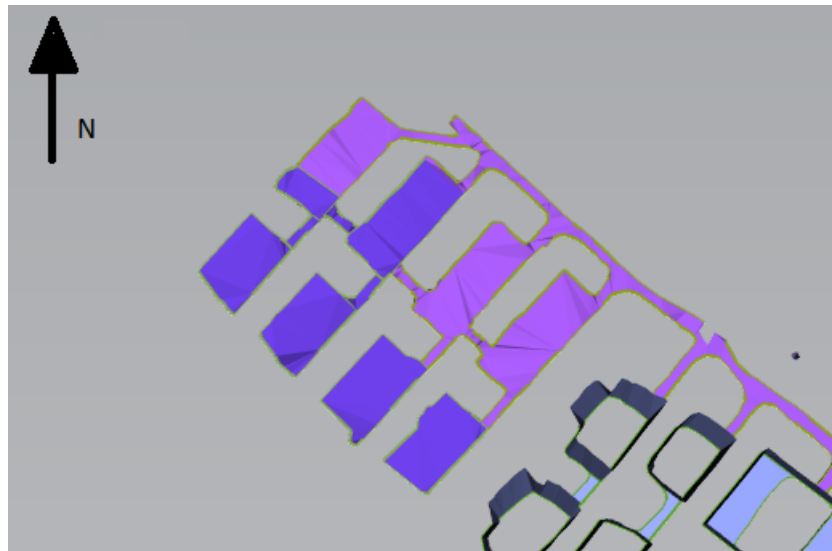


Figure 1.6: Layout of the stopes of Mine 2, plan view. Visible are the footwall stopes (closest to the drift and the hangingwall stopes).

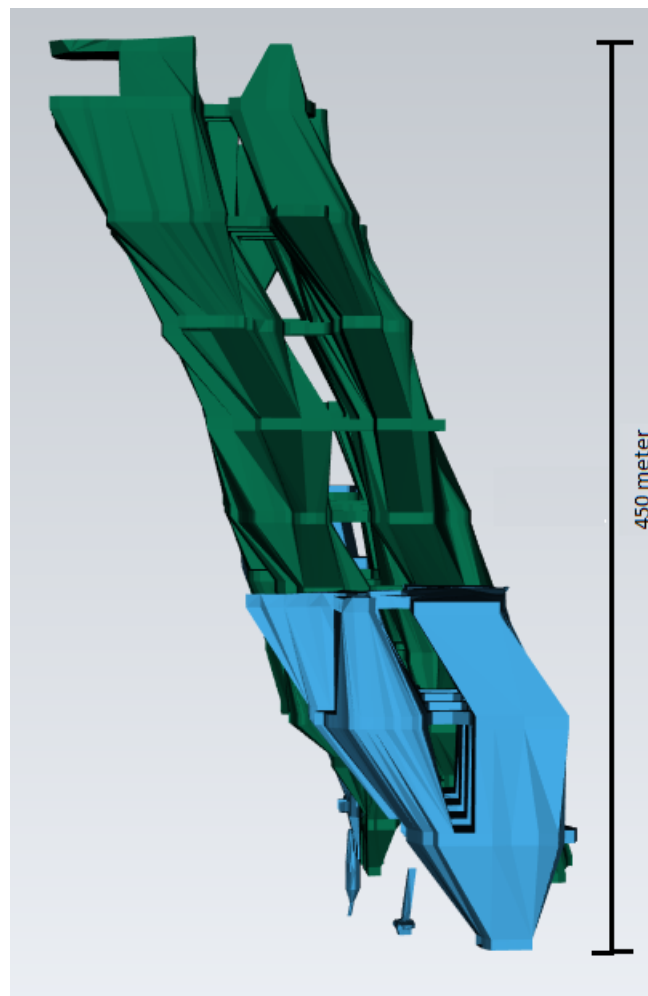


Figure 1.7: Side view of the stopes. Mine 1 is visible in green and Mine 2 is visible in blue.

1.2. Problem Statement

The first part of the underground mine has been mined with sublevel open stoping. The second part of the underground mining area, called mine 2, is partly developed, and is going to be developed further in the coming years. The mining costs for the first part of the underground mine are not clear and they need to be determined before a thought-out mining plan can be made. Furthermore, a pillar between the old mining area and the new area is critical for a safe mining operation and it is critical for the whole mining infrastructure. The required thickness of this pillar is not known.

One key aspect of both mine plans is the location of the new stopes relative to the rib pillar that is between the old mine (Mine 1) and the new mine (Mine 2). The rib pillar is approximately under a 45 degree angle, which makes the assessment of the pillar more complicated. The optimum scenario will be that the stope can be directly above the stope that is located one level lower, this will result in most ore recovered. However, if the new stopes are too close to Mine 1, the rib pillar is too thin, the stability of the mine will become uncertain. Currently, there is no method to assess the thickness of a rib pillar in this kind of complicated situation. To determine the optimal thickness of the rib pillar, a geotechnical model will be made in RS2, which is a two dimensional numerical modelling software. The results from the model will be incorporated in the mine plans for both mining methods.

Therefore, it is necessary to get an overview of the current mining cost, and if possible, to lower the costs. The focus of this thesis is to determine the optimal mining method that will be used while mining Mine 2 in the underground part.

1.3. Goal and Objectives

With the gap defined in the problem statement, it is now possible to define the goal, the hypothesis and the research questions, which are given below.

The goal:

This research aims to prepare a mine plan to continue mining in Mine 2 with the most suitable mining method. Differences between the vertical crater retreat method and sublevel open stoping method must be analyzed and described. Additionally, the effect of the mining activities on stability of the mine should be analyzed.

The hypothesis for this thesis is based on literature review of both methods The hypothesis:

The use of Vertical Crater Retreat for the new mining method will result in a lower mining cost compared with the current method sublevel open stoping.

While the operation proved that sublevel open stoping is a profitable mining method, it is possible that the use of a different mining method will result in lower the mining costs. The following objectives are defined to test the hypothesis:

1. Techno-economic assessment of sublevel open stoping,
2. Techno-economic assessment of vertical crater retreat,
3. Stability of the barrier pillar between Mine 1 and Mine 2.

The following research questions should be answered to provide a solid foundation to attain the objectives.

1. For how long is the use of the sublevel open stoping mining method economically feasible?

2. Is the use of Vertical Crater Retreat as a mining method in this operation economically feasible and technically possible?
3. How does the proximity of stopes affects the stability of the barrier pillar?
4. What is the optimal stope size to continue mining without affecting the stability?

1.4. Method

The method that has been used in this thesis consists of multiple steps, and it followed the Sibelco geotechnical design steps (Schmitz 2018). These steps are a observational method based on monitoring. The first thing to do is to have a conceptual design or approach for the problem, which was that a different mining method should be reviewed. The following step was to acquire data and to incorporate this data into the design. This consisted of the gathering of data during fieldwork in the mine. During this time at the mining operation, information for the cost model was acquired as well. Before the time at the mine and during the cost models have been created and adjusted. Samples that were taken in the field, have been tested in a laboratory in Liege, Belgium. With the data acquired in the fieldwork and from the lab testing, the geotechnical work has been done. This included the geotechnical modelling and the empirical methods used to assess the stability of the mine.

1.5. Scope

The following table will state subjects that have been included into this thesis and what subjects are out of scope.

Table 1.1: Research Scope

In Scope	Out of Scope
VCR & sublevel open stoping	Other mining methods
Cost model underground Mine 2	Cost model processing & open pit
Mine planning for the future stopes in Mine 2	Detailed production planning (Monthly/weekly/daily planning)
2D numerical model	3D numerical model
Empirical mine stability assessment	

1.6. Thesis Outline

This report is consists of the following parts:

1. Introduction

Chapter 1: Introduction

An introduction to the topic with information about the mine site and the research objectives for this thesis.

2. Theory

Chapter 2: Mining

An overview of the theory of mining that is used in this thesis. Mining principles and mining methods are explained.

Chapter 3: Rock Mechanics

A basic overview of the theory of rock mechanics that is used in this thesis.

3. Methodology

Chapter 4: Fieldwork

The steps for the fieldwork in the mine are discussed in this chapter.

Chapter 5: Numerical modelling

Explanation of the steps taken to create the numerical model in the software.

Chapter 6: Mine Planning

The executed steps are explained for the planning of the mine. The steps for the cost model for both VCR and sublevel open stoping are discussed as well.

4. Results & Discussion

Chapter 7: Fieldwork & laboratory testing

The results of the fieldwork & laboratory testing will be given in this chapter.

Chapter 8: stability analysis

The results of the stability analysis will be given in this chapter.

Chapter 9: Cost model

The results of the cost model will be given in this chapter.

Chapter 10: Discussion

Discussion about the methodology that has been applied and the data that has been used to solve the problem.

5. Conclusion & Recommendation

Chapter 11: Conclusion

A conclusion of the findings of this research related to the scope of this thesis.

Chapter 12: Recommendations

Recommendations about the path forward for the mining operation that are based on the findings in this thesis.

Part II

Theory

2

Mining Theory

This chapter describes the various aspects of mining that are important to understand the mining operation at Stjernøy. It starts with the two different mining methods. These mining methods are sublevel open stoping and vertical crater retreat (VCR). The mining method is determined by the geology of the deposit. Each mining method works in a certain sequence, which is why after the mining method, the sequencing will be discussed. When the mining methods are explained, another factor affecting the mining operation will be discussed; mine stability.

2.1. Sublevel Open Stoping

Sublevel open stoping is an underground mining method that uses large-scale open stopes. The method is used if there is a strong orebody, which requires minimal support, and the ore is surrounded by a strong country rock. Furthermore, the ore should be well defined and in a fairly regular shape (Hustrulid 1982). The method is based on providing access to the orebody at different sublevels, between the main haulage levels, to drill and blast the ore. The workers are not supposed to enter the open stope, the activities take place at the sublevels (Hartman & Murmanský 2002). The orebody should be dipping with an angle between 50 degrees and 90 degrees, to make sure that the blasted material falls down to the drawpoint (Darling 2011). One other characteristic of open stoping is that it generally is a natural supported mining method. This means that deformation and displacement is limited to elastic orders of magnitude (Hudyma 1988).

Sublevel open stoping requires a lot of development with high capital expenditures before the production can begin. The layout of a typical sublevel open stope can be found in Figure 2.1. The development of a sublevel stope starts with a shaft or slope that is sunk in the footwall of the ore. This is to be unaffected by the negative aspects of blasting on the production drifts (Hustrulid 1982). The haulage drifts are located at the bottom of the stope, with access crosscuts at intervals. A slot raise is driven from the bottom of the stope to the top, which is enlarged to full stope width (from hanging wall to footwall) to act as a free face for the production blasts and to accommodate the swell (Darling 2011). The stope drilling is done from drilling drifts which are located on the sublevels. The drilling types that are most common are long-hole ring and fan drilling. If the orebody is narrow, the whole width of the orebody can be developed, which accommodates parallel drilling (Hustrulid 1982).

There are two basic types of sublevel open stoping, longitudinal and transverse. The longitudinal approach is used if the orebody is narrow, less than 15 meters thick. It uses stopes that are parallel with the strike of the orebody. The transverse approach uses stopes that are perpendicular to the strike of the orebody, with the possibility to use pillars between primary stopes (Villaescusa 2014).

Blasting in sublevel open stopes is done in slices. The stope is divided into slices of a certain thickness and the holes for that slice are drilled from the top to the bottom of the stope. The holes are plugged at the bottom and filled with 1 or 2 meter(s) of stemming. On top of the stemming comes the explosive

of choice, with a detonator at the bottom of the charge. If the hole is very long, it is also possible that a second detonator is used between 10 to 20 meters from the top of the hole.

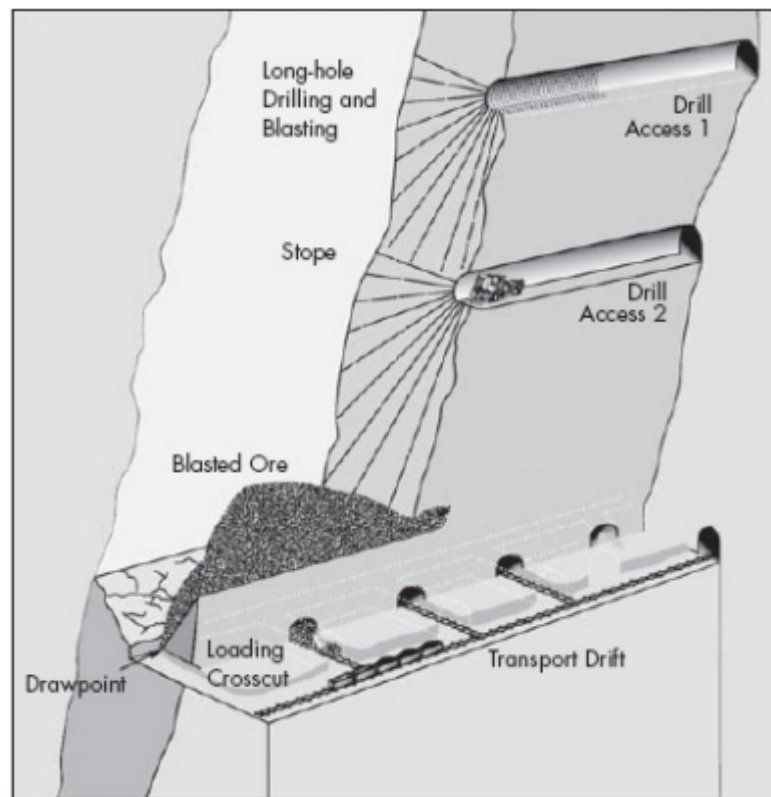


Figure 2.1: Sublevel open stoping. SME Mining Engineering Handbook, 2011. Modified.

One of the main advantages of sublevel stoping is the efficiency of the drilling, blasting and loading operations. The operations can be performed independently from each other. This creates a high potential for mechanization with higher productivities with a minimum level of personnel. Furthermore, most of the operations are located into a few locations, which lowers the transport in the mine (Villaescusa 2014). The main disadvantages are that the development is complicated and comprehensive, and that the shape of the orebody must be regular. Which means that waste inside this regular shape is also mined, or that ore outside this shape is not mined.

A case study of sublevel open stoping is the Olympic Dam mine in Australia. It is a sublevel open stoping operation that produces 1.5 million tonnes per year. The rock mass conditions at this operation are difficult to assess due to massive nature of the rock mass. A mean RMR value of 80 is used for this rock mass, which means "very good rock". The height intervals of the stopes vary between 30 and 60 meters, with a maximum width along strike of 60 meters and a maximum length of 35 meters. The size ranges are caused by the local differences in geological structures, mineralization and geotechnical structures. The production holes are 102 mm in diameter. The burden that is used is 3 meters, and the spacing is 4 meters. A powder factor of 0.25 kg of explosive per tonne of ore is used. The first opening that is created is a raiseborehole to accommodate the swelling of the material. The loading of the holes is done by 2- by 2-men crews working 14 shifts a week. Blast sizes range from 500 tonnes for slot creation to 250.000 tonnes during stope production. During each production week, six to ten blasts are performed (Ugalla 1999).

2.2. Vertical Crater Retreat

Vertical Crater Retreat (VCR) is a variation of sublevel stoping, where the free face is not the open stope vertically in the orebody, but a horizontal stope at the bottom of the block that is mined. The production blasts are horizontal slabs three to four meter in thickness, after which the ore is recovered at the base of the stope (Darling 2011). The last five to ten meter beneath the top, the crown is blasted in one session, with different delayed crater charges or with same delay decks (Chadwick 1992). VCR uses large borehole diameters, ranging from 140 mm to 205 mm holes, with the most common diameter being 165 mm (Jiang et al. 2015). The development is similar to the development of sublevel open stoping, except that there are less sublevels and it is recommended to have the drift at the top of the block as wide as the whole block. This is to provide a drill horizon for the parallel drilling that is necessary.

VCR is based on the cratering theory, which reduces the amount of explosives used in production (Hartman & Murmanský 2002). If a column charge is detonated, blasting rules state that the energy of the explosion is all vertical to the axis of the borehole (Katsabanis 2018). The energy released perpendicular to the axis is only a small part of the total energy. Spherical charges create an energy release pattern along a radial axis from the centre of the charge in a spherical homogenous pattern (Ye 2008). The charges that are used in VCR have a length/diameter ratio of 6:1. If the explosive column length to hole diameter ratio is six or less, the charges behaves as a spherical charge. The maximum burying depth of the charge for the appearance of a crater is called the optimal burying depth. The burying depth of the charge at which there is no crater visible at the surface, only cracks, is called the critical burying depth (Ye 2008). The blasting sequence that is used in VCR mining can affect the borehole above the blast. The damage of the blast will extend upwards and the fragmented material will fall down. It is possible that the shock of the blast will create movement of material higher in the borehole, what can cause blocking of the borehole. If the borehole gets blocked, it can be unblocked by simple measures from an operator or, if the blockage is significant, by re-drilling (Hawker & O'Connor 2011).

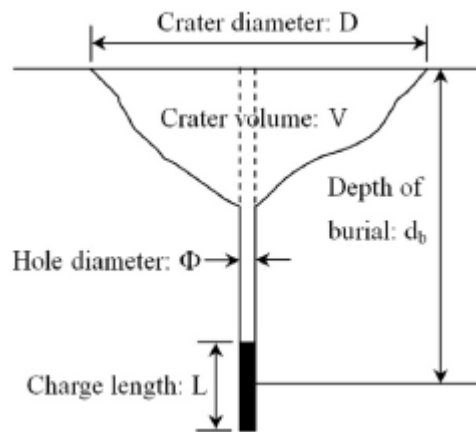


Figure 2.2: Cratering Dimensions. Liu et al 2018.

The different parameters of a cratering blast are given in Figure 2.2, with the depth of burial measured to the centre of gravity of the charge. The hole diameter, the charge length and the depth of burial determine the crater volume and the crater diameter. There is a relationship between the energy of the explosive and the crater volume (Liu et al. 2018). Livingstone determined a constant factor between the critical depth of burial and the cube root of the weight of the charge, which is given in equation 2.1. N is the critical depth of burial; E is the strain energy factor for a given type of rock explosive combination and Q is the weight of the charge.

$$N = E * Q^{1/3} \quad (2.1)$$

Where,

N : critical depth of burial in meters.

E : Strain energy factor for a given type of rock explosive combination in meters per

kilogram.

Q: weight of the charge in kilogram.

This equation can also be written as follows:

$$d = \Delta * E * Q^{1/3} \quad (2.2)$$

Where,

d: depth of burial in meters

Δ : ratio between depth of burial and critical depth of burial

Where d is the depth of burial and Δ is the ratio between the depth of burial and N, the critical depth of burial. Equation 2.2 becomes equation 1 if the depth of burial is equal to the critical depth of burial (Katsabanis 2018). With these equations, the crater volume divided by the charge weight (V/Q) can be plotted versus the ratio between the depth of burial and critical depth (Δ). The curve can be used to determine the optimum depth ratio to get the biggest crater (Katsabanis 2018). For Figure 2.3, the optimum is a ratio of 0.56. This has been determined for charge with a constant weight of 3.00 kg and a strain energy factor of 1.32 m/kg^{1/3} (Liu et al. 2018). One remark that is important for the correct use of this graph is that the curve dips drastically on both sides of the optimum. To ensure best practices, a safer value on the climbing side of the curve should be used.

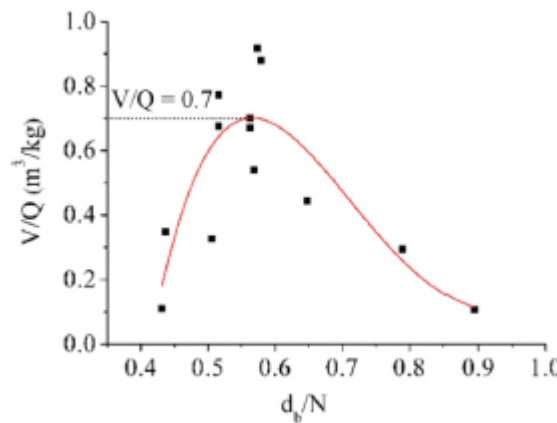


Figure 2.3: Volume/Charge weight ratio versus Depth of burial ratio/critical depth. Liu et al, 2018

This mining method eliminates different development steps, such as raise boring and vertical slot cutting. This reduces the time and costs for development. Furthermore, the uphole drilling and blasting is eliminated from the process. VCR uses holes drilled vertically, which makes the drilling less difficult. Another advantage is that the in-stope drilling is reduced (Villaescusa 2014). At the start of the stope, all the holes are drilled in the upper horizontal development. When the production phase starts, the only steps are loading and blasting of the explosives and mucking of the material from the draw points. A disadvantage of this method is that the horizontal development at the top of the stope must be created, which costs a lot of time and effort. Another disadvantage of this method is that rock breakage, caused by the cratering blast, can negatively affect the fragmentation if not properly designed. And the blast design should be made in such a way that the larger blasts do not affect the final walls of the stopes.

Previous research done on vertical crater retreat focusses mostly on blasting and vibrations. The VCR technique is being used to recover pillars that were left during previous mining activities or a new form of raising. The length that a face can be advanced depends on the hole layout, charging pattern, delay interval, expansion room, hole deviation and rock properties (Liu et al. 2018). The slice height was changed, to make sure that the material of the new blast had enough expansion room. They concluded that smaller slice height and alternating initiation sequence is the key to larger VCR blasts.

2.3. Dilution

Dilution is affecting the mining costs of each mining project. Dilution is the waste material that is not separated from the ore during the operation and is mined with the ore. The waste material is mixed with the ore and sent to the processing plant (Ebrahimi 2013). The total tonnage of the ore is increased, and the overall grade is decreased. There are multiple types of dilution; planned dilution and unplanned dilution. Planned dilution (or internal dilution) is the waste that must be mined due to the geometry of the orebody and the requirement to mine rectangular areas in sublevel open stope and vertical crater retreat mining. The waste material is ingrained within the deposit, which is the reason why it is difficult if not impossible to avoid (Crawford 2004). Unplanned dilution (or external dilution) is the dilution that is created by rock failure or selectivity of mining equipment. The material is originating from outside of the blasted stope boundary (Darling 2011). For both the mining methods that are discussed in this thesis, unplanned dilution is not created by selectivity of mining equipment. This is because there is no digging taking place outside the muckpile. Unplanned dilution can be controlled using the right equipment and mining practices (Crawford 2004). The two types of dilution are shown in Figure 2.4.

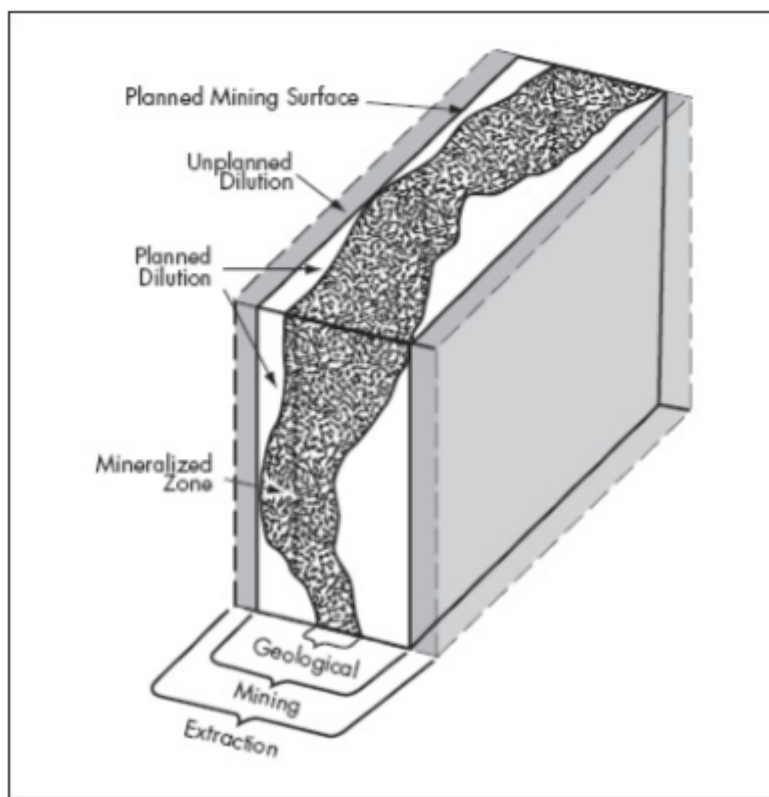


Figure 2.4: Planned and unplanned dilution. SME mining engineering handbook, 2011.

It is not possible to avoid dilution entirely, but it can be quantified and then controlled. Calculating dilution is a difficult process, which involves comparing after crushing samples with the resource and reserve models. The accuracy of this calculation is dependent on the accuracy of the sampling and of the resource modelling (Crawford 2004).

Stope geometry is an important aspect of dilution control. The stope hanging wall is the zone that is sensitive for overbreak. Henning and Mitri (2007) have shown that tall slender stopes with short horizontal and large vertical dimensions are more stable than large rectangle stopes (Henning & Mitri 2007). One parameter that is also very important to predict the dilution is the local stope setting in the mining sequence. Stopes with rocks on both sides have less potential to have higher dilution, this are primary stopes. Stopes with backfill on one or both sides have a higher potential for dilution, this are

secondary stopes.

2.4. Sequencing

A limiting factor to each underground mining operation is the maximum size of the opening that can be created without failure. In most operations, the volume that can be mined safely is significant smaller than the orebody itself. That is why multiple stopes are needed to extract all the material. In most mining operations, the different stages of the stope life cycle happen at the same time, which are: development, production and potential filling. To keep production at the same rate, multiple stopes are needed in different life cycle stages. In general, stope sequencing is driven by ore grade requirements, operational issues and induced stress considerations (Villaescusa 2014). One of the important aspects to remember is to avoid creating highly stressed blocks of rock in the orebody.

2.5. Rib Pillar

Open stope mining is the most economic if the entire orebody can be mined in one longitudinal stope. However, this mining technique creates the potential for serious stope instability. This instability can be solved by using rib pillars and or backfill. The role of a rib pillar is to increase stability to a mining section by limiting rock mass displacements and restricting the exposure of the rock mass in the stope back and walls (Hudyma 1988).

Pillar design is a critical step in the stope design process. The stability analysis of pillars is also very important in the stope design process. The most basic and well used calculations for the factor of safety for a pillar can be found in equation 2.3 (Villaescusa 2014). Stability of a rib pillar refers to the ability of the structure to undergo a small change in loading without resulting in a sudden release of energy of large deformations (Brady & Brown 2006).

$$\text{Factor of safety} = \frac{\text{Pillar strength}}{\text{Average pillar stress}} \quad (2.3)$$

In the equation above, the average pillar stress can be calculated by determining the area that is supported by the pillar, multiplied times the depth of the pillar and the density of the rock mass. The pillar strength can be determined with the strength of the rock and the dimensions of the pillar (Martin & Maybee 2000). The equation for the strength of a pillar is given by Hedley (1978) and is given in equation 2.4.

$$\sigma_p = K * \frac{W^{0.5}}{H^{0.75}} \quad (2.4)$$

Where,

- σ_p : pillar strength in MPa.
- K: strength of a unit volume of rock in MPa.
- W: width of the pillar in meters.
- H: height of the pillar in meters.

By analyzing rib pillar data from different Canadian open stope mines, Hudyma (1988) created a database with a wide variety of rock types and pillar loads. The pillar load data was derived from three-dimensional linear elastic modeling. Hudyma plotted the pillar load divided by the UCS on the y-axis and the pillar width divided by the pillar height on the x-axis. This results in figure 2.5. The graph is divided into three different zones: failed, transition and stable. Furthermore, 13 case studies of rib pillars are included in which the pillars were initially stable and yielded after a certain time. The cases were observed to move correctly through the graph (Villaescusa 2014).

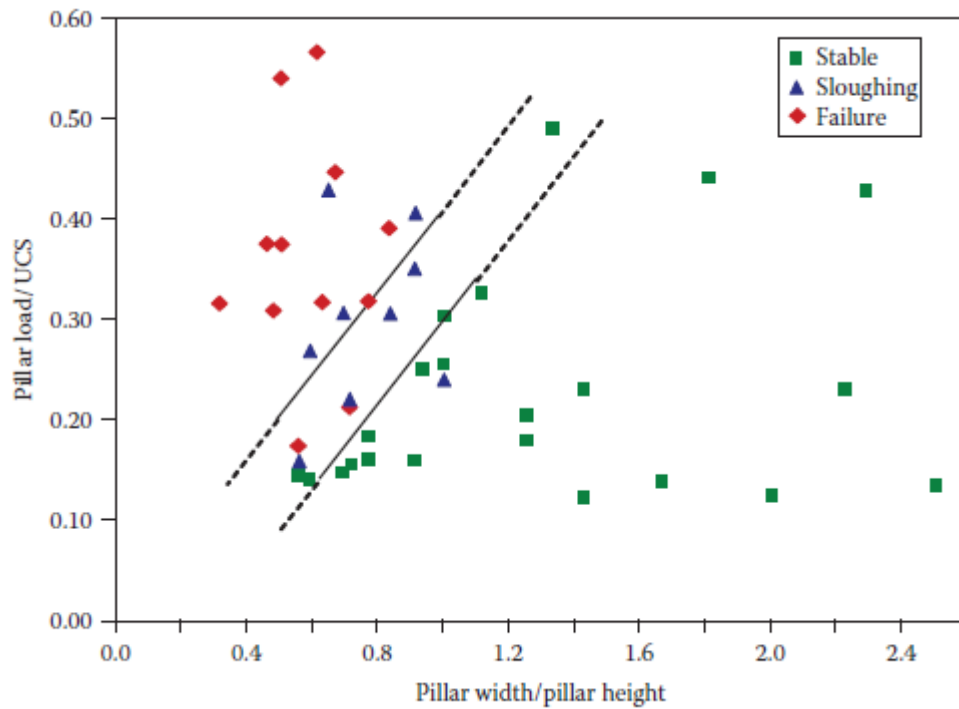


Figure 2.5: Rib pillar stability graph, showing: stable, transition and failed zones. Villaescusa 2014.

2.6. Stereonet Projection

A stereonet is a way to plot a hemispherical projection on a two-dimensional diagram. The projection allows to represent and analyse three-dimensional relations between planes and lines on a two-dimensional diagram. An imagined sphere is placed on an inclined plane, which is shown in Figure 2.6. The intersection of the sphere and the plane is called the great circle. A perpendicular line to the plane through the centre of the sphere intersects the sphere in the lower hemisphere, this is called the pole, see Figure 2.6. If multiple discontinuities are plotted on the same stereonet, an analysis of the joint sets can be made (Brady & Brown 2006). An example of an equal angle stereonet that can be used to manually analyse the planes and lines is given in Figure 2.7.

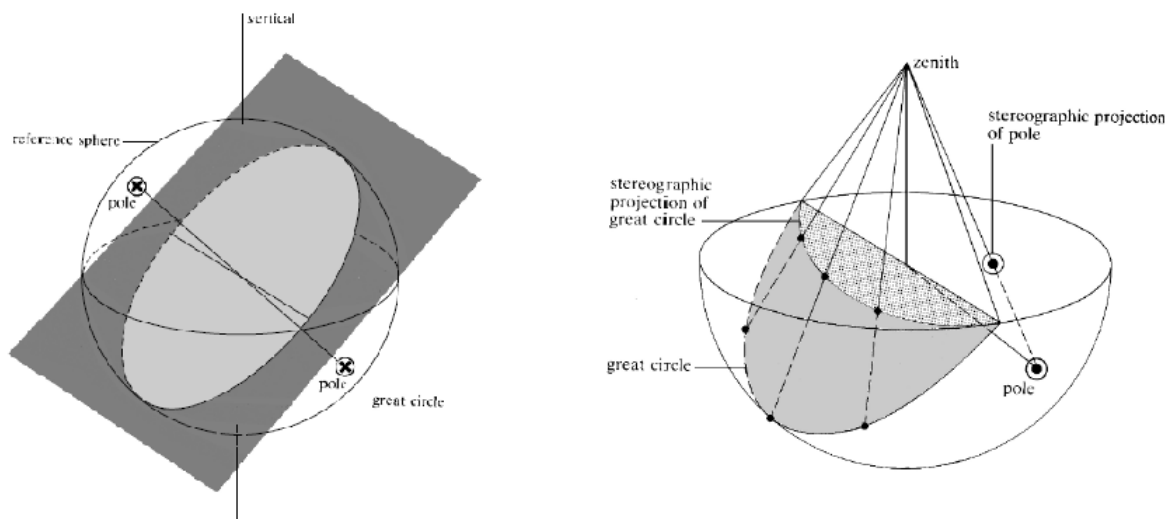


Figure 2.6: Stereonet projection. Left part shows the imagined sphere on the plane. Right part shows the great circle and the pole on the lower hemisphere. Brady & Brown (2004)

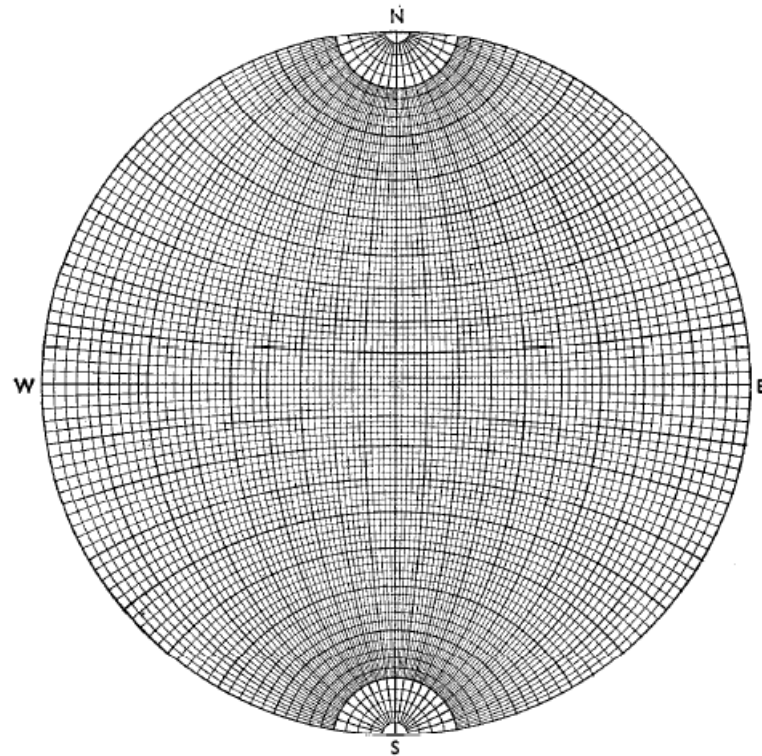


Figure 2.7: Example of an equal angle stereonet used for plotting the planes. Terzaghi (1965)

When orientation measurements are made, discontinuity sets that are perpendicular to the scanline are recorded more frequently than sets that have a lower angle towards the scanline. To account for this bias, the Terzaghi weighting factor can be used. The weighting factor is based on the angle between the scanline and the discontinuity and the distance between the discontinuities (Terzaghi 1965).

2.7. Mine Stability

Sublevel open stoping and vertical crater retreat both work with large open stopes. The stope should be stable, for safety reasons and to prevent too much dilution. The methods that are used to assess stope stability are empirical methods or numerical modelling. Mathews stability graph is one of the empirical methods that will be used for the stability assessment.

Mathews developed an empirical method to determine the stope dimensions. The stability graph is based on 189 case histories of unsupported open stopes. The graph divides the stopes in three categories: stable, unstable and caved. The stable stopes show little to no deterioration during the production time. Unstable stopes can have limited wall failure and/or block failure involving less than 30 % of the face area. Caved stopes have suffered unacceptable failure. The stability graph is based on a plot of stability number N' against a shape factor (or hydraulic radius) HR (Suorineni 2012). Equations 2.5 and 2.6 define the stability number and the hydraulic radius. In the equation for the stability number, the modified Q system is used instead of the Q system. The difference between the two systems is that in the modified Q system, the values for the joint water reduction number (J_w) and for the stress reduction factor have been set to 1. The reason behind this is because in the Q system, the factors J_w and SRF account for stresses in the rock mass. The equation for the stability number involves factor A , which accounts for the stresses in the system. To prevent that the stresses have a double effect on the stability number, they are set to 1 in the modified Q system.

$$N' = Q' * A * B * C \quad (2.5)$$

Where,

- N: the stability number.
- Q': modified Q factor.
- A: stress factor.
- B: joint orientation factor.
- C: Mode of failure factor.

In Equation 2.5 is Q' the modified Q factor, based on the Q system. The modified version is used, because the A factor also accounts for the strength of the rock and part of the formula for the Q system also takes that into account. The factor A in equation 2.5 is the stress factor, which accounts for the effects of induced stress around the stope. It ranges from 0.1, meaning high compressive stresses, and 1, meaning relaxing conditions (Potvin et al. 1988). The stress factor is determined from the ratio of the intact rock strength (UCS strength) to the induced compressive stress at the center line of the surface. Factor B is the joint orientation adjustment factor, which is the relative difference in dip between the critical joint set and the stope surface. The last factor, C, accounts for the mode of failure that may be in the form of gravity fall, slabbing or sliding. Figure 2.8 gives the different graphs for the factors and how to calculate them.

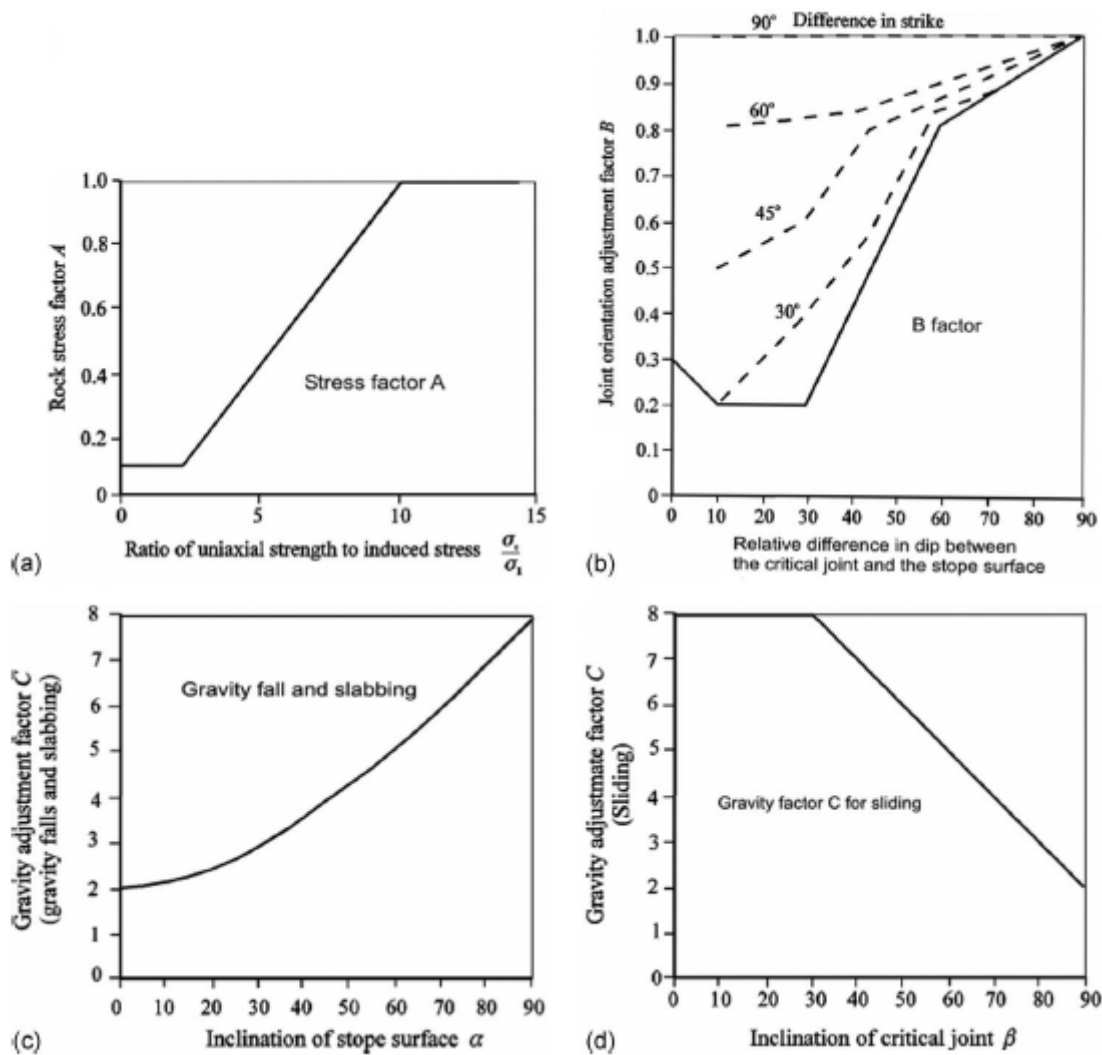


Figure 2.8: The different factors for the stability graph. (a) Stress factor A. (b) Joint orientation factor B. (c) Mode of failure factor for gravity fall and slabbing. (d) Mode of failure factor for sliding. Suorineni 2010.

The final part of using Mathews stability graph is the shape factor or hydraulic radius (HR). Most classification systems define the span in a two-dimensional plane. This is because the methods are based on tunneling, in which the long span can be assumed infinite and the short span is the critical opening. To account more accurately for the combined influence of size and shape on the stope stability, the hydraulic radius is used (McKinnon 2018a). Equation 2.6 shows the formula for hydraulic radius, which is the area divided by the perimeter. Figure 2.9 clarifies the stope dimensions that are used in equation 2.6.

$$HR = Area/Perimeter = \frac{w * h}{2 * w + 2 * h} \quad (2.6)$$

Where,

HR: Hydraulic radius in meters.

w: width of stope in meters.

h: Height of the stope in meters.

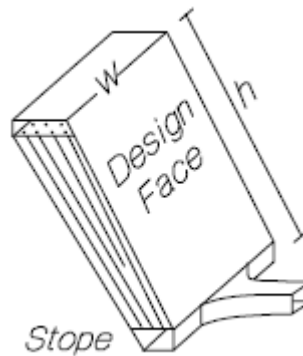


Figure 2.9: Dimensions of the stope that are used to calculate the hydraulic radius. McKinnon 2018.

The stability graph is given in Figure 2.10, and it shows the stable, transition and caved zone. If the stope is located to the left of the uppermost curve, the stope is capable of being stable for a reasonable service time. If the need arises to have personnel in the stope, a light pattern of rockbolts and/or mesh should be used (Hutchinson & Diederichs 1996).

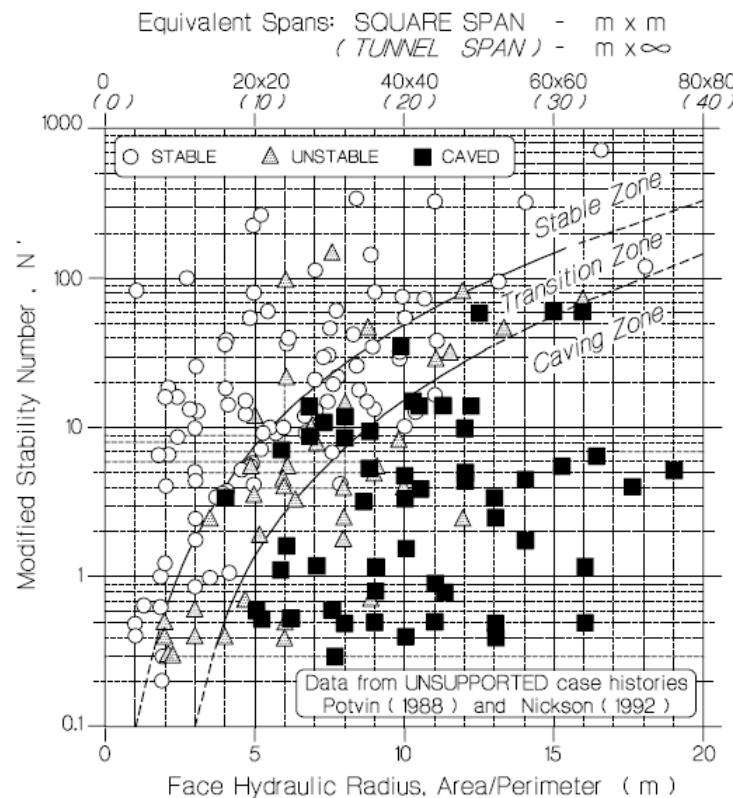


Figure 2.10: Stability graph. Hutchinson & Diedrichs 1996.

The Mathews stability graph uses the following assumptions as a base for the graph. The most significant assumptions are (Suorineni 2012):

- Faults are not in proximity of the stope surface.
- For the determination of Q' , only joints with a length of longer than 3 meters should be used.
- The open stope stability graph is only valid if there is no backfill as any of the surfaces.
- Stopes are mined in 6 months, and time has no effect on the stope stability.
- The method is applicable to 2-way exposed stope surfaces.

2.7.1. Case Study

A case study of Thompson Mine in northern Manitoba, Canada, gives insight in the used VCR method. The mine produces mainly nickel ore from open pit and underground operations. The underground operation produces approximately 6000 tons per day. To holes that are used have a diameter of 114 mm or 165 mm. The 114 holes are loaded with charges ranging from 8 to 12 kilograms, and the 165 holes are loaded with 25 kilograms of explosives. This results in a powder factor for both hole types of 0.45 kilogram of explosive per ton of broken material (Greer 1989). One of the concerns was the powder factor in combination with the medium strength rock. The blasts could damage the walls of the stopes in such a way that the dilution would increase. To create a summary of the mine's open stoping experiences, 126 previously mined stopes were analysed with an empirical method, Mathews stability graph (Hudson 1995). The stopes have been plotted in the graph, and the result is shown in Figure 2.11. A few things can be noted in the graph of the hanging wall cases, one of them is that unstable stopes are plotted in the stable region, which indicates that the correlation with the general failure curve is not sufficient. Also, the plot of the stable points correlates well with the failure curve. The graph of the stope back cases shows a better correlation with the graph, all 11 unstable cases are in the unstable zone or in the transition zone. However, stable points are scattered all over the graph. The differences

between the stopes and the graph are caused by the effect of the high powder factor with the rock quality. Hudson suggests that the stability graph for this mine should be adjusted. The original graph is based on case studies from all over Canada. The true design line for this mine should be calibrated with the data from the site. The left graph of the figure shows the new proposed design line for stable and unstable zones. The recommendation made by Hudson (1995) is that if there are enough data entries, the Mathews stability graph should be updated for the operation in which it is used.

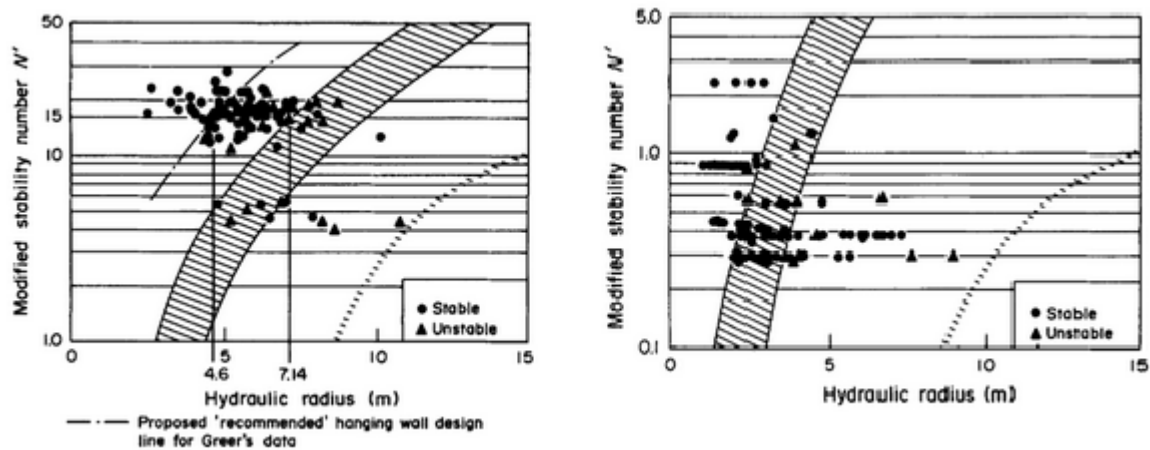


Figure 2.11: Analysis of 122 stope hangingwalls (left graph) and 101 stope back walls (right graph). Hudson 1995.

2.8. RS2

The software that will be used to model the stopes and the rib pillar is RS2. It is developed by Roc-Science, a company specializing in 2D and 3D software for mining, civil and geotechnical engineers. RS2 is a 2D finite element program for soil and rock applications. Finite element method is a way to represent the continuum. The whole domain is divided into elements, which can have multiple shapes but often triangles (Mckinnon 2018b). Modelling the subsurface in RS2 consists of various steps. The first step is to create a cross section of the area of interest. That will be the stopes with the topography of the mountain. The next step is to create a stress field in the model that equals the measured and values found in literature of the stress field. The third step is to assign the materials used in the model with the right rock mass properties. Properties that are included are strength, failure mechanism and the number of joints present in the rock mass. The next step in the progress is to create a mesh of triangular elements with the right density to not miss any detail. The mesh can be larger in areas where limited information is needed, and the mesh can be smaller if there is a need for more information.

RS2 is often used for the evaluation of built up stresses. Gonen and Kose developed a model for the stability analysis of open stopes and backfill in longhole stoping method. They investigate the stresses that would occur around stopes and pillars which will be created when certain parts of the orebody at depth will be mined. The stopes are planned to be at a depth of approximately 400 meters. They first performed laboratory testing to determine the geomechanical properties. The properties are used to model the behavior of the different material types. Gonen and Kose study three different cases, the first being a case of one stope extracted, the second is a case with two stopes and a pillar in between and the last case is when the production reached the 650 meter level (Gonen & Kose 2011).

For the first case, the model showed that the critical stresses occur in the corners and the sidewalls of the stope. For the second case, the critical stresses occurred in the roof and sidewalls of the stopes and in the pillar. The third case showed that there would be no stability problems with the design. To come to this conclusion, they compared the stresses from the model with the geomechanical features. The conclusion from Gonen and Kose was that a triangular or diagonal shaped production sequence starting from the bottom is very important for the stability of the mine (Gonen & Kose 2011).

2.9. Conclusion

With the knowledge of sublevel open stoping and vertical crater retreat described in this chapter, a basis is created to make a decision between both methods. The differences between the methods are clear. Furthermore, other principles that are used during the mining operation of an underground mine are discussed, as well as Mathews Stability graph method. This method will be used later on in this thesis to assess the stope size empirically. The software that will be used, RS2, to assess the stability of the whole mine is described.

The next chapter is going more in-depth to the rock mechanics that are important for each mining operation. A good understanding of rock mechanics and the force that are active in the mine will result in a better assessment of the stability of the mine.

3

Rock Mechanics

To understand the rock behaviour, an understanding of rock mechanics is needed. Rock mechanics is the subject concerned with the response of rock to an applied disturbance. For engineering principles, the disturbances are man induced.

Rock masses can be complex to understand and to use the current engineering principles to analyze the rock behaviour can be complicated. In complex cases, the design decisions can be based on previous experiences in the mine or elsewhere. To make it possible to use experiences from other locations, classification methods have been developed.

This chapter will explain the classification systems and the principles of rock mechanics that have been used in this thesis. These methods are significant, because without a clear understanding of the stability in the mine, unstable conditions can be created. One of the reasons is that Mine 2 is very close to a stability barrier pillar in the mine that gives stability for vital infrastructure parts of the mine. The rock mechanic methods have been used to make sure that the mining methods that are considered result in stable conditions. A focus lies on the area of the barrier pillar, which is of high importance to the mine.

3.1. Stress-Strain Relation

Stress is the intensity of internal forces in a certain body under influence of external surface forces. Stress is the force per unit area. Strain is the proportional deformation of a body under stress. The relation between stress and strain can be described in different ways, the constitutive models. The constitutive models describe the time dependent and time independent response of a material to an applied load. The models describe the responses in terms of elasticity, plasticity, creep, viscosity and combinations (Brady & Brown 2006). The difference in most models is in the after failure behaviour of the material (Mckinnon 2018b).

The most common constitutive model is the model of elasticity, it is the constitutive model for many rocks and a basis for other models. Figure 3.1 shows two different models for elasticity, linear elastic and elastic-plastic model. The x-axis is the strain and the y-axis is the stress. The linear elastic model is a model stress equals the strain. The elastic plastic model first behaves as a elastic model, till the point of failure. From there, the strain becomes a straight line (William 2002).

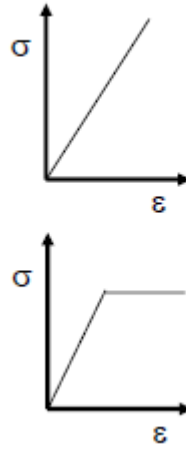


Figure 3.1: Top graph: Elastic constitutive model. Bottom graph: elastic-plastic constitutive model. McKinnon 2018.

3.2. Young's Modulus

The Young's modulus is a property that measures the stiffness of a solid material. It defines the linear elastic relationship between strain and stress in a material during uniaxial deformation. The modulus shows the ability of a material to withstand changes in length when under tension or stress in the lengthwise direction. The equation for Young's modulus is given in equation 3.1. The Young's modulus is also called the elastic modulus.

$$E = \frac{\sigma_{zz}}{\epsilon_{zz}} \quad (3.1)$$

Where,

E : Young's Modulus.

σ_{zz} : uniaxial stress.

ϵ_{zz} : strain.

The stress strain curve for rocks are almost always non-linear, which makes it more difficult to calculate the Young's modulus. However, there are multiple ways to calculate the modulus. The first method is to calculate the slope at a fixed point, generally at 50% of the UCS strength, this is called the tangent method. The next method is the average modulus, which is the slope of the straight line part of the stress-strain curve. The third method is the secant modulus, which is the slope of a line through the origin of the curve to a fixed point (Pourhosseini & Shabanimashcool 2014).

3.3. Poisson Ratio

The Poisson ratio is the negative of the ratio of transverse strain to axial strain in an elastic material subjected to uniaxial stress (Gercek 2007). The Poisson effect is the tendency of a material to shrink or expand in a direction perpendicular to the loading direction. The equation for Poisson's ratio is given in equation 3.2.

$$\nu = -\frac{\epsilon_{trans}}{\epsilon_{axial}} \quad (3.2)$$

Where,

ν : poisson ratio.

ϵ_{trans} : transverse strain.

ϵ_{axial} : axial strain.

The transverse strain is negative when there is axial stretching (tension) and positive for axial compression. The axial strain is negative for axial compression and positive for axial tension.

3.4. Rock Quality Designation Index

The Rock Quality Designation Index (RQD) is based on fracture spacing along scanlines. The RQD is the percentage of intact lengths greater than a threshold value of 10 centimeters, to the total length in the drill run (Sen 2014). If there is a core sample, the RQD can be determined with the sample in a fairly easy way. This task can be assigned to the drillers or to the geologists analyzing the core for grade assessment (Hutchinson & Diederichs 1996). If there is no core sample, RQD can be calculated using the spacing of the joint sets that are present. The RQD can be calculated using equation 3.3. The mean spacing is needed to use this formula, which can be determined from fieldwork (Mckinnon 2018a).

$$RQD = -3.68 * \frac{1}{meanspacing} + 110.4 \quad (3.3)$$

3.5. RMR

The Rock Mass Rating (RMR) system is developed by Bieniawski in 1973 based on experience in shallow tunnels in sedimentary rocks (Singh & Goel 2011). Several adjustments have been made to the RMR system during the years. This is why it is important to state which version of the RMR system is used. To classify a geological structure, the following six parameters are needed:

- UCS strength of intact rock material
- RQD
- Joint spacing
- Joint Condition
- Groundwater condition

The parameters listed above are incorporated in the system by creating ranges for the parameters. Each range for each parameter is assigned a rating value. These rating values allow for the fact that not all parameters contribute equally to the response of the rock mass. Some parameters have higher rating values than other parameters. When for each parameter a rating value is determined, the values can be combined to get the overall RMR. The value for RMR can be adjusted for the influence of joint orientation. For the table with values for the RMR and the adjustment for joint orientation, see Appendix 13.1 & 13.2.

An example of the calculation can be seen in table 3.1. The values for the five parameters have been determined with the table in Appendix 13.1. The dip and dip direction of the dominant joint set are determined with an adit perpendicular to the joint axis. The dip is 35 degrees against the drive direction. With table 13.2 the situation is described as unfavourable and the final RMR rating is to be adjusted with -10 for this case. The final rock mass rating is 54.

Table 3.1: Determination of Rock Mass Rating

Parameter	Value or Description	Rating
strength of intact rock material	150 MPA	12
RQD	70	13
joint spacing	0.5 m	10
condition of joints	Slightly rough surfaces	25
groundwater	water dripping	4
	total RMR	64

3.6. Q system

The Q system is a classification system to characterize rock mass quality developed by the Norwegian Geotechnical Institute (Mawdesley et al. 2001). It is an empirical method to assess the stability of an underground excavation. The system is mostly based on civil engineering tunneling cases in low to moderate depth. Tunnels for civil purposes are being used with a higher frequency and are built for a longer lifespan than mining stopes. That is why they use a more conservative system than what is needed for most mining stopes. The civil standards can be used for equipment rooms, high traffic roadways and lunchrooms where stability is very important (Hutchinson & Diederichs 1996). The equation for the Q system is given in equation 3.4.

$$Q' = \frac{RQD}{J_n} * \frac{J_r}{J_a} * \frac{J_w}{SRF} \quad (3.4)$$

Where,

RQD: Rock Quality Designation.

J_n : joint set number.

J_r : Joint roughness number.

J_a : Joint alteration number.

J_w : Joint water reduction number.

SRF : Stress reduction factor.

The joint set number (J_n) is the number of joint sets present in the rock mass. Figure 3.2 shows the stereonet projection of the different possible joint set numbers, with the accompanying value of J_n . The joint roughness number (J_r) is based on the critical joint set and it describes the large- and small-scale surface texture. It ranges from 0.5 (unfavorable) to 4 (favorable) (Hutchinson & Diederichs 1996). The values for J_r for large- and small-scale are given in Figure 3.3. The joint alteration number (J_a) describes the alteration and frictional resistance of the critical joint set. It ranges from 0.75 (favorable) to 20 (unfavorable). The abbreviated table which is used in hard rock mining to determine the joint alteration factor is shown in Table 3.2. The joint water reduction factor (J_w) is based on inflow and water pressure observed in underground openings. Joint water can soften or remove infill and reduce the friction of joint planes. The stress reduction factor describes the relation between stress and rock strength around an underground opening (*Q system handbook* 2015).










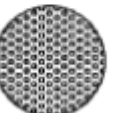
# of Joint Sets		J_n			# of Joint Sets
Intact Rock No Joints		0.5	1		Few Random Joints Only
1 Set		2	3		1 Set + Random
2 Sets		4	6		2 Sets + Random
3 Sets		9	12		3 Sets + Random
> 4 Sets Heavily Jointed		15	20		Earthlike, Crushed Rock

Figure 3.2: Number of joint sets visible in a stereonet projection. McKinnon 2018.

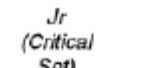







	Large Scale:	Planar	Undulating	Discontinuous
				
Small Scale:				
Slickensided		0.5	1.5	2.0
Smooth		1.0	2.0	3.0
Rough		1.5	3.0	4.0
Gouge-Filled No Wall Contact		1.0	1.0	1.5

Figure 3.3: Joint Roughness number. Hutchinson & Diederichs 1996.

Table 3.2: Joint alteration number (Ja). Hutchinson & Diederichs 1996.

Typical description (critical joint sets)	Ja
tightly healed	0.75
surface staining only	1.0
Slightly altered joint walls. Space mineral coating	2.0 - 3.0
Low friction coating (Chlorite, Mica, Talc, Clay) <1mm thick	3.0 - 6.0
Thin gouge, low friction or swelling clay 1 - 5 mm thick	6.0 - 10.0
Thick gouge, low friction or swelling clay >5mm thick	10.0 - 20.0

3.7. Geological Strength Index

The Geological Strength Index (GSI) is a system for characterization of rock masses. The GSI was created in 1992, but the version that is used today was finalized by Hoek and Marinos in 2005 (Hoek et al. 2005). It was realized that a rock mass classification system needed to be related to geological observations that could be made quick and easy in the field by a qualified person. The RMR and Q system are less reliable swelling, squeezing, clearly defined structural failures or slabbing, spalling and rock burst under high stress (Hoek et al. 2005). The GSI was created because a system was needed that placed greater emphasis on basic geological observations. The new system needed to better reflect the material, structure and geological history and it is developed specially for the estimation of rock mass properties instead of tunnel design (Singh & Goel 2011). The RMR and Q system both rely on RQD, however, RQD is in weak rock masses meaningless or essentially zero, the RQD is not included in GSI.

The GSI classification is a qualitative engineering rock mass description. Numbers are used as little as possible, because the numbers for the Q system and RMR are meaningless for heterogeneous and weak rock masses. The GSI is only used as an estimation tool for rock mass properties, not to replace the RMR and Q system. The index is based on an assessment of the condition of discontinuity surfaces, structure and lithology (Hoek et al. 1998). It combines the blockiness of the mass and the surface conditions of the discontinuities and respects the main geological constraints that are important in a formation (Hoek et al. 2005). The general chart for GSI can be found in 13.3. The two choices described previously have to be made on the chart. This is done by simple field observations. The second GSI chart for heterogeneous rock masses is given in 13.4, which is similar to the general chart, however the maximum GSI value is lower (Hoek & Brown 2019).

3.8. Hoek-Brown Criterion

The Hoek-Brown Criterion is a way to describe a non-linear increase in peak strength of isotropic rock with confining stress. Hoek-Brown follows a parabolic form, which differs from the linear Mohr-Coulomb form. An assumption that is made with Hoek-Brown is independence of the intermediate principle stress. This assumption is based on tests by Brace (1964), that resulted in negligible influence of intermediate stress (σ_2) on failure (Eberhardt 2012). The criterion was developed by Hoek and Brown in 1980 by fitting parabolic curves to triaxial test data. Accordingly, the criterion is an empirical criterion with no fundamental relationship between constants (Hoek 1998).

The first version of the Hoek-Brown Criterion is shown in equation 3.5 (Eberhardt 2012). The parameters σ_1 , σ_3 and σ_c are parameters that can be determined in not too complex laboratory tests. The parameters m and s are a bit more complex. The parameter m can be seen as the frictional strength of the rock, it ranges from 0.001 for highly disturbed rock masses to around 25 for hard intact rock (Hoek 1983). A low value for m indicates a low friction angle. Large values for m give steep Mohr envelopes and high instantaneous friction angles (Eberhardt 2012). The effect of lower or higher m can be seen in Figure 3.4. The figure shows that higher values of m give steeper Mohr circles, which indicate a higher friction angle than lower values of m . The parameter s is representing the degree of fracturing of the rock mass. The maximum value of s is 1, for an intact rock mass, to 0 for a highly fractured rock mass. This is related to the cohesion of the rock mass, for a value for s of zero, the tensile strength has

been reduced to zero (Hoek 1983). An assumption that has to be made is that the fractures present are numerous enough to affect the whole rock mass (Eberhardt 2012).

$$\sigma_1 = \sigma_3 + \sqrt{m * \sigma_c * \sigma_3 + s * \sigma_c^2} \quad (3.5)$$

Where,

- σ_1 : major principle stress at failure.
- σ_3 : minor principal stress at failure.
- σ_c : uniaxial compressive strength.
- m: dimensionless empirical constant.
- s: dimensionless empirical constant.

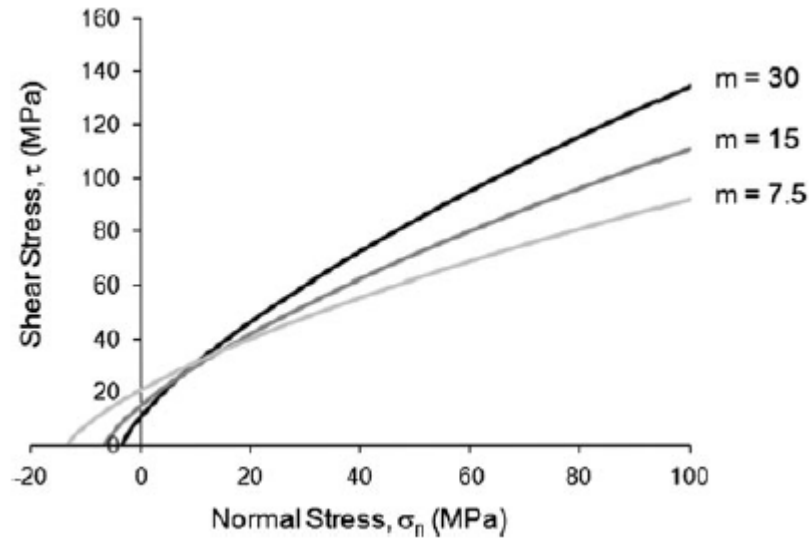


Figure 3.4: The effect of lower and higher values for the parameter m in the Hoek-Brown Criterion. Eberhardt 2012.

Based on experience with the Hoek-Brown criterion, the generalised Hoek-Brown criterion was published in 1994 (Hoek 1994). The generalised version is given in equation 3.6 (Hoek & Brown 2019).

$$\sigma_1 = \sigma_3 + \sigma_c \left(m_b \frac{\sigma_3}{\sigma_c} + s \right)^a \quad (3.6)$$

The parameters m, a and s are the rock material constants, and are given in this version by the following equations: parameter m_b is given in equation 3.7, parameter a is given in equation 3.9 and parameter s is given in equation 3.8.

$$m_b = m_i \exp \left(\frac{GSI - 100}{28 - 14D} \right) \quad (3.7)$$

$$s = \exp \left(\frac{GSI - 100}{9 - 3D} \right) \quad (3.8)$$

$$a = \frac{1}{2} + \frac{1}{6} \left(e^{\frac{-GSI}{15}} - e^{\frac{-20}{3}} \right) \quad (3.9)$$

Where,

- m_b : material constant for rock mass.
- m_i : material constant for intact rock.
- GSI: Geological strength index.
- D: disturbance factor.

The value m_b is based on the value of m_i , which is derived from curve fitting triaxial test data of intact rock. M_b is a reduced value of m_i , which is determined by the strength reducing values of the rock mass conditions determined in GSI (Feng et al. 2018).

3.9. Disturbance Factor

After excavation in rock masses, the removal of rock leads to a stress relief which causes the neighbouring rock to relax and dilate. A good design of a tunnel or other excavation controls this dilation and displacement too limit rock failure. Methods to control this are: selecting the right excavation shape, method of excavation or to install rock support or reinforcement. Draining of the rocks can also help in maintaining the stability of an excavation (Hoek & Brown 2019). In a tunnel, the method of excavation and the control of the blasting. The limited amount of space in a tunnel means that a failure in the tunnel will have a large impact on safety and schedule (Sonmez et al. 2004).

The table that is used to determine the disturbance factor is given in Appendix 13.5. The top part shows a tunnel with excellent blasting results. The design has been carefully made and executed accordingly. The tunnel wall control was done carefully, which resulted in smooth tunnel walls. This indicates that the damage to the surrounding rock is minimal and the disturbance factor D can be set to 0. The second example is a tunnel made with the heading and bench method. The excavation of the lower part can result in rock failure. A disturbance factor of $D=0.5$ is appropriate for this kind of excavation technique. The next example is of a bad design and execution. The damage to the walls is the result of poor drillhole alignment and lack of detail for design and detonation. A disturbance factor of $D = 1.0$ is appropriate for this example. The fourth example is of a slope with two different blasting types, the pre-split blasting on the left part and the mass blasting on the right part. The pre-split blasting part has a disturbance factor $D = 0.5$ and the mass blast has a disturbance factor $D = 1.0$. The mass blast factor is higher, because the blast was less controlled and caused more damage to the remaining rock mass. The last example shows an open pit slope with different qualities of blasting. From production blasting with more damage to the surrounding rock to wall control blasting with almost no damage to the surrounding material (Hoek & Brown 2019).

3.10. Generalised Hoek & Diederichs

The Young's modulus that can be determined with axial compression tests or direct shear tests on rock samples is more applicable to the intact rock than to the whole rock mass. To get the right stiffness for the in-situ rock mass, the value should be reduced (Jiao et al. 2012). The equation for generalised Hoek & Diederichs is given in equation 3.10.

$$E_{rm} = E_i * \left(0.02 \frac{1 - \frac{D}{2}}{1 + e^{\frac{60+15D-GSI}{11}}} \right) \quad (3.10)$$

Where,

E_{rm} : Young's modulus for the rock mass.

E_i : Young's modulus for the intact rock.

GSI: Geological strength index.

D : disturbance factor.

3.11. Kirsch Equation

To calculate the stresses distribution around excavations, the Kirsch equations can be used. The equation can be used to calculate the stresses around a circular excavation, such as the example in

figure 3.5. The equations are given in equation 3.11, 3.12 and 3.13. If the opening has a different shape, the equations and ratios in figure 3.6 should be used to calculate the stresses (Hoek & Brown 1982).

$$\sigma_r = \frac{1}{2}(p_1 + p_2) \left(1 - \frac{R^2}{r^2}\right) + \frac{1}{2}(p_1 - p_2) \left(1 - \frac{4R^2}{r^2} + \frac{3R^4}{r^4}\right) \cos(2\theta) \quad (3.11)$$

$$\sigma_\theta = \frac{1}{2}(p_1 + p_2) \left(1 + \frac{R^2}{r^2}\right) - \frac{1}{2}(p_1 - p_2) \left(1 + \frac{3R^4}{r^4}\right) \cos(2\theta) \quad (3.12)$$

$$\tau_\theta = -\frac{1}{2}(p_1 - p_2) \left(1 + \frac{2R^2}{r^2} - \frac{3R^4}{r^4}\right) \sin(2\theta) \quad (3.13)$$

Where,

σ_r : Radial stress
 σ_θ : circumferential stress
 τ_θ : Tensile stress
 θ : Angle from the horizontal
 p_1 : highest stress in plane
 p_2 : lowest stress in plane
 r : Distance from the center of the circle.
 R : radius of the circular opening

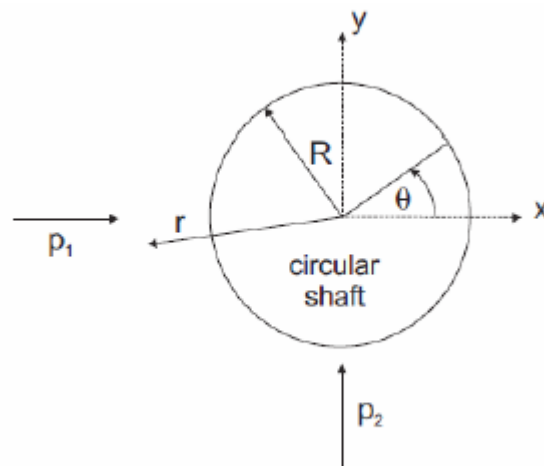


Figure 3.5: Stresses around a 2D circular excavation with a bi-axial stress field. McKinnon 2018

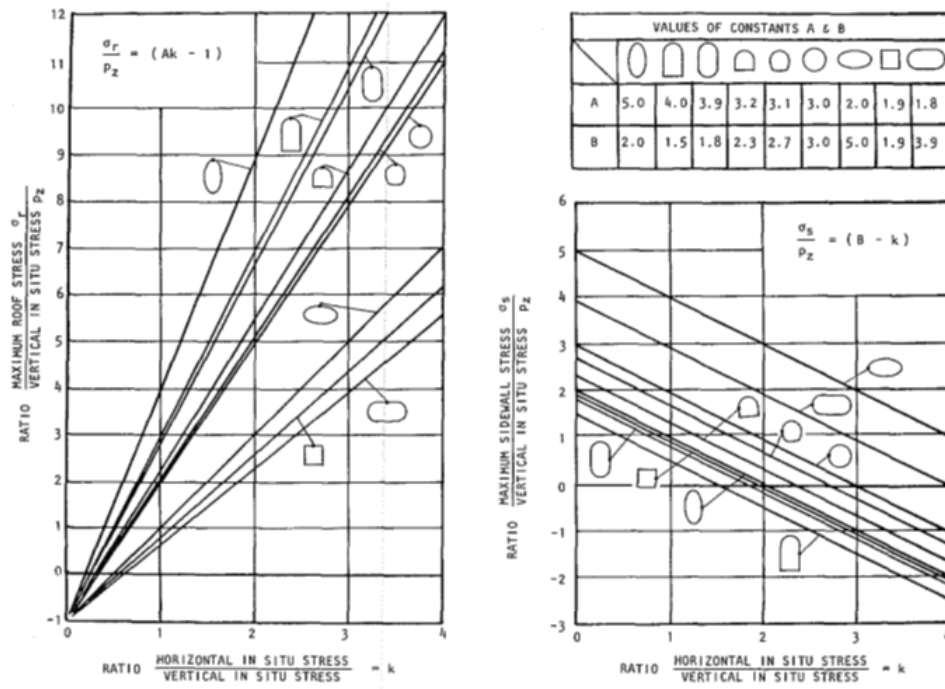
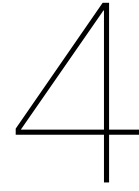


Figure 3.6: Influence of excavation shape and ratio of applied stresses on boundary stress. Hoek and Brown 1980

Part III

Methodology



Field work & laboratory testing

The steps taken in this thesis follow the steps of Eurocode 7 (British Standard EN 1997-1:2004) and uses the concept of the Geotechnical Category described herein which have been described by Schmitz et al 2020. This thesis is part of the conceptual design of the new mine. Based on the results of the conceptual design, the next phase, the final design can start.

The geotechnical modelling is partly based on data acquired in the mine and partly on data acquired in the laboratory. This is done with various methods and according to the sibelco guidelines (Schmitz 2020). A list of methods used is given below:

- scanline mapping,
- rock mass rating,
- Laboratory testing.

4.1. Scanline Mapping

Scanline mapping is a method to obtain information on the engineering properties and structure of the rock mass. The basic method used to map a surface is scanline mapping. A scanline mapping is a simple operation that consists of a long line along the surface of the rock mass and all discontinuities that intersect the line are mapped (Brady & Brown 2006). It is important to do the scanline mapping on an area that is of interest and is representative for a larger section of the mine. The following features are mapped in the scanline survey:

- distance along the scanline that the discontinuity intersects with the scanline,
- number of endpoints of the discontinuity,
- discontinuity type,
- orientation of discontinuity,
- roughness of the discontinuity,
- planarity of the discontinuity,
- trace length of the discontinuity,
- termination type of the discontinuity,
- remarks on the infilling, seepage or aperture.

The features that are listed above are used to get a better insight in the discontinuity sets and to what extent they affect the strength of the rock mass. The roughness and the planarity of a discontinuity are indicators of sliding failure of rocks. The discontinuity type, trace length, termination type and the number of endpoints provide information about the joint set, if it are random joints or maybe a set that is present in the whole survey. The final part of the scanline survey is to check if there is any infilling, seepage or aperture that can affect the strength of the discontinuity. All these parameters are logged during the scanline survey and used in a later stage to determine the joint sets that are present.

The scanline is done at the barrier pillar, and consists of a length of 43 meters. This is slightly wider than the pillar at level 460 in the mine. This level is chosen because the new stopes will be planned up to this level, and the joint sets present will affect the mine layout.



Figure 4.1: Example of the scanline survey in the underground mine. The measuring tape has been placed along the wall.

4.1.1. Stereonet Projection

To evaluate the results from the scanline mapping, the discontinuity data is used to check if the discontinuities are part of larger sets or random discontinuities. This is done with a stereonet projection in Dips software from RocScience. Dips is a stereographic projection program for the analysis and presentation of orientation based data. With the program, it is possible to analyze and visualize data with the techniques used in manual stereonet. Dips is created for the engineering analysis of rock structures (RocScience n.d.).

All the discontinuities that are measured during the scanline survey are uploaded into Dips. The first step is to adjust the measurements for the magnetic declination at the mine site. The magnetic declination is the deviation of the compass from the true north (*What is declination?* n.d.). The magnetic

declination at the mine site is 11.58 degrees. This value can be entered into the software and it compensates the measured values.

The discontinuities are plotted in a stereonet projection, which then shows the poles of each discontinuity. If the poles of multiple discontinuities are located close together, the discontinuities can be part of a set. By finding the centre of a set of poles the pole of the joint set can be found. With the pole of the joint set, the dip and dip direction of the joint set can be determined, for further analysis of the rock strength.

4.2. Rock Mass Classification

Two rock mass classifications have been done in the mine. The first one is done in Mine 2, Stope 1 at the 380 meter level. The part of the stope that is analyzed is the part of the pillar between Mine 1 and Mine 2. This is done to get more insight in the quality of the pillar after blasting of the top slice. The top slice has been developed in this stope and the first slice of the stope has been blasted. The second rock mass classification that has been done is located at the barrier pillar at the 460 level. The second location is part of the scanline survey, however the survey consisted of a longer line than the length of the classification. This is done because a rock mass classification over the same length as the scanline survey is too large.

The rock mass classification that has been done in the field combines multiple methods in one session, to make sure that the classification has been done accurate. If the values for one method do not correspond, or are approximately in the same range, it is most likely that a mistake was made in the classification.

The focus of the first part of the rock classification is on the quality of the drifting work that has been done to create the stope. Parameters that are discussed here are blasting influence and excavation type. Blasting influence can be seen in a drift in multiple ways. If half barrels are visible, the drift was blasted using wall control blasting, which indicates that the rock mass in the sides of the drift are not heavily affected by the blast. Another way to classify the blasting influence is the disturbance class D. An estimation of the disturbance class D can be made in the field by assessing the quality and structure of the wall. The excavation type of a drift can be determined by indicators visible on the wall or by information provided by the mine planner. If there is any mode of failure present in the area of the rock mass classification, this is marked here as well, with a description of the mode of failure.

The next part of the classification is the quality of the rock mass itself. Parameters that are evaluated in this part are the m_i value, degree of weathering, GSI value and rock strength. The GSI value is determined using the method described before in Part II. The rock strength can be determined in multiple ways, with the use of a schmidt hammer or simple geological tools such as a hammer or a pocket knife. The degree of weathering is based on a visual assessment of the rock mass. Weathering states range from fresh to residual soil. Indicators of weathering are discoloration of (discontinuity) surfaces and disintegration of rocks (Brady & Brown 2006). The m_i value is determined, if laboratory testing is not possible, by finding a rock type with similar properties in a table of values for basic rock masses (Hoek 2007). The table that has been used is given in 13.6.

Following the description of the rock mass, the discontinuity parameters are assessed. For each set of discontinuities, the following parameters are reviewed:

- dip and dip direction,
- linear joint count,
- joint roughness,
- discontinuity spacing and length,
- discontinuity separation,

- discontinuity infilling.

For some of these values, different classification methods can be used. To make correlation between different methods possible in a later stage, some parameters are described in multiple ways. Such as the Joint Roughness, it is described with the joint roughness number, joint roughness coefficient and the joint roughness profile. These three parameters are all similar, but vary slightly, and used in different methods.

Following the description of joint sets, an overall description of the joint parameters is required. This is not necessary an average value of the parameters determined before. For the parameters listed above, the value that is most representative for the whole area that is included in the rock mass rating. The following parameters are added to the description:

- block shape factor,
- tilt test,
- volumetric joint count.

The block shape factor is a parameter to describe the shape of the blocks, which can have an effect on the strength of the rock mass (Palmström 1995). The volumetric joint count is the volume of joints in a cubic meter. This is a difficult parameter to assess while in the field, because an imaginary cube should be placed against the rock mass. Every joint that passes through the cube should be added. The tilt test is used to determine the shear strength of the material. The test can be performed in the following way; two blocks are put on top of each other, the lower block is tilted till the top block starts to move. The angle at which the top block starts to move is the tilt angle (Alejano et al. 2012).

The last parameters that are part of the field survey are the inflow of water and the stress reduction factor (SRF). The inflow of water can be qualified between completely dry and flowing. The SRF is a coefficient that represents the stress that is acting on a rock mass. It ranges from 0.5 high stress in a good quality rock to 400 for a massive rock with heavy rock burst conditions.

4.3. Laboratory Testing

To get a better understanding of the rock mass properties for the analysis of mining method and the stability, laboratory testing will be done. With the results of the laboratory testing, the numerical model will give more realistic results for the mine. The parameters that are needed for the model are the following:

- density,
- UCS,
- Young's modulus,
- Poisson ratio,
- tensile strength.

4.3.1. Samples

Multiple samples at different levels have been taken to use in the lab testing. In total, nine different samples have been taken from various levels in the mine. Each sample was taken at the location of the barrier pillar in that area of the mine and at three different levels in the mine. The levels at which samples have been made are: 340 level, 420 level and 460 level. This was done with a handheld core drill. The drill head had an inner diameter of 3.9 centimeters, which results in cores with a diameter of approximately 3.9 cm. The length of the cores should be at least 2 time the diameter of the core to

make it suitable for different types of testing. Furthermore, the diameter should be at least ten times the largest grain size (ASTM 2017). The characteristics of the core samples are given in table 4.1, the level column is the height in the mine at which the sample was taken. If the core is not suitable for testing in the current size, it is possible that the core is redrilled to create a core with the right ratio for testing.

Sample	Level	Height (mm)	diameter (mm)	Height/Diameter
1a	460	24	39.8	0.60
1b	460	32.1	39.8	0.80
2	460	54.6	39.8	1.37
3	460	23.6	39.8	0.59
4	340	60.4	39.8	1.52
5	420	74.7	39.8	1.88
6	420	53.1	39.8	1.33
7	460	75.1	39.8	1.89
8	340	66	39.8	1.66

Table 4.1: Core samples location, length and width

4.3.2. Density

The method to test the density of a material is a standard method which is not difficult. The volume of the sample needs to be determined as well as the weight of the sample. The weight of the sample can be determined with a scientific scale. The volume of the sample can be determined in two ways. The first method is applicable to the sample if the sample is drilled in good conditions and the core is straight. Simple volume calculations are sufficient to calculate the volume of the cylinder. The second method is to submerge the sample in a volume of water and calculate the increase in volume of the overall setup.

4.3.3. UCS, Poisson Ratio and Young's Modulus

The set up for an unconfined compressive strength test consists of a pressure bench that can apply an axial load on a sample. If needed a radial- and axial strain gauge can be added to the set up to measure the radial- and axial strain. The data from the pressure bench and the gauges is digitally recorded. The data from the pressure bench can be used to calculate the UCS of the rock sample. With the UCS strength and the radial and axial strain, the Young's modulus and the Poisson ratio can be determined with the formulas given previously in the chapter rock mechanics. For reliable test results, at least five samples should be tested (ASTM 2017)

Not all the cores that have been made are suitable for ucs testing if the length to diameter (L/D) ratio should be 2. However, a shape correction factor has been determined to calculate the right UCS value for a different L/D ratio (Thuro et al. 2001). The equation for the correction is given in equation 4.1.

$$C = \frac{C_a}{0.88 + \left(0.24 * \frac{D}{L}\right)} \quad (4.1)$$

Where,

- C: Calculated UCS.
- C_a : measured UCS for specimen tested.
- D: Test core diameter.
- L: Test core height.

4.3.4. Sonic Velocity

The sonic velocity of a core sample can be tested by measuring the time a sonic wave needs to move through a sample. The tests are becoming more and more common, due to the non-destructive way of

testing, high precision and a low cost. There are multiple ways to test the velocities, but the ultrasonic method has been used in this thesis. (Chawre 2018)

4.3.5. Tensile Strength

The tensile strength of a material can be tested with the Brazilian Tensile Strength test. This tests is performed on a disk shaped sample, which is easy to prepare. This test is an indirect measurement technique for the tensile strength. An indirect tensile strength test is a test that determines the tensile strength without performing a straight pull test. A core is loaded by two opposing strip loads, until failure occurs in the core. The equation that is used to calculate the tensile strength uses the theory of elasticity for isotropic continuous media. The strength calculated is the tensile strength at the moment of failure perpendicular to the loaded diameter at the center of the disc. The thickness/diameter ratio for the sample should be 0.5 or 0.6. If flat loading plates are used, the equation for the tensile strength is given in equation 4.2. If curved loading plates are used, the equation for the tensile strength is shown in equation 4.3 (ASTM 2016).

$$\sigma_t = \frac{2P}{\pi * t * D} \quad (4.2)$$

$$\sigma_t = \frac{1.272P}{\pi * t * D} \quad (4.3)$$

Where,

σ_t : splitting tensile strength

P: Maximum applied load indicated by the testing machine.

t: thickness of the core sample.

D: diameter of the core sample.

5

Stability Analysis

To select a mining method and to create a mine planning, it is necessary that the mine is stable. The stability of a mine can be assessed in multiple ways. The methods used in this thesis are an empirical method and numerical modelling. First, how Mathews stability graph has been used will be explained. Second, the steps that were done to create the numerical model will be analysed.

5.1. Mathews Stability Graph

The stability graph has been used to determine the stability of the new stopes at the 380 level. The 380 level has the highest induced stress due to the highest depth of the new stopes. The steps of the stability graph have been explained in chapter 3 in Part II of this thesis. The input data from the fieldwork has been used to determine the values for the graph.

The first value that has been calculated is the stress factor A. The UCS of the material does not vary in the rock, so the only variation in this factor is the induced stress at the location of the stope that is assessed. For the 380 level, the induced stress can be determined from the numerical model. The next factor that is going to be calculated is the joint orientation factor, or factor B. For this factor, the orientation of the roof and the stope hangingwall is needed. The orientation for the roof, begin a flat surface, is assumed to be 320/00. The orientation for the hangingwall is 320/70. With these two values know, and the values for the major joint sets that have been determined with the data from the fieldwork, the difference in dip between the joints and the stope surface can be determined. Because it is not known which joint set is the critical joint set, the value for B factor should be determined for all and the lowest value should be used for the calculation. With the program DIPS from RocScience, the angle between different planes can be calculated. The roof and the hanging wall were added into the stereonet results from the fieldwork. The next factor that is determined is factor C, the factor for the mode of failure. In the mine, the modes of failure are slabbing and gravity fall. With the inclination of the stope surface, the value for C can be determined.

The next parameter that has been calculated is the modified Q factor. The modified Q factor is based on the results of the fieldwork that has been done. The parameters that are needed can be filled in the formula given in Chapter 2. With all the factors above known, the stability number N can be calculated.

The last parameter that is needed to use the stability graph is the hydraulic radius (HR). This radius is equal for all hanging wall stopes and equal for all footwall stopes. The HR for the roof will be different than the HR from the hanging wall. For both scenarios the radius will be determined and for the roof and hanging wall the stability will be assessed.

To check if the this empirical method is reliable to use in this mine with the conditions present, the stability in another area was analysed. This area is a new cavern for a new workshop. It has a similar

size as the stopes, however, it is a horizontal excavation instead of an inclined stope. Furthermore, support has been installed in the new cavern. There is a different stability graph for supported stopes, that has been used for the new cavern.

During this thesis events happened that highlighted a part of Mine 2 stope 5 that could be affected by the fault that was located close by. To assess the stability of the area, the stope size has been decreased in the numerical model. For this smaller stope size, the stability graph method was used as well.

5.2. Numerical Model

To assess the stability of the planned stopes, a numerical model has been made. This model was created in the program RS2, by RocScience. The model is a 2 dimensional finite element model. The steps that are important when creating a numerical model for rock mechanic purposes are given in the steps below:

1. Determine the purpose of the model
2. Assess controlling mechanics
3. Gather problem related information
 - stress
 - geology
 - geometry
 - scale
 - geomechanics info
4. Geomechanical model
5. Physical to numerical representation
6. Boundary of the model
7. Create the actual problem geometry
 - material boundaries
 - excavation steps or internal changes
8. Discretization
 - Where to put the most and least detail of the model
9. Create a mesh
10. select constitutive models and material properties
11. Create initial stress conditions
12. apply boundary conditions
13. set up monitoring points to check the model
14. initial unmined model consolidation steps
15. start excavation process
 - follow actual extraction sequence
16. examine the model behaviour
 - development of stresses
17. calibrate the model
18. make necessary adjustments to initial model
19. production runs

5.2.1. Pre-Modelling

The first five points of the list are done before the actual numerical modelling. It is important to have a good plan for the model, to make sure that it is clear why the modelling is done and what questions are answered. After this stage it should be clear how the real problem should be modelled into a 2 dimensional model. It is also important to identify mechanics of the model, like modes of failure and deformation. The model for this thesis is going to be a two dimensional model, which includes the stopes and large production areas in the mine. The two dimensional model is chosen because it is a simpler modelling structure than a three dimensional model. Furthermore, the stopes are of a size which allows two dimensional modelling. the cross sections in stopes are quite similar, and show no large variations. The drifts are not included in the model because the amount of drifts would create a very complex two dimensional model. The major failure mechanisms that are present in the mine are slabbing and gravity fall, which have been assessed in the field work part of this thesis.

5.2.2. Model Generation

The next part of the modelling is to create the model itself. The boundary of the model should be determined at a sufficient distance from the model so that it has no effect on the model. After the model boundary has been defined, the problem geometry should be created. What areas of the mine should be created in the model and what parts of the mine should be left out of the model? The mine should be modelled how it has been developed, because with plastic rock conditions, the excavation sequence can have a high impact on the stability. It can be useful in the start of a project to simplify the model, so that the results of the simple model give insights on weaknesses of the model. At this step, the faults are added into the model.

The next part is to determine the discretization and to create a mesh. The discretization process uses the gradation factor and the number of excavation nodes to change the continuous model to discrete parts. The gradation factor is the ratio of the average length of discretizations on excavation boundaries to the length of discretizations on the external boundary at the maximum distance from the excavation boundaries. The number of excavation nodes determines the amount of finite element nodes on the excavation boundary. With the discretization certain areas can have higher detail than other areas. This is useful to get more information around excavations, but to keep the number of elements of the model low. There are different types of mesh that can be used: graded, uniform or radial mesh. The graded and uniform mesh are the options that are used the most. The graded mesh puts a higher emphasize on the excavations in the model and the uniform mesh creates a mesh that is the same everywhere. The graded option is the type of elements that are used in the mesh. The nodes and the shape of the elements can vary. Commonly used shapes are triangles and quadrilaterals. These two shapes can have nodes on the corners, or on the corners and in the middle of each side. To determine the shape and the amount of nodes of the mesh elements is similar to the mesh style. More nodes in the elements gives a higher level of detail, but it also increases the computation time of the model.

The parameters that are used to create the mesh are given in table 5.1. This table shows the mesh type, element type, gradation factor and the default number of nodes on excavation. The graded mesh type has been chosen because it lays the focus of the model close to the excavations. The 6 noded triangle element type has been chosen because it increases the level of detail, without increasing the computation time too much. The gradation factor has been set to 0.1 and the default number of nodes on excavation has been set to 1000, because these settings create a mesh network that is suitable for the goal of this model.

Table 5.1: Mesh parameters

Mesh type	Graded
Element type	6 noded triangles
gradation factor	0.1
Default number of nodes on excavation	1000

The following part is the selection of the constitutive model and to use the right material properties for each material. The major choice in constitutive model is between plastic and elastic. If the material is not allowed to fail during the computation, elastic should be used. This option also has the lowest computation time. The other possibility is plasticity, which allows elements to fail, if the stress becomes too high. This option has a higher computation time. The plastic constitutive model can be divided into other models, which represent the behaviour in the rock mass in different ways. Because the parameters of the rock mass are hard to estimate after failure, the elastic plastic constitutive model can be used. The post-failure strength of this model is the same as the peak strength of the rock. With the constitutive model selected, the other material properties can be determined. First, the failure criterion has been chosen. The Hoek and Brown failure criterion has been used in all the models, because the criterion is based on the brittle fracture concepts which give a good representation of the behaviour.

A list of all the materials in the model is given in table 5.2, with all the parameters that are used for each type of material. The values for the materials have been determined in other parts of this thesis or are values based on literature. The Nepheline Syenite is the rock type that is dominant in the model, most of the model consists of this rock type. The Syenite K rock type, is a very similar rocktype. However, it has been set to elastic because of the consistent failure of the area above T-stollen, which made the model unstable. The model parameters schwebe 33% and schwebe 66% are the modelled material types that are used in the schwebe in stope 1 and stope 2. The schwebe is the part of the stope that is still left in place when part of the stope has been mined. The schwebe 33% has one third of the stope still in place and the schwebe 66% has two thirds of the material still in place. These materials are included in the model, because that is the current situation and they may have an effect on the stability of the pillar. The backfill material is elastic and weaker than the rock mass. The material that is used to backfill is broken rock from the open pit mine. This kind of material will have lower material properties than the original rock.

Table 5.2: Parameters used in the RS2 model

Parameter	Unit	Nepheline Syenite	SyeniteK	Schwebe 66%	Schwebe33%	Backfill
E_{rm}	MPa	35000	35000	25000	15000	20000
E_i	MPa	61000	61000	-	-	-
GSI	-	75	75	75	75	75
D	-	0.4	0.4	0.4	0.4	0.4
Density	g/cm3	2.67	2.67	2.67	2.67	2
Poisson	-	0.24	0.24	0.2	0.15	0.24
UCS	MPa	135	135	135	135	135
M_b	-	9.172	9.172	6.172	3.172	4.172
S	-	0.041	0.041	0.028	0.014	0.00043
-	-	Plastic	Elastic	Plastic	Plastic	Elastic

The next step is the application of the initial stress conditions and the boundary conditions for the model. The boundary conditions for the model are set in the modelling software and can be a roller lateral constraint and fixed base. If a roller lateral constraint is used, the displacement is limited. The gridpoint is only able to move freely in the plane of the base. For a model with a large size, the roller lateral constraints are commonly used for the sides and the bottom. However, if the model is large enough, fixed base constraint can also be used. For the top of the model, which is the topography of the area, the fixed based constraint is used, because it is not allowed to move. The initial stress conditions for the model should be set in such a way that the are similar to the initial stress for the mine. The initial stress conditions are difficult to determine, because there were no stress measurement before the mining operation. The first stress measurements that have been performed were in 1973, when the mine was already in production. The first part of mine 1 was mined out and the stress measurements were performed in the area close to mine 2, in a drift. This test will be discussed in the data used chapter, part of the results. The initial stress condition is gravity driven, which makes in possible to work with horizontal divided by vertical stress ratios. One ratio for the horizontal in plane stress and one for the horizontal out-of-plane stress. If the modelled stress levels are not in the same range as the stress

levels that were measured, locked in horizontal stresses can be added into the model to increase the horizontal stresses.

The last step is to let the model compute and to make sure that the model is representing the real rock mass behaviour. This can be done by determining the stress in some points in the mine and to compare the modelling results with the results from the testing. To check this, three areas have been chosen. In two of the areas flat jack testing has been performed. One of the tests was done recently and the other test was done in 2018. The other area that was used is a large cavern that is used for the first mineral processing steps in the mine. This is an area where rock burst and/or spalling has taken place, which indicates that the stress levels in this area are high. For the last point, a value is not known for the stress in the area. However, for the two flat jack tests, the stress values are known. With these test areas defined, the computation of the model could start. The first stage is the model without the mine. With the results from the first run, the behaviour of the model can be analysed, which can lead to some changes in the model. As well the results of the computation for the three monitoring zones that have been defined can indicate that some changes are necessary. The calibration of the model is an iterative process, until the results are satisfactory.

The process of getting the right stress field for the initial or early mining stages is an iterative process. A location is selected from which stress data in an early stage is known. The stress at this location is reviewed with each adjustment till it is at the right level.

Table 5.3: Stress field parameters

Field stress type	-	Gravity
Effective Stress ratio	Horizontal/vertical in plane	1.2
Effective Stress ratio	Horizontal/vertical out-of-plane	1.8
Locked-in horizontal stress	in plane	0 MPa
Locked-in horizontal stress	out-of-plane	0 MPa

The effect of the new stopes on the stability of the mine will be investigated with the model. Different mining layouts will be reviewed and also the effect of leaving part of stopes in place or the use of rock bolts. These scenarios will be reviewed by looking at the stresses at the pillar between mine 1 and mine 2 and other key areas. Furthermore, the strength factor will be reviewed for each model. The strength factor is a factor that can be calculated by dividing the rock strength by the induced stress at each point in the mesh. All the stress parameters (σ_1 , σ_z and σ_3) have an influence on the strength factor, which is why it is a three dimensional factor.

One of the areas that is used as a reference is a drift that is located at the 460 level. The drift has been developed for exploration purposes and located approximately two stopes higher than the current stope level. The drift is one of the locations where a flat jack tests has been done. The results for the tests will result in higher values than the far field stress in that location. That is why Kirsch equations have been used to calculate the far field stresses and so calibrate the model further.

5.3. Data Used

The data that was used to create the model can be divided into two categories. The first one, is data from fieldwork and laboratory research. The other category is the data that was used from previous research projects or measurements. An important source for data for the numerical model were reports from SYNTEF, a norwegian consulting company and a report from the university of Liege. Two different syntef reports were used for this thesis a report. The first report is about two-dimensional stress measurements on the 320 level (Johannsson 2001). The second report is about basic numerical modelling of Mine 1 (Dahle 2007). The last report that has been used is a partly finished report from the university of Liege about numerical modelling. The report of syntef 2007 focusses on the general stress conditions at the mine site, before Mine 2 was created. The report of the University of Liege focusses on the location of a new underground processing plant.

To validate the numerical model, stress data is used that has been acquired by flat jack testing in during different areas of the flat jacks that were placed in the walls of tunnels or stopes. The results of the flat jack tests are stresses in a certain direction. By combining multiple flat jack test results, the stress field can be determined. The results from the numerical model should be approximately the same. The flat jack testing has been done by employees of Sibelco.

Table 5.4: Stress testing historical values to be used to validate model.

Parameter	Unit	SYNTEF	Flat jack stope 1	Flat jack above stope 3
vertical stress	MPa	10	35	37
horizontal stress	MPa	7.5	Unknown	27
out of plane stress	MPa	18	25	Unknown

6

Cost Model & Mine Planning

The mining method theories about sublevel open stoping and vertical crater retreat have provided theoretical information about the mining methods. This information will be used to review the mining method that is used and to make two plans to continue mining with each method.

This chapter will describe the methods that have been used to answer the objectives for the cost model and the mining methods that have been stated earlier. The approach which was used to achieve the objectives will be explained.

The following steps will be:

- cost calculations for sublevel open stoping,
- cost calculations for vertical crater retreat,
- mine planning for sublevel open stoping,
- mine planning for vertical crater retreat.

6.1. Approach

The decision which mining method will be used for the new levels is influenced by the production and by the costs of the method. Therefore, it is necessary to have a clear understanding of the different aspects of the costs and the production of each method. The calculations are based on an approach from the bottom up. Currently, there is not a clear overview of costs available, which is why the costs for each step in the mining process are calculated. All these costs are added and adjusted so they are correct for the units used. To start, the unit that is used is a stope. The costs of drilling, loading, blasting, materials and more are calculated for a stope. From the cost value of a stope, the costs of a tonne of ore or a cubic meter of material is calculated.

Other cost values that are calculated are the drifting cost and development cost. These two values are calculated based on the sublevel open stoping method, and used as well for the vertical crater retreat method.

Lastly, the two mine plans are compared.

6.2. Sublevel Open Stopping Cost Model

The cost models for sublevel open stopping and vertical crater retreat are based on a bottom up approach. This means that no clear overview of costs existed within the company. To get an overview of the total costs, the important steps in the mining process were reviewed and categorized. the steps in the mining process are divided into the following groups:

- blasting,
- operations,
- personnel,
- equipment.

6.2.1. Stopes

The first part of the model is the blasting section. In this section, the steps involved for blasting are reviewed. This involves calculations to determine the number of explosives that are needed to blast a certain area. The first step is the borehole volume calculations for footwall stopes, hangingwall stopes, drifts, vertical slot, top slice development footwall stope and top slice development hangingwall stopes. The volume of explosives can be calculated with the following equation:

$$V = \frac{d^2}{4} * \pi * l - 20 * d \quad (6.1)$$

Where,

- V: volume of explosives in borehole in cubic meters (m3).
- d: diameter of borehole in meters (m).
- l: length of borehole in meters (m).

The first part of equation 6.1 is the volume calculation of the whole borehole. However, not the whole borehole is filled with explosives, the top part is filled with stemming or left open. The last part of the equation, twenty multiplied with the diameter, is the stemming height, which needs to be deducted from the total volume of the borehole to get the volume of the explosives used in one borehole. The stemming height is determined by using a rule of thumb that is frequently used in mining. The rule of thumb is that the stemming height is 10 to 20 times the diameter of the borehole.

The following step is to determine how many boreholes there are in one stope. To determine the number of boreholes in a row, the width of the stope is divided by the spacing between the holes. The spacing is the distance between boreholes in the same row. To calculate the number of rows, the length of the stope is divided by the burden between the rows. The burden is the distance between different rows. However, dividing the width and the length by the spacing and burden will give one row and one borehole per row more than in reality. This is because there is no hole at the edge of the stope, the first hole is located a certain distance from the final wall of the stope. the number of boreholes in a stope can be calculated with the following equation:

$$N = \left(\frac{W}{S} * \frac{L}{B} \right) - \frac{W}{S} \quad (6.2)$$

Where,

- N: number of boreholes in a stope.
- W: width of the stope in meter (m).
- S: Spacing between the boreholes in a row in meter (m).
- L: Length of the stope in meter (m).
- B: Burden between the rows in meter (m).

6.2.2. Drifts & Top Slice

This process is followed for the footwall stopes and for the hangingwall stopes. For the drifts, the same process is followed, except that the boreholes are horizontal instead of vertical and the length of the boreholes is 5 meter. The other steps are similar. For the vertical slot that is used to create a free face for blasting, the calculation steps are similar to the steps for the stopes. The calculation for the top slice development is partly the same as the calculation for the drift. The top slice is developed by creating drifts next to each other, so the whole top slice is created by the drifting method. This results in the calculation for the top slice being the materials and cost for the drift multiplied by the number of drifts in the top slice. This number can be determined by area calculations.

6.2.3. Working Hours

The next step is to determine the amount of man hours that is required for each process. This has been done by reviewing mine plans, by personal communication with the people that work in the mine and with personal communication with the people in the office. The communication resulted in estimates from the people that plan the work and people that perform the work, which were quite similar. No actual timing of work on stopes or drifts has been done, because during the time of the field visit other work was performed in the mine. This resulted in time estimates for the drilling and loading of the holes.

For the mucking of the drifts and the top slice, estimates from the Caterpillar handbook are used, which is indicated in the model. The estimation that have been used are for the scooping of material, dumping and for the travel time underground. The assumptions also correlated with very rough estimates done by the people in the mine.

6.2.4. Consumables

The next part of the underground operation that is important is the estimation of the consumables that are used underground. Consumables that are considered in this model are:

- explosives
- Diesel,
- electricity,
- lubricants,
- track,
- tires,
- drilling rod,
- drilling bit,
- bucket teeth.

Each of the consumables are used in a different way. Most of the consumables can be estimated by reviewing maintenance and cost reports or by comparing them to similar machines in mining engineering handbooks. These handbooks contain guidelines for different equipment sizes and the right size can be selected.

With the number of boreholes and the volume of each borehole known, the weight of explosives for a stope can be calculated. The information required of the explosive that is used is given by the manufacturer of the explosive. The information required about the explosive is the density of the explosive. With the density known, equation 6.3 can be used to calculate the total weight of explosives for a stope:

$$Q = V * N * \rho \quad (6.3)$$

Where,

Q: total weight of explosives used for a stope in kilogram (kg).
 ρ : density of explosive in kilogram per cubic meter (kg/m³).

With the weight of explosives per stope and with the stope size dimensions, the powder factor for the blast can be determined. The powder factor is the weight of explosives per tonne of material original in place. The powder factor serves multiple purposes, such as a guide to plan shots and an indicator for hardness of the material. The powder factor can be calculated with equation 6.4.

$$PowderFactor = \frac{Q}{W * L * H} \quad (6.4)$$

Where,

H: Height of stope in meter (m).

The other consumables that are used for blasting are detonators, boosters and shocktube. The usage of these consumables depends on the length and size of the borehole and are mostly standard for a certain type of borehole.

With the costs for each individual process known, the overall costs for drifting per meter can be determined. Or per cubic meter of material.

6.3. Mine Planning

The mine planning is based on the annual underground mining rate and mining layout. It is affected by the stability of the mine and the mining method that will be used. The maximum height of the underground stopes of mine 2 is the 500 level, due to the advance of the open pit mine. The mine planning will focus on how much material is needed and how many stopes are needed to achieved this goal. As well as the development needed to make sure that the stopes are accessible during the planned time. A drift is already created at the 460 level, which will be reviewed if it is profitable to use that drift in the coming mining plan.

6.4. Mining Method

The mining method will be selected based on the mine planning, costs and the stability assessment of the planned work. The aspects for the mining methods will be compared and the most suitable will be selected. The most suitable mining method is the method that is not too complex to use in the mine, results in reaching the production targets in the underground mine and the method that is not significantly more expensive than the other mining method. It is possible that the cheapest mining method is not always the best in the mine. To review the complexity of the mining method, the different steps of the process are compared to make sure that it is achievable.

6.5. Data Used

The data that has been used for the cost model comes from different sources. The biggest difference for data used for this part is that part of the data is acquired during the visit at the mine or during review of mine specific files, such as cost overviews. The other part of the data that is used is from handbooks or guidelines that are common in the industry. This has been done for data that was not available at the company itself, but was needed to get a comprehensive cost model. The data that was acquired from guidelines and other assumptions is given in table 6.1 with reference where the assumptions were based on. The data that is acquired from personal communication is from correspondence with a Principal Geotechnical Engineer at Vale Base Metals, who is experienced with the Vertical Crater Retreat mining method.

Table 6.1: Assumptions in Cost model

Parameter	Unit	Value	Source
Shocktube length	meter	35	based on hole length
Set up time drifter	min/hole	1	SME handbook
Cycle time mucking	sec	15	SME handbook
speed front loader	km/h	12	Caterpillar handbook
explosive length VCR	m	0.912	Personal Communication
thickness VCR slice	m	4.572	Personal Communication
consumables for equipment			
drill rig: lubricants	liter/hour	0.89	costmine handbook longhole rig 3.0 to 6.5 in
drill rig: track	number/hour	0.002	costmine handbook longhole rig 3.0 to 6.5 in
drill rig: electricity	kWh/hour	100.55	costmine handbook longhole rig 3.0 to 6.5 in
drill rig: maintenance	labour hour/hour	0.42	costmine handbook longhole rig 3.0 to 6.5 in
explosive truck: diesel	liter/hour	15.13	costmine handbook ANFO loading truck
explosive truck: lubricants	liter/hour	0.49	costmine handbook ANFO loading truck
explosive truck: tires	number/hour	0.017	costmine handbook ANFO loading truck
explosive truck: maintenance	labour hour/hour	0.28	costmine handbook ANFO loading truck
drifter: electricity	kWh/hour	77	costmine handbook 2 boom jumbo 6.1x8.3
drifter: lubricants	liter/hour	0.63	costmine handbook 2 boom jumbo 6.1x8.3
drifter: tires	number/hour	0.00053	costmine handbook 2 boom jumbo 6.1x8.3
drifter: drilling bits	number/hour	0.1125	costmine handbook 2 boom jumbo 6.1x8.3
drifter: drilling rod	number/hour	0.05	costmine handbook 2 boom jumbo 6.1x8.3
drifter: maintenance	labour hour/hour	0.35	costmine handbook 2 boom jumbo 6.1x8.3
loader: gasoline	liter/hour	45.62	costmine handbook 9.3 cu yard wheel loader
loader: lubricants	liter/hour	1.05	costmine handbook 9.3 cu yard wheel loader
loader: tires	number/hour	0.002	costmine handbook 9.3 cu yard wheel loader
loader: bucket teeth	number/hour	0.01	costmine handbook 9.3 cu yard wheel loader
loader: maintenance	labour hour/hour	0.33	costmine handbook 9.3 cu yard wheel loader
support vehicle: gasoline	liter/hour	15	costmine handbook utility vehicle UG
support vehicle: lubricants	liter/hour	0.313	costmine handbook utility vehicle UG
support vehicle: tires	number/hour	0.018	costmine handbook utility vehicle UG
support vehicle: maintenance	labour hour/hour	0.13	costmine handbook utility vehicle UG

Part IV

Results & Discussion

Fieldwork & Laboratory testing

The results from the fieldwork and the laboratory testing will be given in this chapter. First, the results from the fieldwork will be given and after that the results of the laboratory testing. The fieldwork results consists of two rock mass classifications and a scanline survey. The rock mass classification results are shown in table form, and the scanline survey with the program DIPS from Rocscience.

7.1. Fieldwork

The results from the rock mass classifications are given in tables 7.1, 7.2 and 7.3. Table 7.1 shows the results for the rock mass classification for the two classifications that have been performed. These results are acquired following international standards (Ulusay & Hudson 2007) (Ulusay 2015) and Sibelco standards and spreadsheets (Schmitz 2016). The first parameters are giving information about the excavation type and the quality of the excavation work. With the disturbance class for Mine 2 Stope 1 being 0.25 and for the drift 460 level 0.4. The next section of the table shows the information that was collected by of the joint sets and of the block shape. The last section of the table shows strength and other parameters. The rock strength is given in the qualification R4 which means a strong rock, the specimen requires more than one blow of geological hammer to fracture it. The stress reduction factor is given in G for the first classification and in H for the second. G means competent mainly massive rock with medium stress with favourable stress conditions. H means competent mainly massive rock with high stress and a tight structure. The weathering grade 1A means that there are no visible signs of rock weathering. The results for both locations is quite similar, although both locations are located 100 meter above each other.

Table 7.1: Results from the fieldwork for three locations

Parameter	Unit	Mine 2 Stope 1	Drift 460 Level
Rock type	-	Nepheline Syenite	Nepheline Syenite
dip	degree	90	89
strike	degree	10	226
width outcrop	m	7.5	4.8
height outcrop	m	6.10	5
Opening type	-	Tunnel intersection	Tunnel intersection
Method of excavation	-	Drill & Blast	Drill & Blast
Half barrels	-	no	no
Blasting Influence	-	Not Affected	Not Affected
Disturbance Class	-	0.25	0.4
joint set number	#	4	3
volumetric joint count	# joints per m^3	10	11
Observed mode of failure	-	slabbing	wedge failure
block shape	-	flat block	long or flat block
block shape longest dimension	m	0.6	1.5
block shape shortest dimension	m	0.16	0.2
Mi	-	28	27
GSI	-	70	75
Rock strength	-	R4	R4
Groundwater	-	completely dry	completely dry
Stress reduction factor	-	G	H
weathering grade	-	1A	1A

The results for the joint sets and Schmidt hammer tests of Mine 2 Stope 1 and for the drift level 460 can be found in table 7.2 and table 7.3. The Schmidt hammer results are the first part of the table, with results from a Schmidt hammer ranging from 0 to 100. The values of the hammer correlated to strength values are given in the table as well. The relation between the value of the Schmidt hammer and the strength value is based on research by Saptono et al. 2013. In the other part of the table, the joint properties are discussed. The joint roughness number, joint roughness coefficient and joint roughness profile are ways to describe the roughness of the joint. The three ways are used, to allow for comparison of results for different methods used. The results for the roughness are approximately the same for each method. The joint alteration number is given in category B, which means that the joint is unaltered and has only surface staining.

Table 7.2: Results from joint analysis fieldwork for Mine 2 stope 1 classification

Mine 2 Stope 1					
		Joint Set			
dip direction	degree	303	65	100	219
dip	degree	89	57	50	90
Parameter	Unit	1	2	3	4
Schmidt hammer	#	100	100	88	100
Schmidt hammer orientation	degree	90	90	90	90
Schmidt hammer Strength	MPa	>200	>200	>200	>200
joint number	#	1	2	3	4
linear joint count	# joints per m	6	2	2	1
Joint roughness number	-	Rough or irregular undulating	smooth undulating	smooth undulating	smooth undulating
Joint roughness coefficient	#	11	8	14	9
Joint roughness profile	#	Rough undulating	Smooth undulating	Smooth undulating	Smooth undulating
Joint Alteration number	-	B	A	F	A
Joint spacing	m	0.07	0.66	0.3	0.09
Joint length	m	0.8	1	0.75	0.25
Joint separation	mm	0	0	<1	0
Joint infilling	#	none	none	hard	none
Joint infilling	#	0	0	<1	0
Length longer than outcrop	-	no	no	no	no
tilt test	degrees	45	45	45	45

Table 7.3: Results from joint analysis fieldwork for drift 460 level classification

Drift 460 level				
		Joint Set		
Parameter	Unit	1	2	3
dip direction	degree	359	30	225
dip	degree	69	72	84
Schmidt hammer	#	72	48	100
Schmidt hammer orientation	degree	90	90	90
Schmidt hammer Strength	MPa	>200	>200	>200
joint number	#	1	2	3
linear joint count	# joints per m	3	3	2
Joint roughness number	-	Smooth undulating	Smooth undulating	Rough or irregular undulating g
Joint roughness coefficient	#	8	9	10
Joint roughness profile	#	Smooth undulating	Smooth undulating	Smooth undulating
Joint Alteration number	-	B	B	B
Joint spacing	m	0.45	0.05	0.5
Joint length	m	1.1	0.6	0.5
Length longer than outcrop	-	no	no	no
Joint separation	mm	0	0	0
Joint infilling	#	none	none	none
Joint infilling	#	0	0	0
tilt test	degree	55	53	55

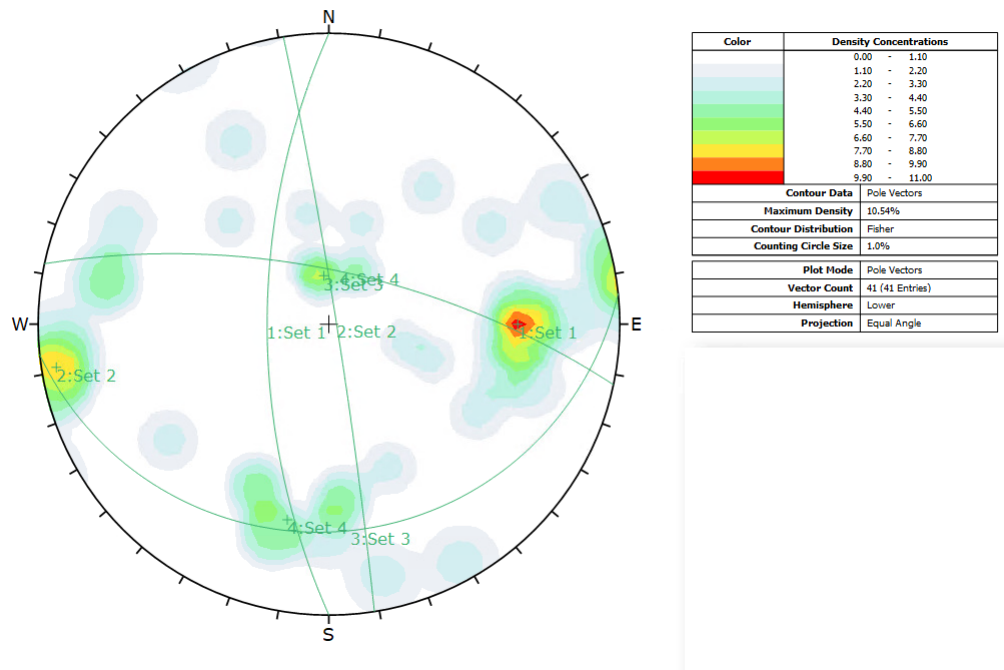


Figure 7.1: Four major joint sets that are present in the rock mass

The scanline mapping that has been performed resulted in four major joint sets that have been included into the stability analysis. The joint sets can be seen in a stereographic representation in figure 7.1, with the dip and dip direction for each joint set in table 7.4.

Table 7.4: Dip and dip direction of each joint set that has been found in the scanline mapping

set	dip	dip direction
1	66	270
2	87	81
3	19	174
4	69	12

7.2. Laboratory Testing

The results of the laboratory testing are given in table 7.5 and table 7.6. The cores that have been tested for the UCS are the largest cores that were created during the fieldwork. The cores that have been tested for the tensile strength, are cores that were smaller. The test results for the UCS test will be reviewed first. The table shows the diameter and height of each core that has been tested for the UCS test. The tests that have been performed are the sonic velocity test, the uniaxial compression test and the deformation modulus (Young's Modulus). The sonic velocity test shows a range in the velocities from 4344 m/s to 6383 m/s. The last column is the Young's modulus divided by the UCS, otherwise known as the modulus ratio. The modulus ratio ranges from 345 to 447, which is a small spread around a mean value of 398. The UCS ranges from 91 MPa to 135 MPa. The samples had a different height to diameter ratio than the recommended value. The column of UCS corrected gives the results after the correction formula has been applied. The formula is given in the chapter about rock mechanics. The UCS test for core 7 was stopped before rupture was observed, because the loading system has a limitation of 155 MPa.

Table 7.5: Uniaxial compression tests results

Sample	Diameter (mm)	Height (mm)	Density ρ (kg/m ³)	Sonic velocity V_l (m/s)	UCS R_c (MPa)	UCS Corrected (MPa)	Deformation Modulus E_d (MPa)	E_d/R_c
Core 2	39.8	54.6	2615	5009	121	115	41 750	345
Core 4	39.8	60.4	2609	4344	91	88	36 800	405
Core 5	39.8	74.7	2604	6383	135	134	56 910	420
Core 6	39.8	53.1	2639	5797	107	101	47 760	447
Core 7	39.8	75.1	2638	6108	155*	-	69 473	-
Core 8	39.8	66.0	2609	4455	119	116	44 690	376

The results of the UCS tests are also given in figure 7.2. Here the stress strain curves of the six different cores are given. The stress in MPa is plotted against the strain for the six different cores, which results in the axial stress-strain curves for the cores. There was no data for the radial strain. What can be seen from the graph is that core 5 and core 7 have a different path than the other four cores. Core 7 was the core that did not yield during the test, so it is possible that something went wrong there or there may be another reason for the high values of this test. Core 5 and core 7 are also from a different level in the mine, so it is not likely that there is a structural reason for the difference between these cores and the rest. The other four cores, are all following a path that is quite similar. Some cores are stronger than others, but the slope of the graphs does not differ significantly.

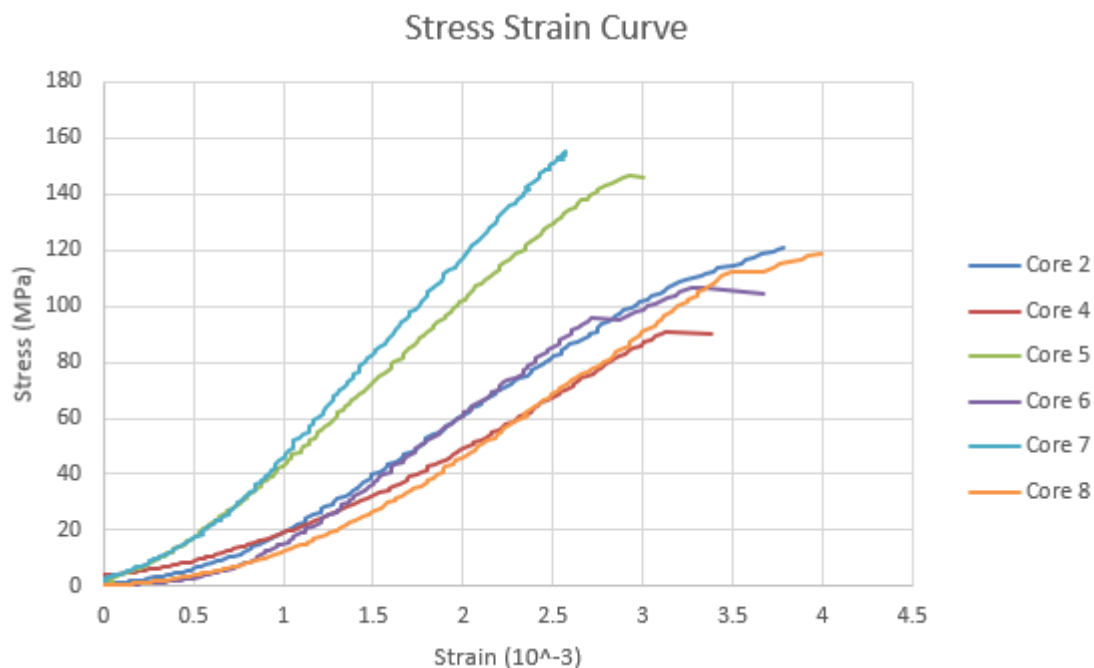


Figure 7.2: Stress strain curves for the six cores that have been tested for UCS strength by Liege University.

The Brazilian tensile strength test results are given in table 7.6. The tests have been performed on three samples with a height diameter ratio less than 1. The density values for these samples are slightly lower than for the samples of the UCS test. The same trend can be seen with the results for the sonic velocity tests, the values for the samples used in this test are slightly lower than for the UCS test samples. The tensile strength of the material ranges from 7.38 MPa to 13.66 MPa.

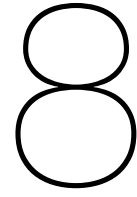
Table 7.6: Brazilian tests results

Sample	Diameter (mm)	Height (mm)	Density ρ (kg/m ³)	Sonic velocity V_l (m/s)	Brazilian strength (MPa)
Core 1-a	39.8	24	2583	4948	7.38
Core 1-b	39.8	32.1	2592	4686	13.66
Core 3	39.8	23.6	2525	4677	11.88

7.2.1. Historical Data Comparison

In this section, the differences between the data acquired during testing and with the historical data are given. The sonic velocity of all the samples is spread out over a large range. This range can be compared with historical data acquired. The sonic velocity should be not dependent on size of the sample that is tested. The smaller cores, which were used for the Brazilian test, have a sonic velocity of 4677 m/s to 4948 m/s. The larger cores, that were used for the UCS testing, show a sonic velocity of 4344 m/s to 6383 m/s with an average of 5349 m/s and a standard deviation of 15%. The value that was acquired in the historical tests for the sonic velocity is 5359 m/s with a standard deviation of 3%. The samples they have tested show results that are clustered together and do not have large outliers. The average values for the sonic velocity are almost the same.

The values for elastic modulus from the historical tests are significantly higher than the results from testing. The results from testing range from 36.8 GPa to 69.5 GPa, with an average value of 49.4 GPa and a standard deviation of 22%. The results from the historical tests give an average elastic modulus of 61 GPa with a standard deviation of 11%. The results for the UCS testing show values ranging from 88 MPa to 134 MPa, with an average value of 121 MPa and standard deviation of 17%. The historical test results show an average value of 135 MPa and standard deviation of 29%.



Stability Analysis

The results of the stability analysis will be shown in this chapter. The stability analysis consists of multiple parts and first the results of the stability graph method will be given. After which the results for the numerical model will be shown. The results for the justification of results with the Kirsch solution is given at the end of this chapter.

8.1. Stability Graph

The stability graph method is used for different areas in the mine, for a stope size with the highest level of stress, for different layout stopes of stope 5 and to test if the method is working with a new workshop at a higher level. The first step of the method is the calculation of the factors A, B, C, Q' and N. Table 8.1 gives the results for the Mine 2 stope and the new workshop.

Different options for stope 5 are discussed in this part of the thesis. Option A is a long and small stope, with a width of 10 meter and the original height and length. The width is set to 10 meter so there is room for an additional pillar in the original stope. Option B is to keep the width and height of the stope the same as the normal stopes, but to change the length to 27.5 meters, so that there is room for a pillar in the middle of the stope.

Table 8.1: Results of the stability graph method for the mine 2 stope and for the new workshop

Parameter	Unit	Mine 2 Stope		New Workshop
		Roof	Hanging Wall	Roof
Induced Stress	MPa	14	18	5
UCS	MPa	120	120	120
Ratio	-	8.6	6.6	24
Factor A	-	0.8	0.6	1
Critical Angle	degree	54	46	44
Factor B	-	0.65	0.51	0.44
Mode of failure	-	Gravity Fall	Gravity Fall	Gravity Fall
dip of stope	degree	70	70	90
Factor C	-	5.8	5.8	8
RQD	-	69	69	70
J_n	-	12	12	12
J_r	-	3	3	3
J_a	-	1	1	1
Q'	-	8.8	8.8	8.8
N	-	26.4	15.5	31.1

The parameters and results for the calculation of the stability number are given in table 8.2 for different layouts of stope 5. The different layouts of stope 5 will have the same parameters for the calculation of the stability number. The parameters for the rock quality, stresses and the joint properties do not change, so the stability number will be the same. The difference with the different layouts is the hydraulic radius.

Table 8.2: Results of the stability graph method for two variations of stope 5

Parameter	Unit	Stope 5	
		Roof	Hanging Wall
Induced Stress	MPa	14	18
UCS	MPa	120	120
Ratio	-	8.6	6.7
Factor A	-	0.3	0.64
Critical Angle	degree	54	46
Factor B	-	0.65	0.51
Mode of failure	-	Gravity Fall	Gravity Fall
dip of stope	degree	70	70
Factor C	-	5.8	5.8
RQD	-	69	69
J_n	-	12	12
J_r	-	3	3
J_a	-	1	1
Q'	-	8.8	8.8
N	-	26.4	17.6

The Hydraulic radius of the different stope layouts can be calculated with the dimensions of the stopes. The results for the four different stopes are shown in table 8.3. The calculation for the hydraulic radius differs for the hanging wall and the roof.

The table also shows the results of the stability graph method, in which zone the stope falls. The first three stope options are reviewed with the stability graph for unsupported excavations. The new workshop has been evaluated with the stability graph for cable bolting, because bolting has been applied in the new workshop area. Most of the stopes fall in the stable zone. However, the hanging wall of the stope mine 2 falls in the transition zone. This is also the case for the hanging wall of stope 5 option A. Both cases that fall in the transition zone are due to a high hydraulic radius in combination with a lower stability number than the other cases.

Table 8.3: Hydraulic radius calculations for the different stability graph versions that have been performed.

Parameter	Unit	Stope Mine 2		Stope 5 Option A		Stope 5 Option B		Workshop
		Roof	Hanging wall	Roof	Hanging wall	Roof	Hanging wall	Roof
Dip	degree	90	70	90	70	90	70	90
Height	m	50	50	50	50	50	50	16
width	m	27	27	10	10	27	27	27
length	m	60	60	60	60	27.5	27.5	60
HR	m	9.31	13.64	4.29	13.64	6.81	8.87	9.31
N'	-	26.4	17.6	26.4	17.6	26.4	17.6	31.1
Zone	-	Stable	Transition	Stable	Transition	Stable	Stable	Stable

8.2. Numerical Model

The results for the numerical model will be given in this section. The first step is the design of the model. After which the results of the model will be shown.

The model is given in figure 8.1 and in this figure the layout of all structures in the model is shown. One of the first things that is visible in the figure are the two faults that are present. These faults are the orange and brown lines that run through the whole figure. The stopes left of the barrier pillar are the old stopes (Mine 1) and the stopes right of the barrier pillar are the new stopes (Mine 2). The pinching shape at the bottom right is the primary processing and blending location. The stopes of Mine 1 and Mine 2 consist of an outer dark blue line, which represents a final stage of the stope. The green lines in the stopes are the different stopes itself. The stopes have been simplified to make sure that the numerical model was able to compute. The real layout is that the stopes of Mine 1 that retreat upwards are connected so that the material from the top right stope still falls to the lowest level. This is the same case for stope 5 of Mine 2, the inclined part of the stope is modelled, however it is not excavated in this model. Furthermore, the large stopes (the most left one in the figure) is a stockpile stope for the raw material from the open pit. However, it used to be two smaller stopes, but the pillar in between those two stopes (partly) collapsed. To make it possible to model this, a small pillar is left in place. Why the inclined parts are modified, will be explained later in this thesis. The green box around the primary processing location is a material boundary and that will be explained later on in this thesis.

Some areas of the model are less relevant for this thesis as other areas, which is why for some results the focus will be on the area around mine 2 and the barrier pillar. It was necessary to recreate the whole mine in the model and not only partly, because of the effects of all excavations on the stress distribution.

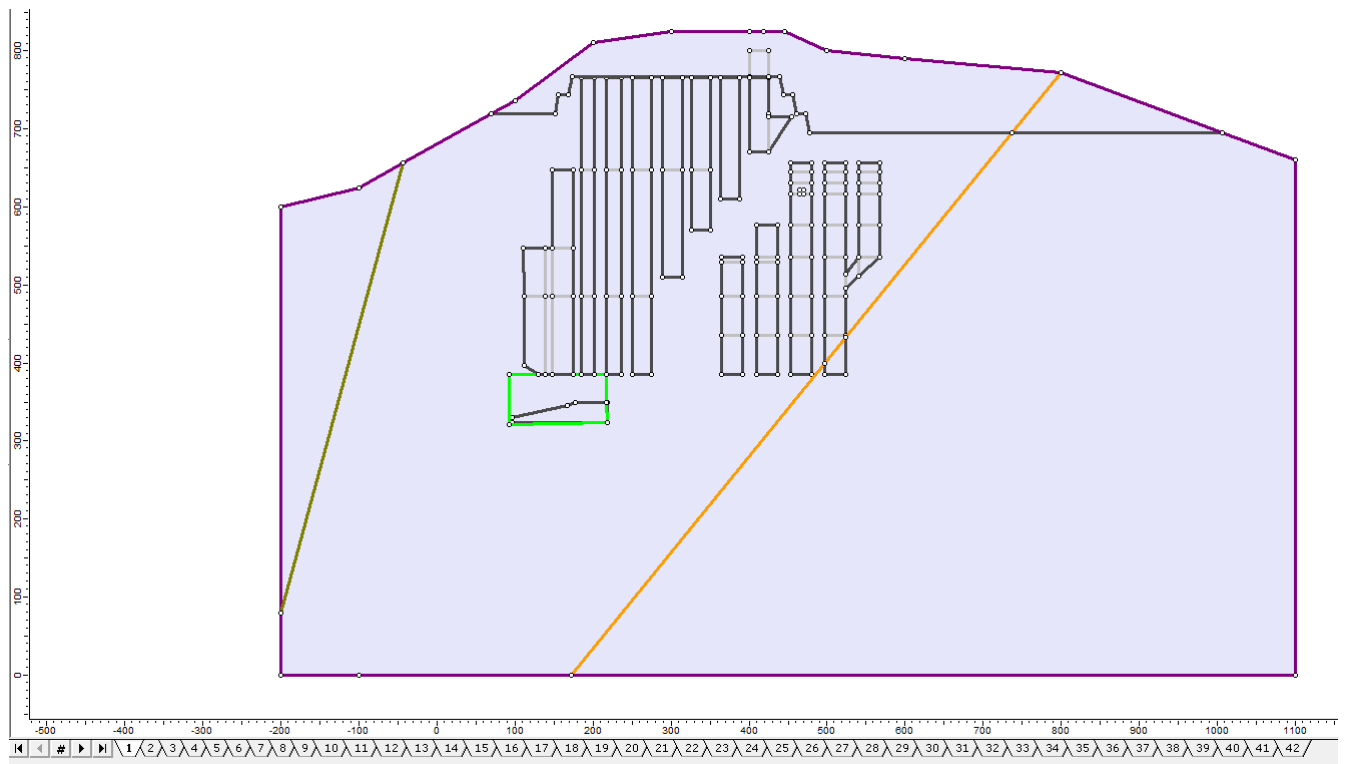


Figure 8.1: The layout of the numerical model. With Mine 1, Mine 2, the primary processing and faults.

8.2.1. Stages

As can be seen in the bottom of figure 8.1, this model consists out of 42 stages, with each stage being a step in the development of the mine. The first step is to calculate the stress distribution without the mine present (nothing excavated). The following steps are to slowly excavate all the stopes in the right order to come to the current situation. The stopes of Mine 1 are excavated in smaller stages than modelled, to make sure the model did not become too large. The first stage is the whole model, without any excavations, given before in figure 8.1. The following eight stages are shown in figure 8.3. Stages

2 to 7 are stages in which Mine 1 is excavated. Stage 8 is the first stage that has material back in the stopes. At these early stages, the material is raw material, which has fallen down from the top of the stopes to the bottom of the stopes. This raw material is modelled as loose material. In stage 9, the primary processing plant location is opened up. This cavern has an elongated shape that pinches at the end, at which it is connected by drifts to the surface of the island. The next eight stages are stage 10 to stage 17 and can be found in figure 8.4. These stages continue the development of Mine 1 and the stopes being filled with material during excavation. What has not been modelled is that change of material when the stopes are fully developed. If the stopes are fully developed, such as in stage 11, the raw material is drawn from the bottom of the stope, the exit has been blocked and the stopes are being filled with waste material from the open pit. At stage 14, the material around the primary processing location has been set to elastic. Stages 12 to 18 show the progress of the development of Mine 1. Stage 18 to stage 25 are given in figure 8.5 and stages 26 to 33 are given in figure 8.6.

At stage 18, the development of Mine 1 is complete and at stage 19 the first stope of Mine 2 is created. The development of Mine 2 continues through stage 20 to 34. Stage 29 shows the development of the first slice of the stope, which is modelled as the stope with lower parameters. In stage 30, the same parameters as stage 29 are set for stope 1 of mine 2. At stage 31, the middle slice of stope 1 of mine 2 is blasted which causes the material qualities to decrease even further. The stages 32, 33 and 34 are build in to make it possible to adjust the stopes that are left in place in this example. After this stage, the mine is at the current situation. Stages 34 to 41 are given in figure 8.7 and stage 42 is given in figure 8.8. Stages 35 to 42 show the development of the future stopes.

Figure 8.2 shows the name of each modelling material that has been used. The N.S. stands for Nepheline Syenite.

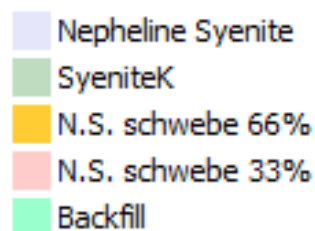


Figure 8.2: The different modelling materials that are used.

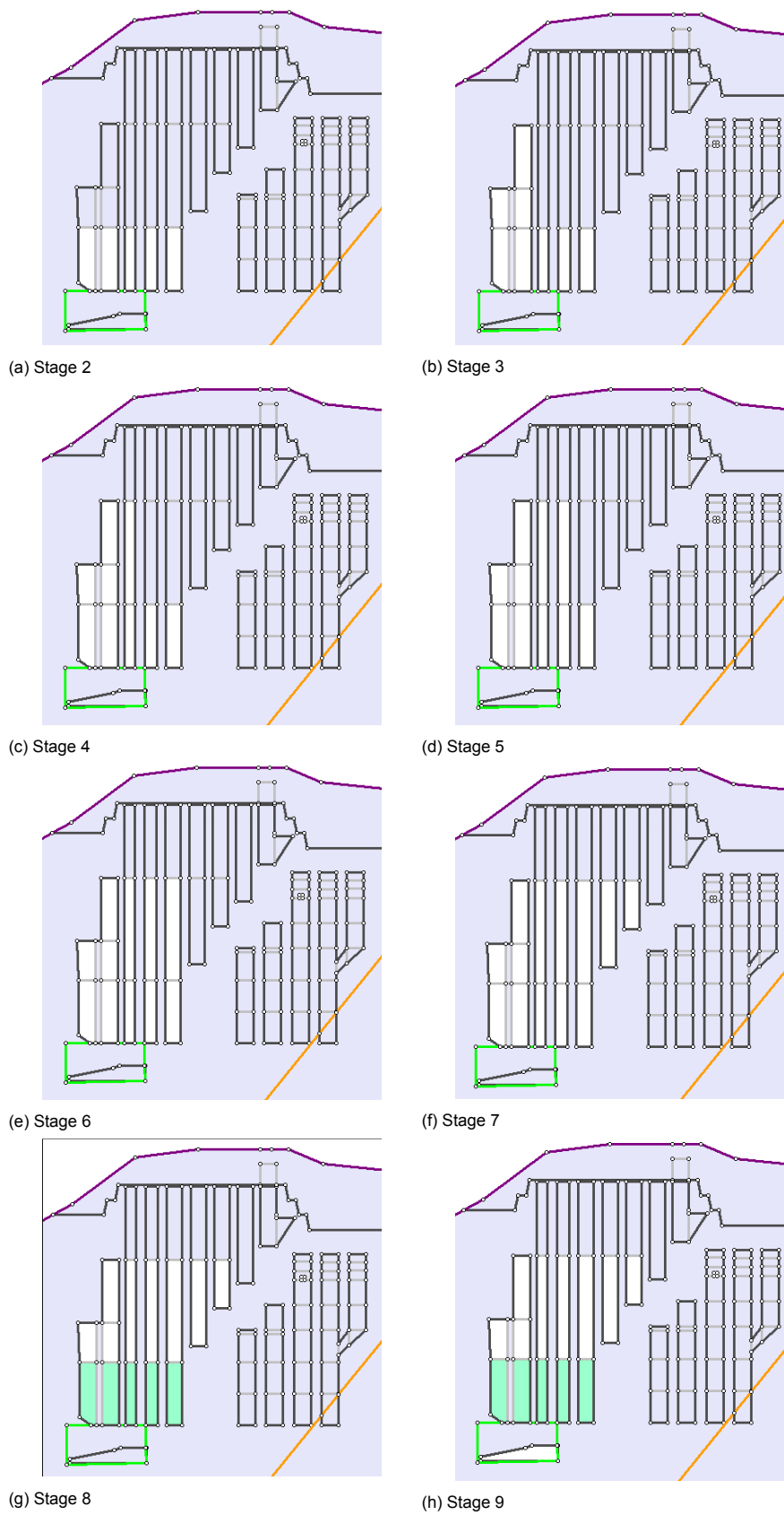


Figure 8.3: Stages 2 to 9 show the development of the model

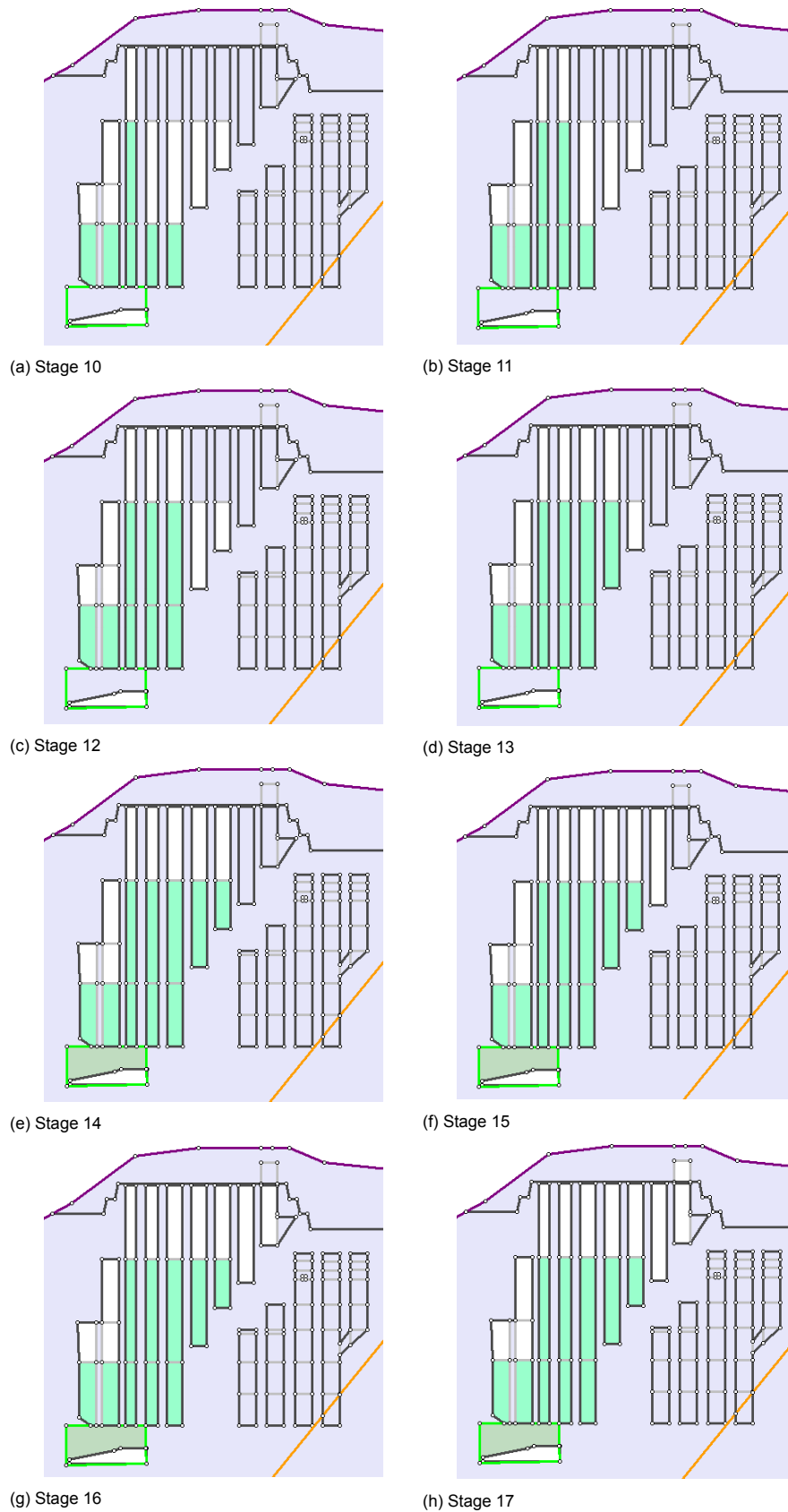


Figure 8.4: Stages 10 to 17 show the development of the model

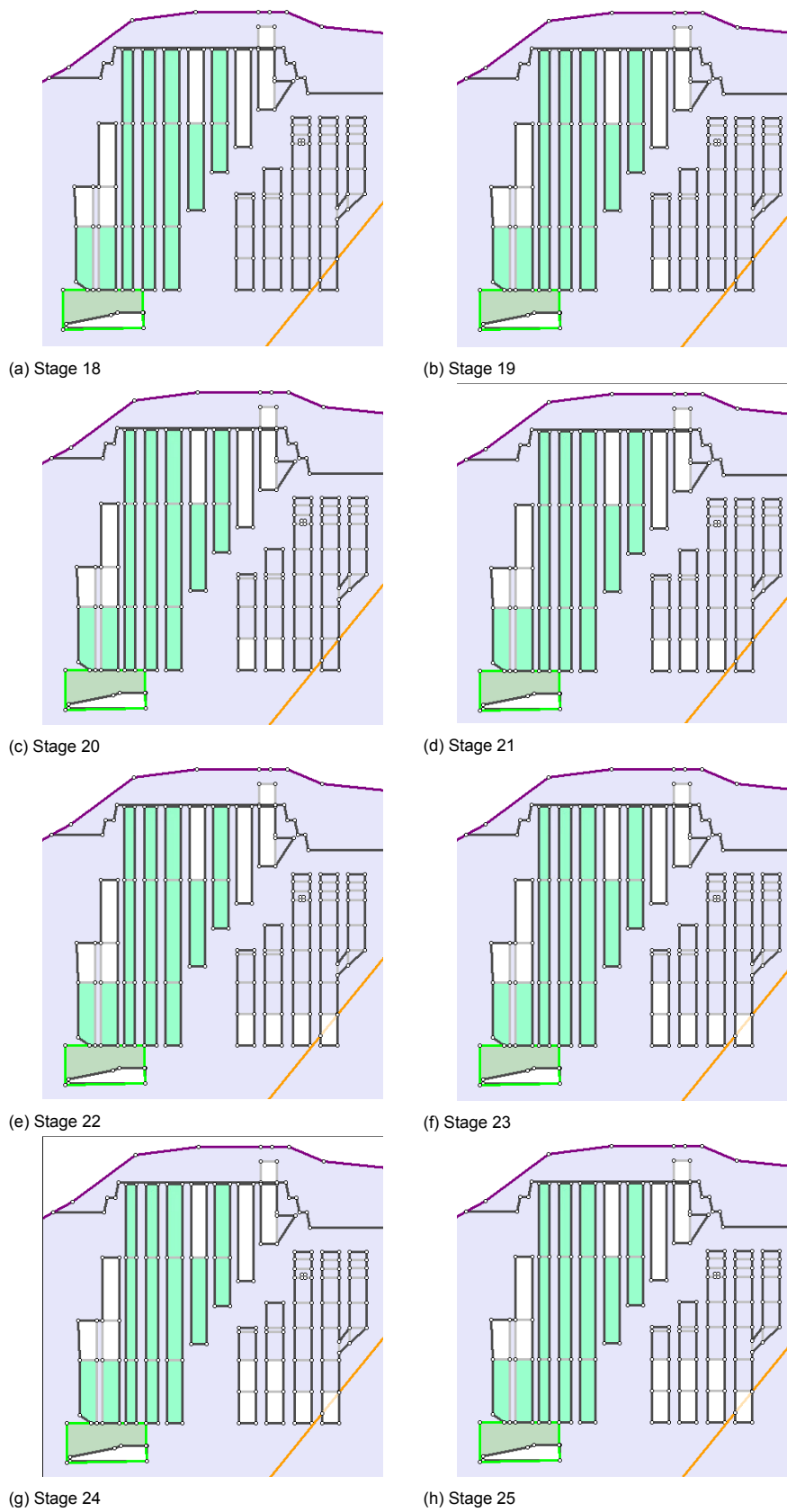


Figure 8.5: Stages 18 to 25 show the development of the model

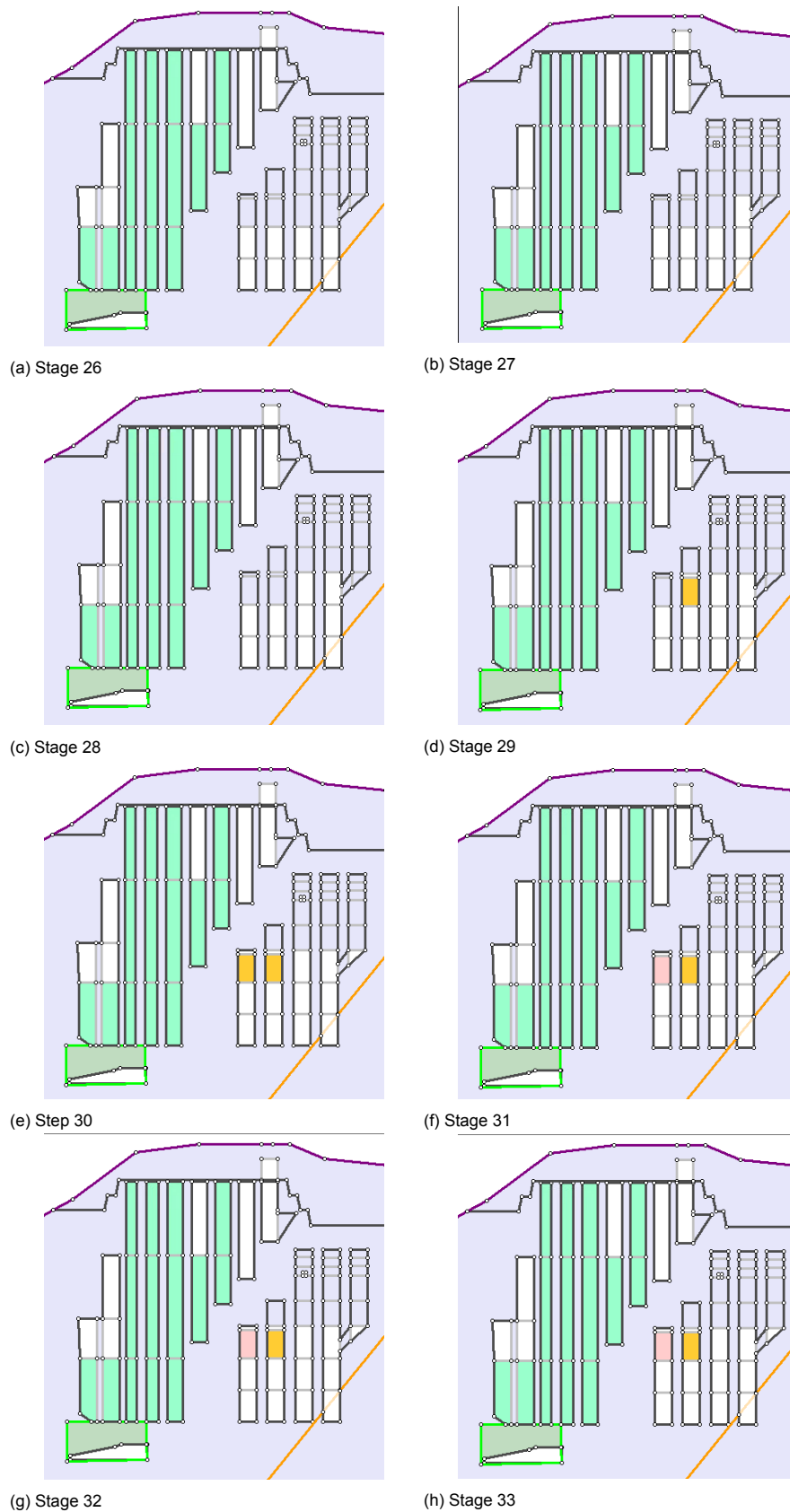


Figure 8.6: Stages 26 to 33 show the development of the model. At stage 29 the first part of slope 2 is blasted. At stage 30, the first part of slope 1 is blasted, and at stage 31, the second part of slope 1 is blasted. This is modelled like this to recreate the current situation.

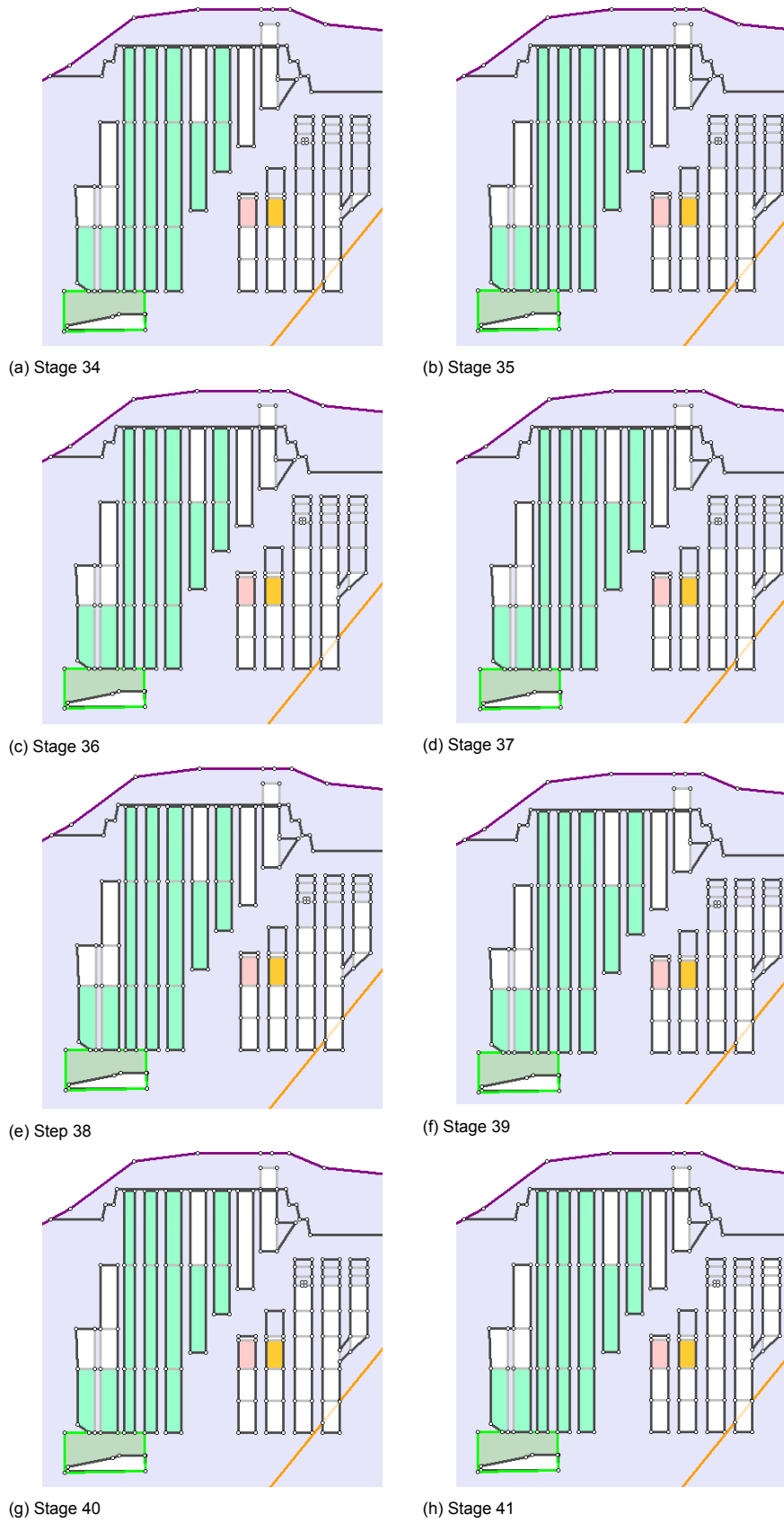


Figure 8.7: Stages 34 to 41 show the development of the model

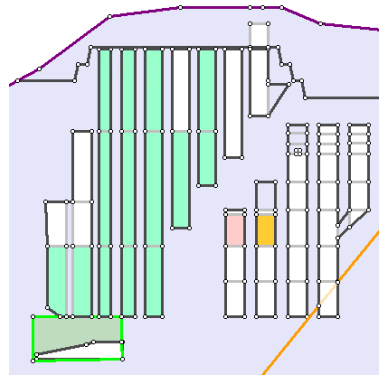


Figure 8.8: Stage 42

8.2.2. Mesh

The discretization and the mesh that has been used for the model is shown in figure 8.9. The mesh consists out of 6465 elements that are focused around excavations. The areas with the highest density of elements is around Mine 1 and Mine 2 and the primary processing location. The other areas, are of lesser interest for this thesis. That is why the density is lower in that area, if those areas had the same density as around the excavations, the model would take significantly longer computation time.

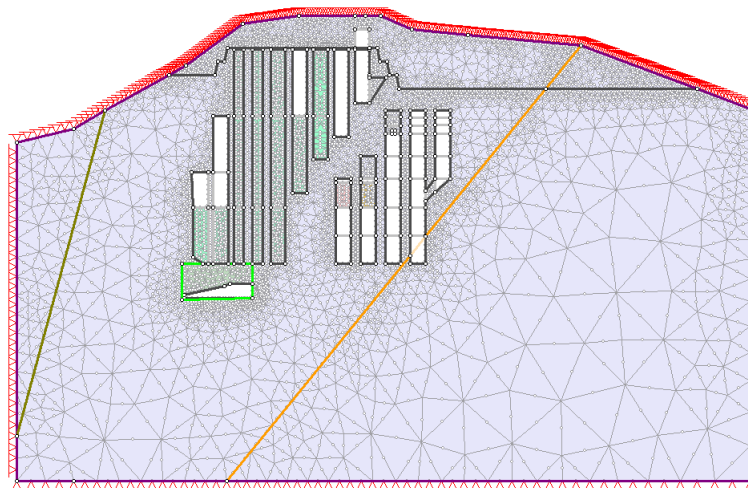


Figure 8.9: Model with discretization and mesh.

8.2.3. Stress Distribution

The stress distribution of the model before any excavation work is done is given in figure 8.10 with the stress in MPa. The stress contours follow the topography of the model. At the top of the model, the stress becomes zero. At the bottom of the model, at the highest point of stress, the stress is 26.10 MPa. For some unknown reason, the outline of the primary processing location is partly not present on this figure, however when zoomed in the whole outline is visible. The stress distribution before all the excavation work has been given to make sure that the stress field behaves naturally. The next step that was done to check the stress distribution was when Mine 1 was partly developed. Stress measurements from SYNTEF research showed different stresses at certain levels. The stress levels that are shown in table 8.4 and in appendix 14.1 are very close to the stress levels that were measured in the 1970's by SYNTEF.

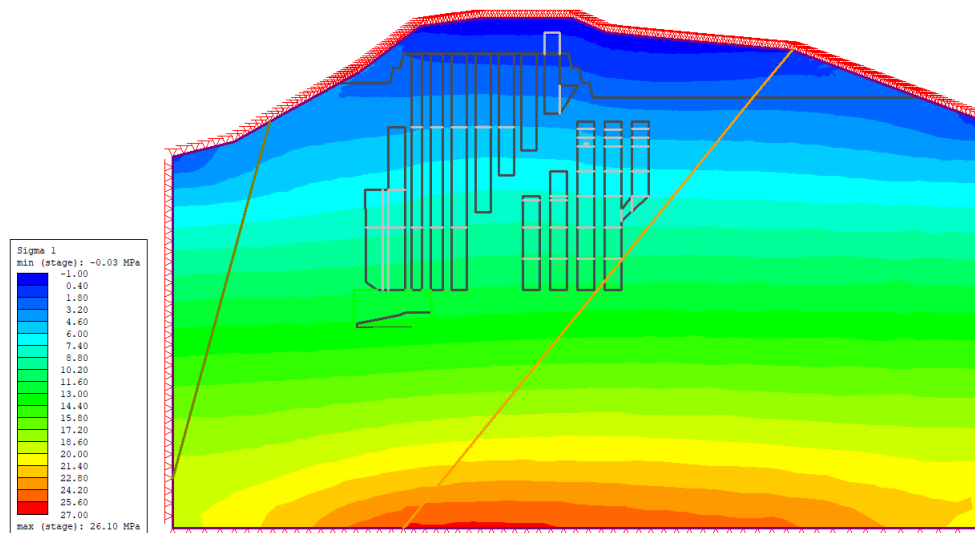


Figure 8.10: Sigma 1 Stress distribution in the model before all excavation work.

Other points that were used to determine if the model represented the actual stress field were in the top of stope 1 of mine 2, and in a tunnel at the 460 level. The tunnel has been modelled in the model at the top of stope 3 of mine 2. Flat jack tests were performed at these locations according to the internal Sibelco standard (Schmitz & Bergtes 2020). Furthermore, above the location of the primary processing, evidence of high stress levels are visible. This is mostly seen as spalling of the rock in the tunnel wall and in a pillar. This indicates that the stress is high at these points. The stress level for these areas are given in table 8.4. The first column has been discussed above and for the top of stope 1, the values are close to the measured values. The rest of the values in the table are all modelled values. The modeled values do not differ that much from the measured values. For the values above the processing location, they are expected to be this high if spalling failure has been found.

Table 8.4: Stress testing historical values to be used to validate model.

Parameter	Unit	Measurement 1970's location	Top stope 1	Top stope 3	Above processing location
vertical stress	MPa	10.70	30.6	6.9	72.26
horizontal stress	MPa	6	4.8	2.10	15.25
out of plane stress	MPa	17	18.5	8.25	32.3

The stress values for the top of stope 3, in the drift at the 460 level, are not correlating with the results of the flat jack measurements. The first thing that should be noted is that the flat jack tests are tests in the tunnel wall, which will have a higher stress than far field stress values. This can be compensated by using the Kirsch equation, which allows for the calculation of far field stresses from measurements in the tunnel wall. However the compensation of the values from the model do not reach the values that were measured. The attempt to back calculate the stresses with the shape factor of $A=1.8$ and $B=3.9$, see figure 8.11, did not give the correct results. The results are for the maximum roof stress 8.4 MPa and for the maximum sidewall stress 15.4 MPa, which is significantly lower than the measured values.

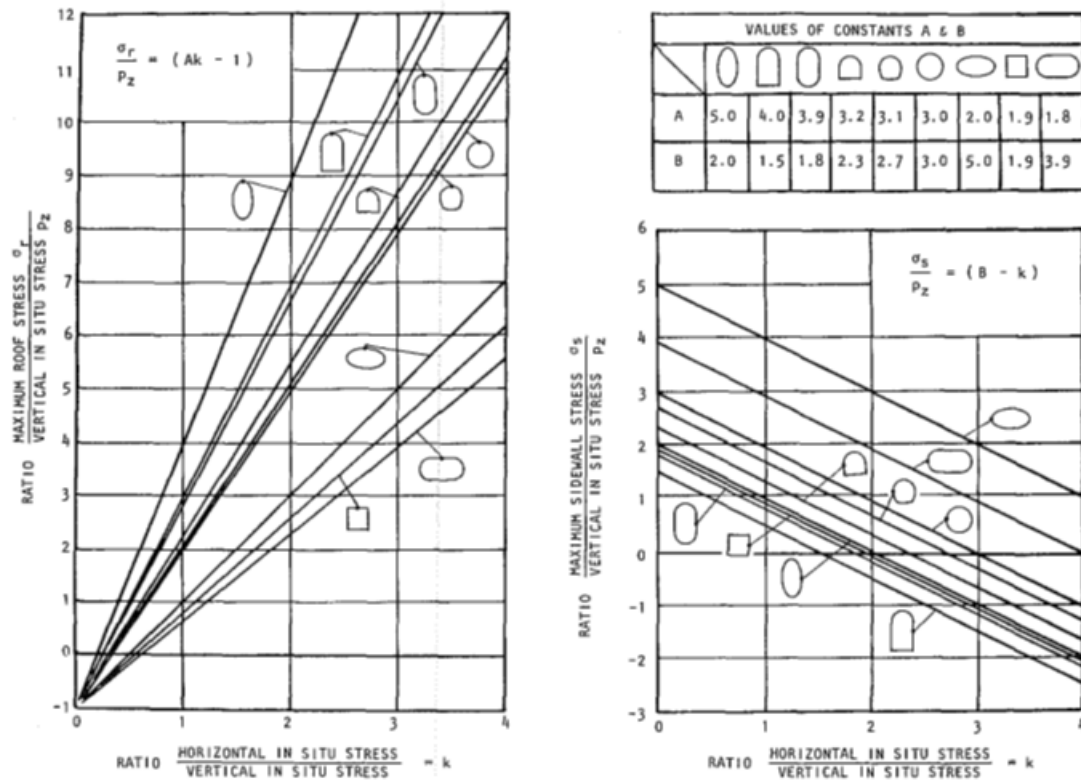
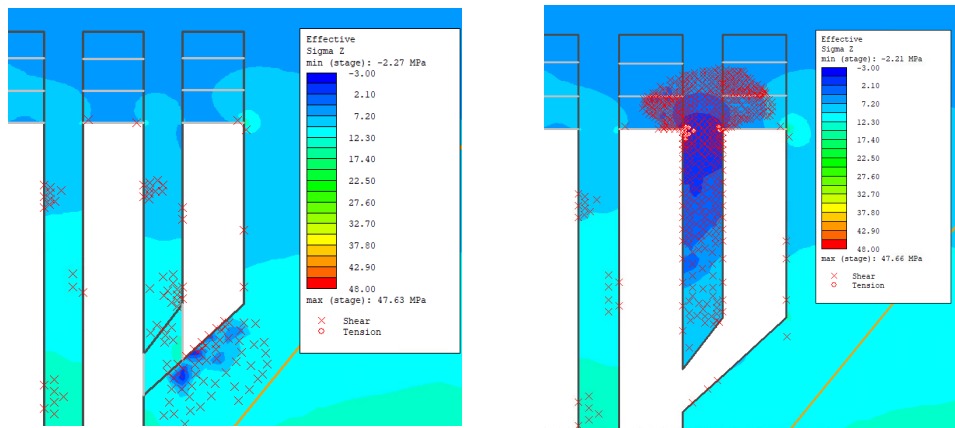


Figure 8.11: Kirsch variation that was used to calculate the stress with a different tunnel shape.

8.2.4. Stope Connections

The reason why there is a difference in the model and the real layout of the mine with aspect to the connection of the lower parts of the stopes is that it becomes unstable in the two-dimensional model. Figure 8.12 shows the scenario what happens in the stopes are connected at the bottom between stope 4 and stope 5 of mine 2. In the figure, the yielded elements are also shown. The yielded elements can be divided into two different categories, the shear yielded elements, which are shown by a cross, and the tension yielded elements, which are shown as a white circle. This is the same situation for part of Mine 1, where some stopes are connected to each other by chutes as well. What can be seen in (b) is that the amount of yielded elements is increased compared to the number of yielded elements in (a). The number of yielded elements is increasing massively in the pillar in (b) However, the number of yielded elements below the pillar is less than in (a). Which is logical, because the stress cannot flow through the pillar anymore and therefore it does not impact the area below the pillar and the stope. This increasing in yielded elements causes a non-convergence in the model, which means that it is not a stable option.



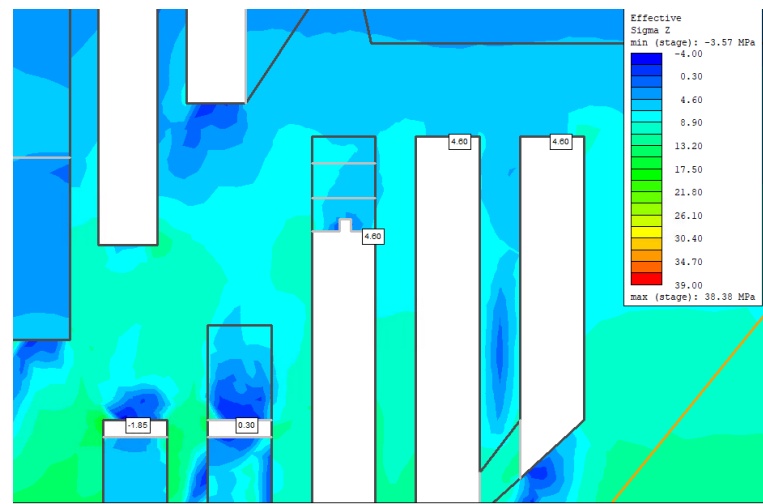
(a) The stopes when they are not connected. Also shown are the yielded elements in this part of the model. (b) The connected stopes with a chute. The yielded elements in this part of the model are also shown.

Figure 8.12: The yielded elements in the pillar between stope 4 and stope 5 of Mine 2.

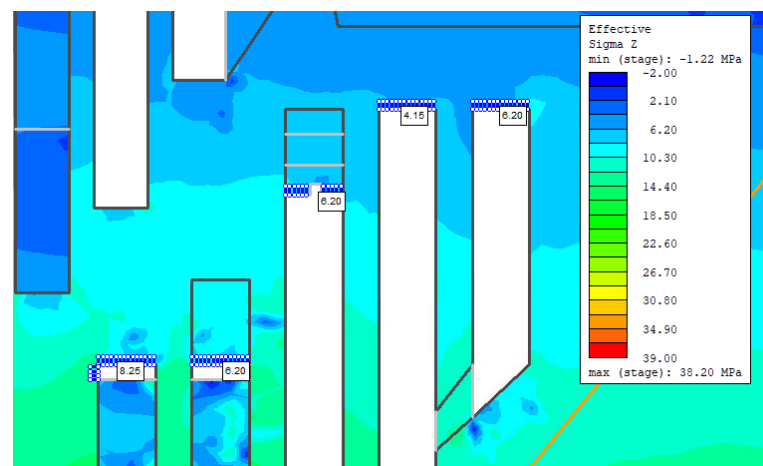
8.2.5. Effect of Bolts

The effect of bolting on the stability has also been modelled. The bolts that are used in the model are four meter long and have a spacing of 2 meter and a out-of-plane spacing of 1 meter. The bolts have been placed in the final stope form in the top of each stope and in stope 1 the side towards the barrier pillar to strength the pillar. Figure 8.13 shows the out-of-plane stress for two scenarios; one without bolts (a) and one with bolts installed in the areas that have been stated (b). The bolts are the blue lines that are visible in (b). The bolts that are used in this model are 19 mm end anchored bolts with a bolt modulus of 200 GPa.

The effect of the bolts on the top of stope 1 is that without the bolts, there is a 1.85 MPa tension in the roof of the stope. However, with the bolts installed, the tension in the roof of the stope is converted into a stress of 8.25 MPa. The stress in the sidewall of the top of stope 1 is decreasing after the installation of the bolts. The stress drops from 29.05 MPa to 25.45 MPa. The effect of the bolts in the top of stope 2 is that the stress of 0.30 MPa (without bolts) is increased to 6.20 MPa (with bolts). The same effect can also be seen in the top of stope 3, 4 and 5. The effect of the bolts in the top of stope 1 and 2 is also that the area of tensile stress is very small or not existent at all.



(a) Without bolts



(b) With bolts

Figure 8.13: The effect of bolts on the stress distribution around the stopes.

8.2.6. Strength Factor Evaluation

One way to evaluate the effects on stability of the different options, is to evaluate the strength factor of the material. This is an option that can be set in RS2, so that it displays the strength factor of that element. Sigma 1, Sigma 3 and Sigma Z have an influence on the strength factor, which makes this strength factor a three dimensional factor. The strength factor is the rock strength (based on failure criteria) divided by the principal stresses.

From now on, the focus of this results section lies on the effects on mine 2 and the changes that have been made in Mine 2. If some changes were made in Mine 1 or somewhere else, this will be stated clearly. The effect of removing the schwebe (the part of the stope that has not been produced yet) of stope 1, stope 2 and the top stopes of stope 2 and stope 3. will be first assessed. Three models will be compared for this problem. One with the schwebe of stope 1 and stope 2 left in place and with the top of stope 2 and stope 3 left in place. This will result in a production loss. The second scenario is to remove the schwebes from stope 1 and stope 2, but leave the top of stope 2 and stope 3 in place. The third model that will be given is one with everything mined out, all the stopes have been developed.

The results for the different options are given in figure 8.15, with in (a) and (b) the first option, (c) and (d) the second option and (e) and (f) the third option. The legend for this figure is given in figure 8.14. These options are compared on their last stage, with all the mining finished. What can be seen is that in (a) and (b), the area of the rib pillar has a safety factor of approximately 1 or higher. A small area has an safety factor of less than 1. In the top of the stopes, above the top slice development in stope 1 and 2, the safety factor become very large, that is due to the low stresses at these points. Subfigure (c) and (d) show the option with all the stopes fully developed. What is a difference between this option and the first option is that the area with a safety factor lower than 1 is larger and it stretches out across the whole stope. From the old stope of Mine 1, low strength areas form towards the stopes of Mine 2.

Subfigure (e) and (f) show the third option, which was to leave in only the top stopes of stope 2 and 3. The zones with a low strength factor are almost connecting the stopes of Mine 1 and Mine 2 with each other. As can be seen in the subfigures, there are more zones with a low strength factor than the first option. The difference with option two is that the low strength factor zones do not get as close to each other. However, there are more zones with a low strength factor at the top of stope 2 and there is one zone with a low strength factor at the middle of the barrier pillar at the top of stope 3.

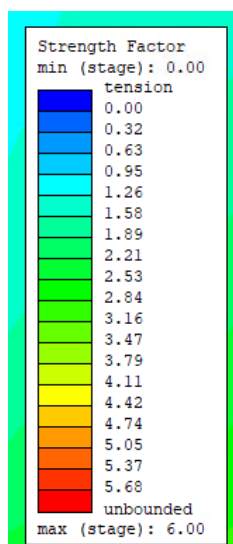
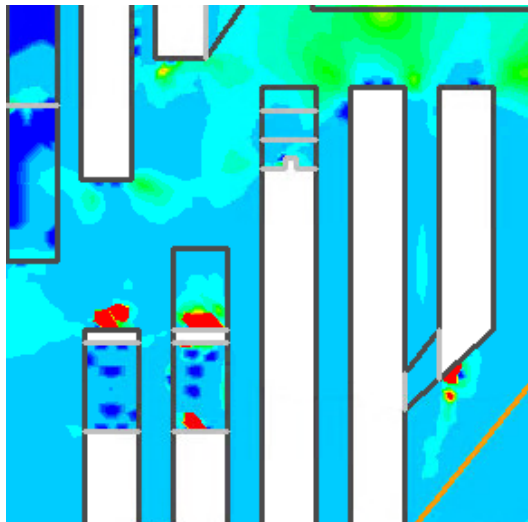
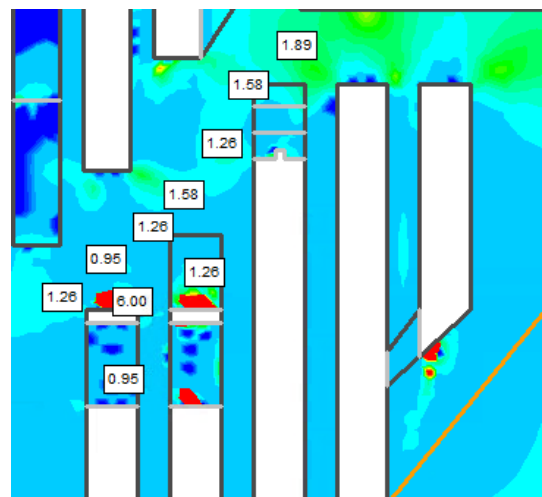


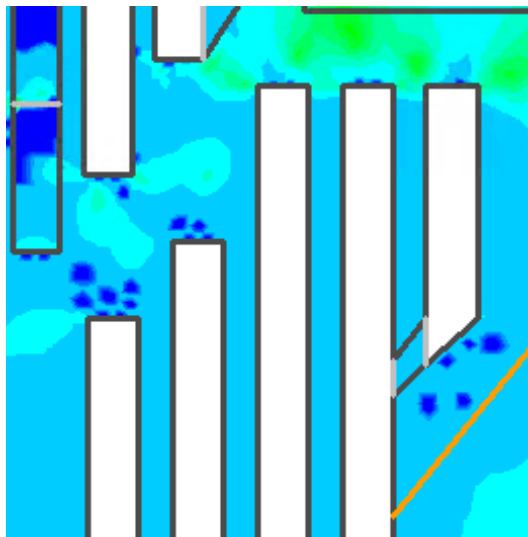
Figure 8.14: The legend for figure 8.15 and figure 8.16



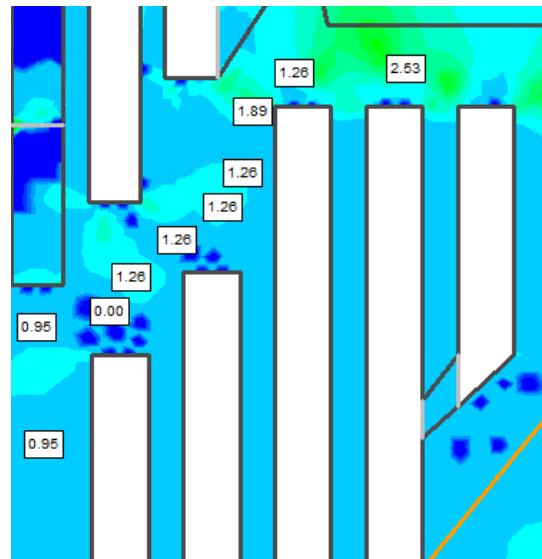
(a) First option results. Close up of the barrier pillar at the final stage.



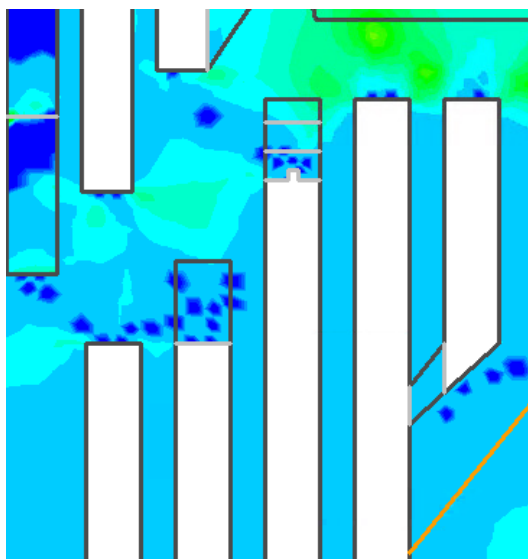
(b) First option results. Close up of the barrier pillar at the final stage with values for the strength factor at certain points.



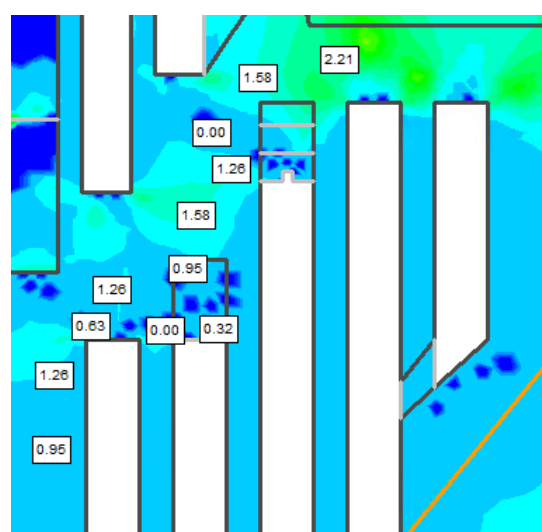
(c) Second option results. Close up of the barrier pillar at the final stage.



(d) Second option results. Close up of the barrier pillar at the final stage with values for the strength factor at certain points.



(e) Third option results. Close up of the barrier pillar at the final stage.



(f) Third option results. Close up of the barrier pillar at the final stage with values for the strength factor at certain points.

Figure 8.15

8.3. Sensitivity Analysis

The UCS strength of the Nepheline Syenite is a very important factor in the model. The effects of a lower strength than used in the initial model can be very large. To test the model, the UCS strength of the Nepheline Syenite has been changed to lower values. With these lower values, the effect on the strength of barrier pillar can be seen. The UCS strength that was used in the initial model is 135 MPa, which was based on historical data. The UCS strength that was acquired from testing, is 121 MPa, which is the strength that has been used in figure 8.16. This is a 10% decrease of the UCS. The figure shows the factor of safety for the final development step in the mine, with certain stopes left in place. What can be seen is that the area with a factor of safety of 1 or lower (see figure 8.14) is larger than with the higher UCS strength. The area of low factor of safety in (a) is quite large, it extends almost to the backfilled stopes of Mine 1. At (b), (c) and (d) the effect on the factor of safety is shown if different stopes are left in place. The difference between (a) and (b) is minimal, however with (c) the area of low factor of safety is significantly decreased. However, the number of stopes that are left in place is also higher than in (a), (b) or (d).

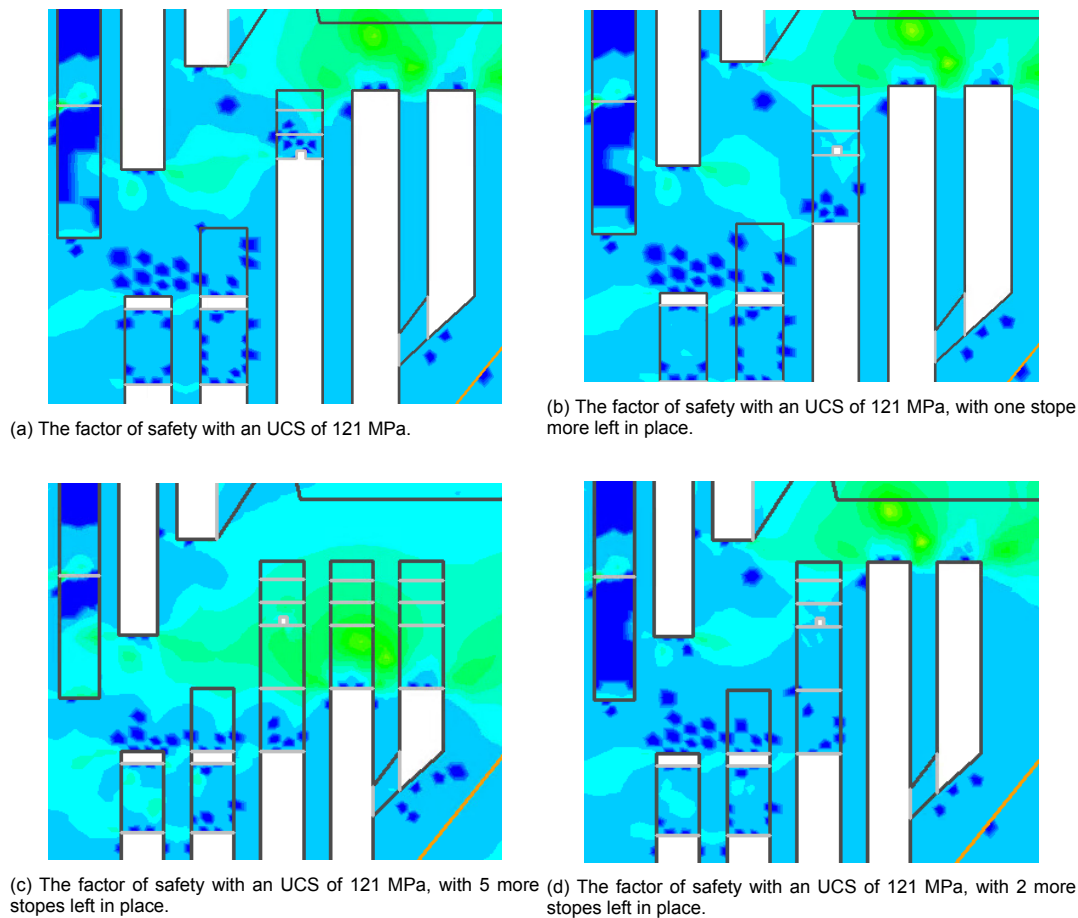


Figure 8.16: The effect of different UCS value on the factor of safety for the barrier pillar.

The next step is to decrease the strength of the material by 20%, so that the UCS is 107 MPa. The effect of this can be seen in figure 8.17. The area with a low factor of safety in (a) is larger than with a strength of 121 MPa, and significantly larger than with 135 MPa strength. What can be seen in (b), (c) and (d) is that the area of low factor of safety is significant, unless the top of each stope is left in place. This will result in a loss of ore. The difference between a UCS strength of 121 MPa and 107 MPa is less, than the difference between those two and a strength of 135 MPa.

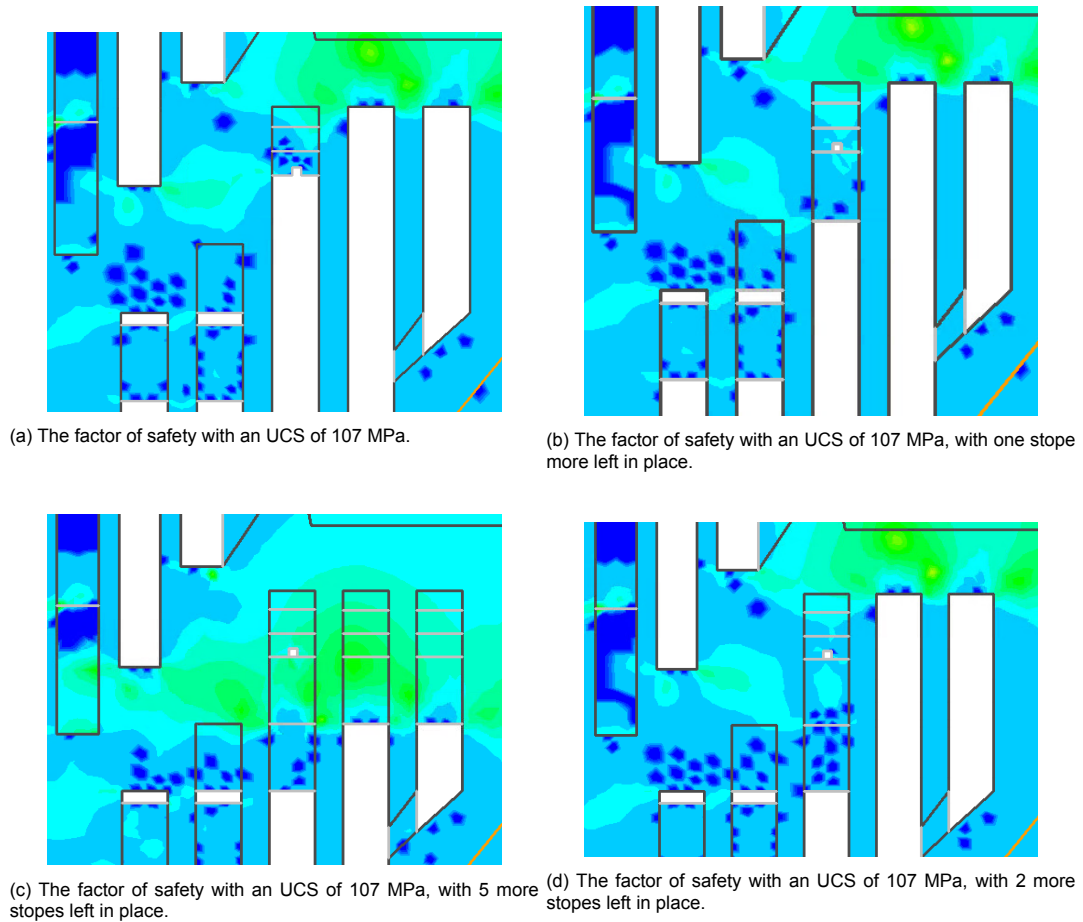


Figure 8.17: The effect of different UCS value on the factor of safety for the barrier pillar.

9

Cost model

The results for the cost model will be given in this chapter. Two different models have been made, one for the sublevel open stoping and one for vertical crater retreat. Both models follow the same procedure to get to the final cost estimation.

9.1. Operations

The results for the operations part of the cost model are given in this section. The cost model was divided into different steps and the first step was the calculation of the the material needed for blasting. Table 9.1 shows information about the time required to create a stope, a drift or to muck the material from a drift blast. The loading of the longhole holes is done in vertical slices for the sublevel open stoping, in horizontal slices for vertical crater retreat and for the drift in blocks of 5 meter. The horizontal slice for VCR consists of all the holes in the stope. The difference between the methods from the table is the drilling time and the loading time. The drilling time for a hole with the VCR method is 0.5 hour longer then with the sublevel open stoping method. The loading time for a slice is increased with almost 17 hours.

Table 9.1: Preparation times for the different operations for sublevel open stoping and vertical crater retreat.

Operation	Unit	Sublevel Open Stoping	Vertical Crater Retreat
Drilling longhole	holes/shift	2.5	3
Loading Longhole	hour/slice	12.85	29.4
Drilling drift	hour/block	2.5	2.5
Loading drift	hour/block	2.5	2.5
Mucking drift	hour/block	1.4	2.5

9.2. Drifting & Production

The results for the drifting and production calculations are given in table 9.2. The first part of the table gives the longhole drilling and blasting costs. The longhole cost are given in NOK per hole and NOK per meter. The drifting costs are calculated for a block with a depth of 5 meter. This is done because the drifting is done in blocks of 5 meter due to equipment constraints. The footwall stope production is the longhole production of the whole footwall stope and the hanging wall stope production is the production for the whole hanging wall stope.

One of the first things that is visible from this table is the higher cost for the drifting per cubic meter of material and per tonne. The difference between drifting and longhole sublevel open stoping production is a factor 6. The factor between drifting and VCR mining is 5.4. The production of vertical crater retreat is more expensive than for sublevel open stoping. The VCR mining method is approximately 0.60 NOK/tonne more expensive than the sublevel open stoping method.

The tables with the values that have been used to get to the results are given in appendix 15.1 to appendix 15.10 for sublevel open stoping and in appendix 15.11 to 15.17 for vertical crater retreat. The powder factor that has been calculated for sublevel open stoping is for the stope 0.165 kg/tonne and for drifting 0.996 kg/tonne. For vertical crater retreat, the powder factor for drifting stays the same and the powder factor for the stope is 0.136 kg/tonne.

Table 9.2: Cost model results sublevel open stoping

	Unit	Sublevel Open Stoping	Vertical Crater Retreat
Longhole drilling	NOK/hole	2,040	2,451
Longhole drilling	NOK/m	45.34	54.47
Longhole blasting	NOK/hole	2913	3089
footwall stope production	NOK	965,976	1,058,213
footwall stope production	NOK/m3	13.06	14.57
footwall stope production	NOK/tonne	4.93	5.50
hanging wall stope production	NOK	797,549	875,381
hanging wall stope production	NOK/m3	12.95	14.47
hanging wall stope production	NOK/tonne	4.89	5.46
drifting	NOK/5m block	25,521	25,521
drifting	NOK/m3	78.53	78.53
drifting	NOK/ tonne	29.63	29.63

9.3. Planning

The mine planning is partly based on the stability assessment of the model. Some parts are left in place which can be mined to make sure that the stability of the pillar is not affected. The stopes that are planned to be mined are the stopes that are given in table 9.3 given below. The table shows the results for each stope, the volumes and tonnages per stope and the costs for the production of that stope in NOK for sublevel open stoping and for VCR. The last two columns are the cost of the stopes per level combined to get an overview of the production costs per level. The costs are given in million NOK for each stope and for each level. The costs for the stopes of the 420 level are slightly lower then the costs for the other two levels, because the stopes are slightly smaller.

Table 9.3: Stopes to be mined in Mine 2 with costs for each stope and per level

Both Cases				Sublevel	VCR	Sublevel	VCR
Level	Stope (#)	volume (m3 x1000)	Tonnage (tonnes x1000)	cost (NOK x1000,000)	cost (NOK x1000,000)	total/level (NOK x1000,000)	total/level (NOK x1000,000)
420	2	93.6	248.0	1.74	1.91	6.95	7.62
420	3	93.6	248.0	1.74	1.91		
420	4	93.6	248.0	1.74	1.91		
420	5	93.6	248.0	1.74	1.91		
460	3	95.0	251.7	1.76	1.93	5.29	5.80
460	4	95.0	251.7	1.76	1.93		
460	5	95.0	251.7	1.76	1.93		
500	3	95.0	251.7	1.76	1.93	5.29	5.80
500	4	95.0	251.7	1.76	1.93		
500	5	95.0	251.7	1.76	1.93		

The drifts are needed to create access to the stopes. One of the drifts has been mined already, so only two new drifts are needed. The length of the drifts is 150 meter. With a width of 10 meter and a height of 6.5 meter, the volume of one drift is 9.8 thousand cubic meter. The cost for each drift are 766,000 NOK.

Table 9.4: Drifts to be mined with length, volumes and costs.

Level	length (m)	Volume (m3 x1000)	Tonnage (tonnes x1000)	Cost (NOK x1000,000)
420	150	9.8	25.8	0.766
500	150	9.8	28.8	0.766

The top slice access for each slope is required to make sure that the drilling and loading can be done properly in each stope. Table 9.5 shows the costs for each top slice to be developed. The costs are given in million NOK for each top slice. The development costs for one top slice are getting in the same range as one stope production cost and the development for a top slice gives less material than a stope production.

Table 9.5: Top slice for each level to be mined.

Level	Stope (#)	Volume (m3 x1000)	Tonnage (tonnes x1000)	Cost (NOK x1000,000)	Total/level (NOK x1000,000)
420	2	18.2	48.1	1.21	4.83
420	3	18.2	48.1	1.21	
420	4	18.2	48.1	1.21	
420	5	18.2	48.1	1.21	
460	3	18.4	48.8	1.23	3.68
460	4	18.4	48.8	1.23	
460	5	18.4	48.8	1.23	
500	3	18.4	48.8	1.23	3.68
500	4	18.4	48.8	1.23	
500	5	18.4	48.8	1.23	

The costs per level are given in table 9.6. The table shows the number of stopes on that level, volume, tonnage, cost and percentages generated from the top slice and drift. The percentages for the drift and top slice are cost percentages, they show what part of the costs is generated by the development and what part is from the stope production. For both methods, the percentage for the developments around 40%. The percentages for VCR are a bit lower than for sublevel open stoping. The volume percentage is the percentage of the total volume is from the development work, the drifts and top slice.

Table 9.6: Cost per level and the percentage of the total cost and volume is from the top slice and drift.

Level	Stopes	Volume (m3 x1000)	Tonnage (tonnes x1000)	Sublevel	VCR	sublevel	VCR	Volume (%)
				Cost (NOK x1000,000)	Cost (NOK x1000,000)	drift + top slice (% NOK)	drift + top slice (% NOK)	
420	4	486.1	1288.2	12.5	13.2	0.45	0.42	0.17
460	3	340.2	901.5	9.0	9.5	0.41	0.39	0.16
500	3	369.5	979.0	9.8	10.2	0.46	0.43	0.15

With a production per year of 50.000 tonnes for the underground mine, the mine can continue for each level for a large number of years. Each stope will provide enough raw material for a production of 5 years, with in addition the volumes of the drifts and the top slice. Each top slice will provide enough raw material for a year of production. The 420 level, as proposed in table 9.6, will provide enough raw material for 25.76 years, the 460 level will provide for 18 years and the 500 level will provide for 19.58 years. Combining the level volumes and the level costs for both methods, results in a cost per ton for each method in NOK/tonne. For sublevel open stoping, the cost per tonne is 9.86 NOK. For VCR the cost per tonne is 10.39 NOK.

9.4. Capital Cost

To be able to drill the holes for the stopes, a new drill rig is needed. There are two options for drill rigs that are considered during this thesis. Both are from Sandvik and the difference between them is the size of the drill holes they can produce. Table 9.7 shows the costs for two different drill rigs and one with a zero emission autonomous package. The DL421 is a rig that should be used if the mining method is sublevel open stoping, and the DU412i should be used if the mining method is VCR. This is due to the difference in drill hole size.

Table 9.7: Costs of different drill rigs

Type	Cost (NOK x1000.000)
DL421	9
DL421 (zero emission)	12
DU412i	12

10

Discussion

In this chapter the results from chapters 7, 8 and 9 will be discussed. First, the results of the fieldwork and laboratory testing will be discussed. After that, the stability analysis results will be discussed. The last part of the discussion is the cost model.

10.1. Fieldwork and Laboratory Testing

The results for the fieldwork and laboratory testing have been given in chapter 7. The first part of that chapter are the results for the fieldwork. The fieldwork has been done in multiple sites in the mine. The fieldwork consisted of two rock mass classifications and one scanline mapping. The two rock mass classifications show a uniform rock type through out the area of Mine 2. With the result that the rock type is uniform, the rock in the numerical model can be set as one rock type.

The results for the Schmidt hammer tests for the classifications are high, the strength of the rock is higher than 200 MPa according to the test. The test results were checked and did not match with previous readings and did not correlate to literature (Ulusay 2015). Therefore the testing was stopped and the Schmidt hammer was sent for calibration to the TU Delft.

The results for the joints of the scanline mapping have been used for the whole mine. After the joint sets had been found in the scanline, the assumption was made that these sets are present in the whole mine, and no other major sets are present. This was done to simplify the stability analysis. It was not possible to use different zones with different joints sets in the program.

The results for the laboratory testing done in this thesis are showing different values for the different samples. The UCS test ranges from 88 MPa to 134 MPa, which is a large range. The difference can be caused by a slight change in mineralogy. It has been observed in historical tests that if the percentage of darker minerals in a sample goes up, the strength of the sample goes down. It is also possible that there is a difference in strength of the cores at different locations in the mine. However, four of the five samples give a UCS tests higher than 100 MPa, which would be more similar to literature. The laboratory testing was performed on samples taken in the field. The samples were created with a handheld drill, which made it difficult work. This degree of difficulty resulted in various quality of the samples. Some were long, others short and not all had the required size guidelines for testing. This is that the length should be at least 2 times the diameter of the sample. For the UCS testing, the corrected values are given in the results section. The three Brazilian tensile tests that have been done, show one result with a lower tensile strength. The difference between core 1-a and core 1-b should be investigated further, because they were part of the same core, that broke in half. It is possible that in one of the parts is a transition between minerals that weakens the rock or there is a difference in mineralogy. The difference in sonic velocity for the UCS test samples and the Brazilian test samples should also be investigated further. The samples that have a lower velocity also have a lower UCS value and vice versa. All samples of the Brazilian test are lower with the sonic velocity than the UCS

test values.

The results from the laboratory testing have been compared to the results from historical testing. The results from the laboratory testing had a large range. However, the average values of the sonic velocity test and the UCS test are in the range of the average values from historical testing. The results for the elastic modulus differ significantly from the results from historical tests.

10.2. Stability Analysis

The results for the stability analysis start with the analysis of the stope size with Mathews Stability graph empirical method. The results for four different excavation sizes have been given in chapter 7. The first point of discussion is that how correct the method is when in close proximity to a fault. There are two faults that run through the area, with one being very close to Mine 2. In literature, it is stated that the method is not as useful in the proximity of a fault. However, it is not stated how large the distance should be between the fault and the zone of interest. Some results of this method should be used with caution if the literature is right. However, the calculations for the stope sizes do apply for areas that are further away from the faults.

The results of the new workshop at the 560 level with the stability graph method mean that the method works for this mine. One remark is that a slightly different stability graph has been used, because rock bolting has been applied in the new workshop area and that affects the type of graph that should be used. Basically, it is the same shape of graph, with the same step sizes on the axes, but the graph is shifted so that the stable zone is larger than the graph that is used for the unsupported stopes.

The results for the different stope 5 options show that a very long stope (stope option A) has a stable roof and a hanging wall that is less stable, the hanging wall is in the transition zone. This can be caused by the fact that this stope option is very long and high compared to the width of the stope. Stope option B is a more square stope size which both the roof and the hanging wall falling into the stable zone. This can be caused by the fact that it is less a thin sheet compared to stope option B. One factor that has not been taken into account with the smaller stope size is the increasing number of pillars. With more smaller stopes, the number of pillars will also increase, which means that there are more pillars that are not allowed to fail.

The results of the numerical modelling are divided over multiple models with 42 stages. Each stage is a different step in the development of the mine. When the schwebes of stope 1 and stope 2, the top of stope 2 and the top of stope 3 are left in place, the factor of safety becomes at one point in the barrier pillar below 1 (0.96) and at the other points, it stays above 1. Some areas right above stope 1 and 2 have a very high factor of safety due to the stress distribution which goes to zero at those points. The second option is to remove all the planned stopes. Which will result in an area with a very low factor of safety in the barrier pillar near the top of stope 1 and stope 2, towards Mine 1. The third option, which leaves only the top stopes of stope 2 and stope 3 in place, shows that the areas with a low factor of safety are larger than in option 1, but smaller than in option 2. However, they are still present in the barrier pillar and they can have a large effect on the stability of the pillar.

The behaviour of the stress field of the model is as expected at most points that were selected to validate the model. The very high stress state around the underground primary processing location in the model is also seen in the mine. Spalling happens around different points near the primary processing location. The very high stresses in the model caused non-convergence in the model in early stages. This means that there was no solution for the model at which it was stable. This is why the different material is added in the rectangle around this location, to make sure that the model did not fail. This material was set to behave elastic. This can be justified by the fact that this area is far from the area that is of interest for this thesis. The high stresses that were measured with a flatjack in the top of stope 1 in Mine 2 were also visible in the model. However at the drift in the 460 level, the stress field model was lower than the measured flat jack results. The stresses in the drift were high, maybe too high to be caused by the stress field only. Some modeling was done to understand this area of high stress. However, no results came close to the measured results. Explanations that were tried are

faults with different orientations and or strength. But this did not recreate the effect.

The effect of decreasing the strength of the Nepheline Syenite by 10% and 20% is significant. The decrease of 10% has the effect that at least the top three stopes in stope three must be left in place to not have a zone of a low factor of safety close to Mine 1. However, this area is still close to Mine 1. If the top two stopes of each stope are left in place, the area of a low factor of safety is significantly smaller and not as close to Mine 1. The decrease of 20% of strength of the material has almost the same effect as a decrease of 10%. The same number of stopes must be left in place, all the top stopes, to make sure that the area with a low factor of safety is not close to Mine 1.

The last point of discussion is the fact that the model is a two-dimensional model. The real situation is three-dimensional, which means that a two-dimensional model is a simplification of the reality. However, within this thesis it was not possible to create a three-dimensional model. The effect of a two-dimensional model is that some stresses can be higher than in reality. When a stress field is created around a circle in a two-dimensional model, the stress can only flow around the circle in one dimension, which can lead to higher pressures around the circle. In a three dimensional model, the stress can move around a sphere in multiple ways, which leads to a better distribution of the stress, and possible lower values for some areas. The layout of the mine was simplified to make sure that the model was converging. The stopes of Mine 1 are in reality connected by a type of chute, which was not possible to model in the two-dimensional model.

10.3. Cost Model

The results for the cost model are given in chapter 9, which shows the results for the sublevel open stoping and the vertical crater retreat method. The last section of the chapter shows the difference between the results for the two mining methods. With the VCR being the more expensive mining method compared to sublevel open stoping. The higher cost for VCR is caused by the higher cost for drilling of a hole. The fact that the number of holes for both methods is the same in the model, caused the higher cost for the method. It maybe possible that the burden and spacing can be larger when VCR is used. However due to no ability to test the effect of changes in the drilling pattern, the choice was made to keep the burden and spacing the same. The increasing diameter of the holes in VCR causes a small increase in drilling time. The costs for blasting for both methods are approximately the same. The larger volume due to the larger diameter for the VCR method is compensated by the fact that only part of the borehole is filled with explosives. Which resulted in a total cost for blasting for VCR that is in the same range as the total costs for blasting for sublevel open stoping. The result of the cost modelling is that the sublevel open stoping is cheaper option than VCR, which is not in line with literature. From literature, it was expected that use of VCR as a mining method would result in lower mining cost. This difference can partly be explained by the variations of sublevel open stoping they are using. It can be possible that the cost savings between VCR and sublevel open stoping is for a more horizontally focussed sublevel open stoping, and not the variation used at Stjernoy.

Drifting cost for each drift on each level is the same, this is because at each level, the size of the stopes is the same. The drift on the 460 level has been mined already. There is a drift, which was probably made for exploration purposes, that continues for the whole width of Mine 2. This is why the development cost for the 460 level is lower than for the other two levels.

The costs for sublevel open stoping and VCR comparing the development work to the production work result in high costs percentages for the development work. The development work for sublevel open stoping is in percentage a bit higher than VCR. This is caused by the fact that the development work is the same for both methods, only the production cost for VCR is higher than for sublevel open stoping.

One of the factors that is comparable between the mine and the cost model that has been made is the powder factor that is used in sublevel open stoping and the powder factor for drifting. The powder factor for stoping that is used in the mine is 0.16 kg/tonne. The result of the model for sublevel open stoping is a powder factor of 0.165 kg/tonne. For drifting, the powder factor used in the mine is 0.96 kg/tonne and the powder factor calculated in the model is 0.996 kg/tonne. Both modelled values for

the powder factor are close to the values that are used in the mine. This indicates that this part of the model is a realistic representation of the reality.

There are potential differences between VCR and sublevel open stoping regarding production rates and manhours that are required for certain tasks. However, the development work that is required for both methods is the same. The only potential differences are created by the drilling of the holes and the loading and blasting of the holes. The drilling of the holes for sublevel open stoping is assumed to be faster than the drilling for the VCR holes. This is due to the larger diameter of the hole, this has been incorporated into the cost model. The difference in loading time for each blast is also incorporated into the cost model by the larger loading time for a slice for VCR blasting. More holes need to be loaded per slice. The loading time for each individual hole is set to the same time. Loading of a part of the hole (for VCR) is quicker than the whole hole (for Sublevel open stoping), however there are more steps to determine the exact height of the hole for VCR. The potential difference in production rates between the methods is not of high importance, because the low production rate for the underground mine (50.000 tonnes per year) is possible for both methods.

The risks of both methods are for a large part the same for both methods. The only difference in risk is that when part of the stope has been blasted. With VCR, there are slices blasted from the bottom, which means that the floor on which the work is done is getting thinner. The last slices are blasted at the same time, which increases the difficulty of the blast, which increases the risk of a negative event. With sublevel open stoping, after the first slice has been blasted, a part of the stope is open. This partly open stope increases the risk for personnel working in the stope. However, the amount of work left in the stope is limited and the need for vehicles in the stope is also limited. This means that there is a larger risk with sublevel open stoping than with VCR, but it should be a manageable risk.

Some costs for sublevel open stoping and for VCR are not determined for this thesis, but are based on industry guidelines and or handbooks. For example the maintenance cost of the equipment that is used underground has been based on these sources. During this thesis, it was not possible to get a clear overview of those costs. This is the same for some consumables that are used. The amount of material that was used for some blasts, blasting cord and bottom charges, did vary for some holes. The estimations for the duration of each part of the process are made with the help of people from the mine, which partake in those steps or who have been working at the mine for numerous years. This gave an indication for most of the processes, however, some of these processes are so variable or they did not know. For these unknowns, industry standards have been used as well.

Part V

Conclusion & Recommendation

Conclusion

This chapter will elaborate the conclusion that can be formed from this thesis regarding the analysis of the two mining methods, the fieldwork and laboratory work and stability. The conclusion will be given as answers to the research questions given in the introduction chapter.

11.1. Cost Model

The first research question that can be answered in the conclusion is: For how long is the use of sub-level open stoping mining method economically feasible. The conclusion that can be made from the cost model regarding this question is that the use of sublevel open stoping as a mining method for this mining operation is economically feasible based on the results of the cost model that was created. The final cost per tonne for this method is 9.86 NOK/tonne. The development work (drifting and top slice) is a large part of the costs of each level. However, it is necessary to continue mining with this method. To continue mining with this method, a new drill rig is needed, which will be a significant capital investment. The investment is justified by the fact that there is no suitable other drill rig that can be used to create the stopes of this size. The mine can continue using this method for almost 65 years, if the annual underground production (50.000 tonnes per year) is kept at the same level.

The next research question that can be answered is: Is the use of Vertical Crater Retreat as a mining method in this operation economically feasible and technically possible? The second conclusion that can be made from the cost model is that the second method that was considered for this thesis is the vertical crater retreat method, which is an economically feasible method if the parameters for the blasting are used as described in this thesis. The final cost per tonne for the use of this mining method is 10.39 NOK/tonne. The method is technically feasible as well, for the extent that was possible to test in this thesis. However, further investigation on the cratering technique is required if this mining method will be used for the next phase. The results from this can effect the burden and spacing of the drilling pattern, which can have a large influence on the economical feasibility of the method. This method will require a large drill rig, which means that there is a large capital investment to make when the method is implemented. However, the fact that there is no suitable drill rig at the moment justifies this capital investment. The production for the underground part of the mine does not differ for this method or when the sublevel open stoping method is used, the use of this method will also result in 65 years of production.

11.2. Stability

The third research question that can be answered is: How does the proximity of stopes affects the stability of the barrier pillar? The stability of the barrier pillar is affected by the mining activities that are done close to the barrier pillar. The barrier pillar will have a lower factor of safety if the schwebes of stope 1 and stope 2 are removed. This make it impossible to also mine the top part of stope 2, because

the material has nowhere to go. Additionally, the removal of the top of stope 2 will also have a negative effect on the factor of safety of the barrier pillar, it will become lower than 1 for areas in the barrier pillar. The last stope that has an effect on the stability of the barrier pillar is the top stope of stope 3. The removal of this stope will also have the effect that the factor of safety in part of the barrier pillar becomes lower than 1. The effect of leaving the stopes in for the stability results in an production loss of approximately 750 tonnes. However, the mine can continue for 65 years with the underground part if the production level stays the same. A loss of 750 tonnes to increase the stability of a vital part of the underground infrastructure is a manageable loss. The effect of a lower UCS of the Nepheline Syenite is that more stopes need to be left in place to get a factor of safety that is larger than 1.

11.3. Stope Size

The last research question that can be answered is: What is the optimal stope size to continue mining without affecting the stability? The stope size is an important aspect for the costs of production and the layout of the mine. Based on empirical stability assessment done with the stability graph method, the current stope size results in a stable roof of the stope and a hanging wall that is in the transition region. Due to the shape of the stope, with a dip of 70 degrees, the roof is the most important part of the stope that should be stable. Two different stope options have been tested for stope 5, with one being a small long stope and one being a more square stope. The more square stope option has a stable hanging wall in contrary to the long stope. However, the changing of stope sizes to smaller stopes, will result in additional pillar in the planned mine area. This will result in extra loss of raw material. Furthermore, it is uncertain what the effects of those small pillars are on the stability of the area. Changing the height of the stopes is also an option when reviewing stope size. However, the current infrastructure that is present is favorable for stopes with the same height as the current stopes. If the height of the stopes is decreased, more development work is needed, which is expensive. If the height of the stopes is increased, the drift that has been made at the 460 level will become abundant and this will cancel the potential savings of using an existing drift.

It is now possible to provided an answer to the goal of this thesis. The goal of this thesis is to:

Prepare a mine plan to continue mining in Mine 2 with the most suitable mining method. Differences between the vertical crater retreat method and sublevel open stoping method must be analyzed and described. Additionally, the effect of the mining activities on stability of the mine should be analyzed.

Based on this research, it can be concluded that the use of sublevel open stoping is the most suitable mining method to continue mining in Mine 2. The difference in costs per tonne between both methods is a small difference. However, the fact that sublevel open stoping is a proven method at this mine and it is the cheaper option according to the cost model, justify the choice for sublevel open stoping. Furthermore it is important to leave certain stopes in place to not negatively affect the stability of the mine. The hypothesis, which is stated in the introduction, was tested with this research and it was not found to be true.

Recommendations

Based on the research and conclusions provided earlier in this thesis, it is now possible to give recommendations on how to move forward.

12.1. Cost Modelling

The first recommendation is to create an overview of different costs and standard operating times which were not available during this thesis. For some of these parameters, assumptions have been made in this thesis. To improve the cost model, the real values are needed. For example, an overview of maintenance work for the underground mine would be beneficial. Maintenance work should be logged with time spend on the process and the materials that were used to fix the problem. An overview of operating times for certain operations is also useful for planning purposes for the operation.

12.2. Stress Modelling

The next recommendation is that there should be more research into the stresses in the Mine 2 area. A three dimensional model can be used to model the mine completely. This will give results that are more reliable than the results from the two dimensional model. This three dimensional model can be used to find an explanation for the stresses at the drift at the 460 level. The high stresses at that point are not predicted by the two dimensional model, but they could have a high impact in the stability of that region. If this region is not modeled in a three dimensional model, other types of research are needed to explain the high stresses. As agreed with the site, the current flat jack testing program will be extended to see how the stress behaves at different areas. It is possible that there are features that have been missed that have a high influence on the area. Furthermore, the effect of a lower UCS strength should be further investigated. If the solution of leaving more stopes in place if the quality of the Nepheline Syenite is not as expected or that some other solution has to be determined.

12.3. New Mining Area

The final recommendation is to investigate the possibility to mine the area behind the fault next to stope 5 at the east side of Mine 2. There is a larger area which has not been mined behind the fault, and this is a possible option for the underground production. A whole new mining method can be used, because it is not dependent on previous used mining methods with stopes and chutes.

Bibliography

- Alejano, L., González, J. & Muralha, J. (2012), *Journal for Rock mechanics and Rock Engineering* **45**, 1023 – 1035.
- ASTM (2016), 'Astm d3967 16 -standard test method for splitting tensile strength of intact rock core specimen', *ASTM International, West Conshohocken, PA* .
- ASTM (2017), 'Astm d7012-14e1 - standard test methods for compressive strength and elastic moduli of intact rock core specimens under varying states of stress and temperatures', *ASTM International, West Conshohocken, PA* .
- Brady, B. H. G. & Brown, E. T. (2006), *Rock mechanics for underground mining*, third edn, Springer.
- Chadwick, J. (1992), 'Creighton's vcr mechanics: vertical crater retreat mining as practiced at inco ltd's creighton mine.', *Mining Magazine* pp. 1–4.
- Chawre, B. (2018), 'Correlations between ultrasonic pulse wave velocities and rock properties of quartz-mica schist', *Journal of Rock Mechanics and Geotechnical Engineering* **10**, 594–602.
- Crawford, G. (2004), 'Dilution and ore recovery', *Pincock, Allen and Holt, Lakewood Colorado* **1**, 1–7.
- Dahle, H. (2007), Numerisk modellering av pilartykkelse mellom eksisterende gruve og fremtidig dagbrudd, stjernoy, report, SYNTEF, Trondheim, Norway.
- Darling, P. (2011), *SME Mining Engineering Handbook, Third Edition*, SME Mining Engineering Handbook, Society for Mining, Metallurgy, and Exploration.
URL: <https://books.google.nl/books?id=5uq-kdfHLWUC>
- Eberhardt, E. (2012), 'The hoek-brown failure criterion', *Rock Mechanics and Rock Engineering* **45**, 981–988.
- Ebrahimi, A. (2013), 'The importance of dilution factor for open pit mining projects', *SRK consulting, Vancouver* pp. 1–8.
- Feick, K. (2019), 'Nepheline'.
URL: <https://uwaterloo.ca/earth-sciences-museum/resources/detailed-rocks-and-minerals-articles/nepheline>
- Feng, W., Dong, S., Wang, Q., Yi, X., Liu, Z. & Bai, H. (2018), 'Improving the hoek-brown criterion based on the disturbance factor and geological strength index quantification.', *International Journal of Rock Mechanics and Mining Sciences* **108**, 96–104.
- Gercek, H. (2007), 'Poisson's ratio values for rocks', *International Journal of Rock Mechanics and Mining Sciences* **44**, 1–13.
- Glazner, A., Bartley, J., Coleman, D., Gray, W. & Taylor, R. (2004), 'Are plutons assembled over millions of years by amalgamation of small magma chambers?', *Geological Society of America Today* pp. 4–11.
- Gonen, A. & Kose, H. (2011), 'Stability analysis of open stopes and backfill in longhole stoping method for asikoy underground copper mine', *Mining Sciences* pp. 375–387.
- Greer, G. (1989), Empirical modelling of open stope stability in a vertical crater retreat application at inco's thompson mine, in '91st annual general meeting of the Canadian Institute of Mining and Metallurgy. Quebec City', pp. 9–16.

- Hartman, H. & Murmanský, J. (2002), *introductory Mining Engineering*, 2nd edition edn, John Wiley and Sons, Hoboken New Jersey.
- Hawker, R. & O'Connor, D. (2011), Keeping open of underground blast holes, in '6th Southern African Base Metlas Conference', Southern African Institute of Mining and Metallurgy, pp. 323–336.
- Hedley, D. (1978), 'Design guidelines for multi-seam mining at Elliot Lake'.
- Henning, J. & Mitri, H. (2007), Mine planning for ore dilution, in '109th CIM annual general meeting', Canadian Institute of Mining, p. 8.
- Hoek, E. (1983), 'Strength of jointed rock masses', *Geotechnique* **33**(3), 187–223.
- Hoek, E. (1994), 'Strength of rock and rock masses', *International Society for Rock Mechanics* **2**(2), 4–16.
- Hoek, E. (1998), 'Reliability of Hoek-Brown estimates of rock mass properties and their impact on design', *International Journal of Rock Mechanics and Mining Sciences* **35**, 63–68.
- Hoek, E. (2007), *Practical Rock Engineering*, Vol. 1, 1 edn, Evert Hoek Consulting Engineer Inc.
- Hoek, E. & Brown, E. (1982), *Underground Excavations in Rock*, revised first edn, E & FN Spon.
- Hoek, E. & Brown, E. (2019), 'The Hoek-Brown failure criterion and GSI - 2018 edition', *Journal of Rock Mechanics and Geotechnical Engineering* **11**, 445–463.
- Hoek, E., Marinos, P. & Benissi, M. (1998), 'Applicability of the geological strength index (GSI) classification for very weak and sheared rock masses. the case of the Athens schist formation.', *Bulletin Engineering Geology and the Environment* **57**, 151–160.
- Hoek, E., Marinos, V. & Marinos, P. (2005), 'The geological strength index: applications and limitations', *Bulletin Engineering Geology and the Environment* **64**, 55–65.
- Hudson, J. (1995), *Comprehensive Rock Engineering*, Vol. 1, first edn, London: Pergamon Press.
- Hudyma, M. R. (1988), 'Development of empirical rib pillar design criterion for open stope mining', *University of British Columbia*.
- Hustrulid, W. (1982), *Underground Mining Methods Handbook*, 1st edition edn, Society of Mining Engineers, New York.
- Hutchinson, D. & Diederichs, M. (1996), *Cablebolting in Underground Mines*, first edn, BiTech Publishers, Richmond BC.
- Jiang, N., Zhou, C. and Luo, X., & Lu, S. (2015), 'Damage characteristics of surrounding rock subjected to VCR mining blasting shock', *Hindawi Shock and Vibration* pp. 1–8.
- Jiao, J., Wu, S., Han, H., Du, X. & Niu, L. (2012), *Rock Mechanics: Achievements and ambitions. Analysis of empirical estimation of rock mass modulus and its application*, Taylor and Francis Group London.
- Johannsson, A. (2001), *Todimensjonal bergspenningsmålinger på nivå 320, gruve II, Stjernøya*, report, SYNTeF, Trondheim, Norway.
- Katsabanis, P. (2018), 'Fragmentation notes cratering for course mine220. Kingston: Dept. mining engineering at Queen's University', pp. 1–89.
- Li, X. (2013), *Alkaline Magmatism, water-rock interaction and multiple metamorphism in the Seiland Igneous Province, Northern Norway*, PhD thesis, Freiburg im Breisgau: Albert Ludwиг University.
- Liu, K., Yang, J., Li, X., Hao, H., Li, Q., Liu, Z. & Wang, C. (2018), 'Study on the long-hole raising technique using one blast based on vertical crater retreat multiple deck shots', *International Journal of Rock Mechanics and Mining Sciences* pp. 52–67.

Martin, C. & Maybee, W. (2000), 'The strength of hard-rock pillars', *International Journal of Rock Mechanics and Mining Sciences* **37**, 1239–1246.

Mawdesley, C., Trueman, R. & Whiten, W. (2001), 'Extending the mathews stability graph for open-stope design', **110**.

McKinnon, S. (2018a), 'classification and joint data analysis', *MINE469 Stability Analysis in Mine Design*, Queens University, Kingston Ontario .

McKinnon, S. (2018b), 'Numerical modeling', *MINE469 Stability Analysis in Mine Design*, Queens University, Kingston Ontario .

Oksfjord, Norway. *The climate in Oksfjord Norway* (2020).

URL: <http://www.weatherbase.com/weather/weather-summary.php3?s=560307cityname=%D8ksfjord%2C+Norwayunits>

Palmström, A. (1995), Rmi - A rock mass characterization system for rock engineering purposes, PhD thesis, University of Oslo, Norway.

Potvin, Y., Hudyma, M. & Miller, H. (1988), 'The stability graph method for open stope design', *Canadian Institute for Mining and Metallurgy AGM* **2**, 1–30.

Pourhosseini, O. & Shabanimashcool, M. (2014), 'Development of an elasto-plastic constitutive model for intact rocks', *International Journal of Rock Mechanics and Mining Sciences* **66**, 1–12.

Q system handbook (2015), first edn, Norwegian Geotechnical Institute.

Roberts, R., Corfu, F., Torsvik, T., Hetherington, C. & Ashwal, L. (2010), 'Age of alkaline rocks in the seiland igneous province, northern norway', *Journal of Geological Society London* pp. 71–81.

RocScience (n.d.), 'Dips'.

URL: <https://www.rocscience.com/software/dips>

Saptono, S., Kramadibrata, S. & Sulistianto, B. (2013), Using the schmidt hammer on rock mass characteristic in sedimentary rock at tutupan coal mine, International Symposium on Earth Science and Technology, pp. 390–395.

Schmitz, R. (2016), 'Rock mass rating on the basis of information contained in rock outcrops', *Sibelco Centre of Excellence Mining Geotechnics, Technical Manual 001 and spreadsheet. Sibelco Internal Document* .

Schmitz, R. (2018), Handbook geotechnics, Technical report, Centre of Excellence Mining and Geotechnics, Sibelco.

Schmitz, R. (2020), 'Geotechnical risk management of slopes in quarries, mines and dredging operations of sibelco: geotechnical monitoring', *North of England Institute of Mining and Mechanical Engineering Newsletter* **2/2020**, 1–7.

Schmitz, R. & Bergtes, M. (2020), 'Improved methodology in flat jack testing in hard rock mines', *North of England Institute of Mining and Mechanical Engineering Newsletter* **3/2020**, 1–7.

Schmitz, R., Nuyts, W., Daems, B. & Karagoz, S. (2020), 'Application of eurocode 7 in mining', *Sibelco Centre of Excellence Mining Geotechnics, Guideline 011 - C Examples. Sibelco Internal Document*.

Sen, Z. (2014), 'Rock quality designation-fracture intensity index method for geomechanical classification', *Arabian Journal for Geosciences* **Volume 7**, 2915–2922.

Singh, B. & Goel, R. (2011), *Engineering Rock Mass Classification*, Butterworth-Heinemann.

Sonmez, H., Cokceolglu, C. & Ulusay, R. (2004), 'Indirect determinatino of the modulus of deformation of rock masses based on the gsi system', *International Journal of Rock Mechanics and Mining Sciences* **41**, 849–857.

- Suorineni, F. (2012), 'A critical review of the stability graph method for open stope design', *Mass Mining* **1**, 1–8.
- Terzaghi, R. D. (1965), 'Sources of error in joint surveys', *Géotechnique* **15**, 287–304.
- Thuro, K., Plinninger, R., Zäh, S. & Schütz, S. (2001), in 'Rock Mechanics a challenge for society', ISRM, pp. 2–7.
- Ugalla, S. (1999), 'Sublevel open stoping: Design and planning olympic dam mine', *10th Australian Tunneling Conference* **1**, 14–17.
- Ulusay, R. (2015), *The ISRM Suggested Methods for Rock Characterization, Testing and Monitoring 2007-2014*, Springer.
- Ulusay, R. & Hudson, J. (2007), *The complete ISRM suggested methods for rock characterization, testing and monitoring: 1974-2006*, Kozan Ofset Matbaacilik, Ankara, Turkey.
- Villaescusa, E. (2014), *Geotechnical design for sublevel open stoping*, 1st edition edn, CRC press.
- What is declination?* (n.d.).
URL: https://www.usgs.gov/faqs/what-declination?qt-news_science_products=3qt-news_science_products
- William, K. (2002), 'Constitutive models for engineering materials', *University of Colorado at Boulder* **3**, 603–633.
- Ye, T. (2008), 'Field experiment for blasting crater', *Journal of China University of Mining and Technology* **18**, 224–228.

13

Appendix A

Table 3.5 Geomechanics classification of jointed rock masses (after Bieniawski, 1989).
(a) *Classification parameters and their ratings*

Parameter	Ranges of Values				
	point-load-strength index (MPa)	uniaxial compressive strength (MPa)	drill core quality <i>RQD</i> (1%)	joint spacing (m)	condition of joints
1 Strength of intact rock material	> 10	> 250	90–100 20	15 17	very rough surfaces, not continuous, no separation, unweathered joint wall rock
rating					
2 drill core quality <i>RQD</i> (1%)	4–10	100–250	75–90 17	0.6–2 15	slightly rough surfaces, separation < 1 mm, highly weathered walls
rating					
3 joint spacing (m)	2–4	50–100	50–75 13	0.2–0.6 10	slightly rough surfaces, separation < 1 mm, highly weathered walls
rating					
4 condition of joints	1–2	25–50	0.06–0.2 8	0.06–0.2 8	slickensided surfaces or gouge < 5 mm thick or separation > 5 mm, continuous joints
rating					
5 groundwater	25–125	0.2–0.5	25–125	0.2–0.5	separation 1–5 mm continuous joints
rating					
6 strike and dip orientations of joints	0	0	0	0	0
rating					

(b) *Rating adjustment for joint orientations*

Rating	tunnels and micro foundations	slopes
very favourable	0	0
favourable	–2	–2
fair	–5	–5
unfavourable	–10	–15
very unfavourable	–12	–25

(c) *Rock mass classes determined from total ratings*

Ratings	100 ← 81	80 ← 61	60 ← 41	40 ← 21	< 20
Class no.	I	II	III	IV	V
Description	very good rock	good rock	fair rock	poor rock	very poor rock

(d) *Meaning of rock classes*

Class no.	I	II	III	IV	V
average stand-up time	20 years for 15 m span	1 year for 10 m span	1 week for 5 m span	10 hours for 2.5 m span	30 minutes for 1.0 m span
cohesion of the rock mass (kPa)	> 400	300–400	200–300	100–200	< 100
friction angle of the rock mass	45°	35°–45°	25°–35°	15°–25°	< 15°

Figure 13.1: Rock Mass Rating (RMR) system rating table. Brady & Brown

Table 3.6 The effects of joint strike and dip in tunnelling (after Bieniawski, 1989).

Strike perpendicular to tunnel axis				Strike parallel to tunnel axis		
Drive with dip		Drive against dip				
Dip 45°–90°	Dip 20°–45°	Dip 45°–90°	Dip 20°–45°	Dip 45°–90°	Dip 20°–45°	Dip 0°–20° irrespective of strike
very favourable	favourable	fair	unfavourable	very unfavourable	fair	fair

Figure 13.2: Rock Mass Rating (RMR) system rating table. Brady & Brown







GEOLOGICAL STRENGTH INDEX FOR JOINTED ROCKS (Hoek and Marinos, 2000) From the lithology, structure and surface conditions of the discontinuities, estimate the average value of GSI. Do not try to be too precise. Quoting a range from 33 to 37 is more realistic than stating that GSI = 35. Note that the table does not apply to structurally controlled failures. Where weak planar structural planes are present in an unfavourable orientation with respect to the excavation face, these will dominate the rock mass behaviour. The shear strength of surfaces in rocks that are prone to deterioration as a result of changes in moisture content will be reduced if water is present. When working with rocks in the fair to very poor categories, a shift to the right may be made for wet conditions. Water pressure is dealt with by effective stress analysis.						
		SURFACE CONDITIONS				
		VERY GOOD Very rough, fresh unweathered surfaces GOOD Rough, slightly weathered, iron stained surfaces FAIR Smooth, moderately weathered and altered surfaces POOR Slackensided, highly weathered surfaces with compact coatings or fillings or angular fragments VERY POOR Slackensided, highly weathered surfaces with soft clay coatings or fillings				
STRUCTURE		DECREASING SURFACE QUALITY →				
 INTACT OR MASSIVE - intact rock specimens or massive in situ rock with few widely spaced discontinuities  BLOCKY - well interlocked undisturbed rock mass consisting of cubical blocks formed by three intersecting discontinuity sets  VERY BLOCKY - interlocked, partially disturbed mass with multi-faceted angular blocks formed by 4 or more joint sets  BLOCKY/DISTURBED/SEAMY - folded with angular blocks formed by many intersecting discontinuity sets. Persistence of bedding planes or schistosity  DISINTEGRATED - poorly interlocked, heavily broken rock mass with mixture of angular and rounded rock pieces  LAMINATED/SHEARED - Lack of blockiness due to close spacing of weak schistosity or shear planes		DECREASING INTERLOCKING OF ROCK PIECES ↓				
		90				
		80				
		70			N/A	N/A
		60				
		50				
		40				
		30				
		20				
		10				
		N/A	N/A			

Figure 13.3: General chart for Geological Strength Index from geological observations. Marinos, Marinos & Hoek 2005

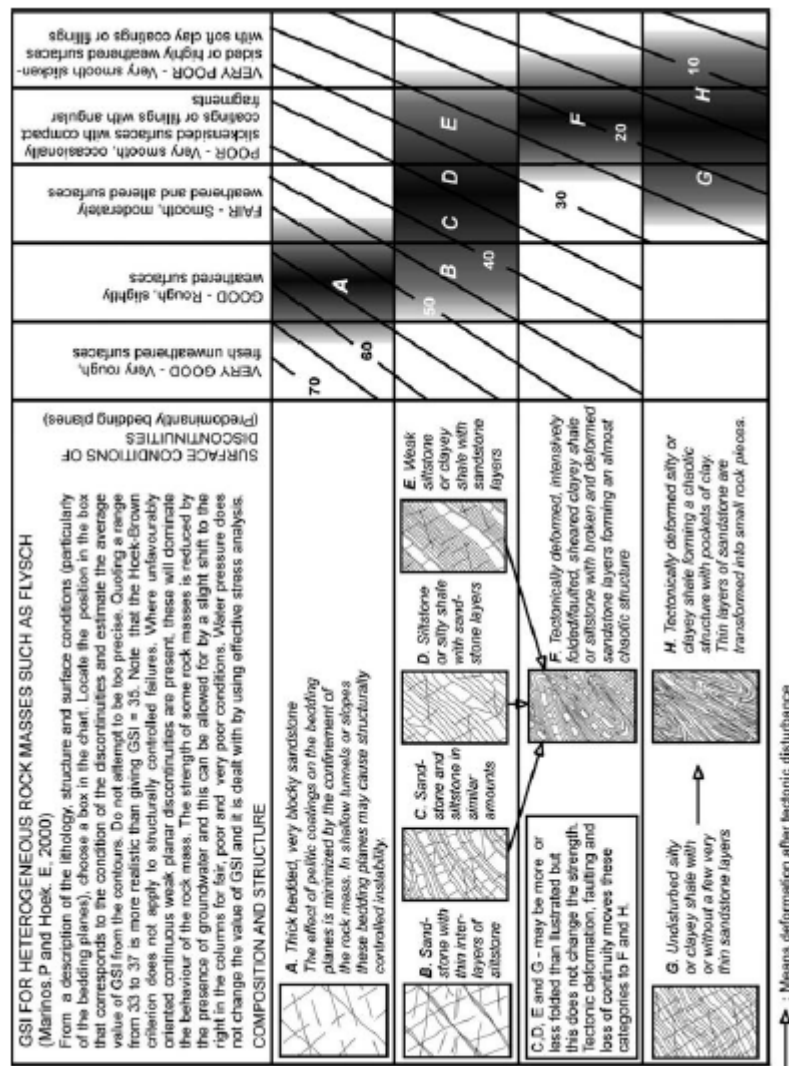







Figure 13.4: Geological Strength Index for heterogeneous rock masses. Marinos, Marinos & Hoek 2005

The disturbance factor D should never be applied to the entire rock mass surrounding an excavation		
Appearance of rock mass	Description of rock mass	Suggested value of D
	Excellent quality-controlled blasting or excavation by a road-header or tunnel boring machine results in minimal disturbance to the confined rock mass surrounding a tunnel. The blasting design for this tunnel is discussed in http://www.roscience.com/assets/resources/learning/hoek/Practical-Rock-Engineering-Chapter-16-Blasting-Damage-in-Rock.pdf	$D = 0$
	Mechanical or manual excavation in poor quality rock masses gives minimal disturbance to the surrounding rock mass. Where squeezing problems result in significant floor heave, disturbance can be severe unless a temporary invert, as shown in the photograph, is placed.	$D = 0$ $D = 0.5$ with no invert
	Poor control of drilling alignment, charge design and detonation sequencing results in very poor blasting in a hard rock tunnel with severe damage, extending 2 or 3 m, in the surrounding rock mass.	$D = 1.0$ at surface with a linear decrease to $D = 0$ at ± 2 m into the surrounding rock mass
	Small-scale blasting in civil engineering slopes results in modest rock mass damage when controlled blasting is used, as shown on the left-hand side of the photograph. Uncontrolled production blasting can result in significant damage to the rock face.	$D = 0.5$ for controlled presplit or smooth wall blasting with $D = 1.0$ for production blasting
	In some weak rock masses, excavation can be carried out by ripping and dozing. Damage to the slopes is due primarily to stress relief. Very large open pit mine slopes suffer significant disturbance due to heavy production blasting and stress relief from overburden removal.	$D = 0.7$ for mechanical excavation effects of stress reduction damage $D = 1.0$ for production blasting A transitional D relationship incorporating the effects of stress relaxation can be derived from the disturbance rating*

Note: *A disturbance rating for open pit slopes has been published by Rose et al. (2018).

Figure 13.5: Guidelines for estimating disturbance factor D . Hoek & Brown 2019.

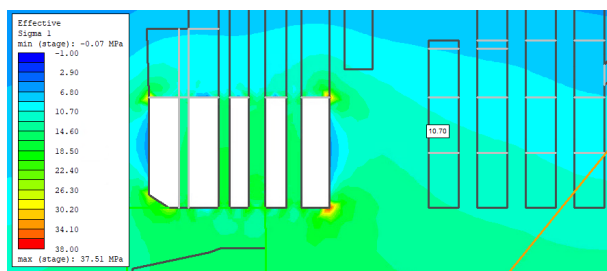
Rock type	Class	Group	Texture			
			Coarse	Medium	Fine	Very fine
SEDIMENTARY	Clastic		Conglomerates* (21 ± 3)	Sandstones 17 ± 4	Siltstones 7 ± 2	Claystones 4 ± 2
			Breccias (19 ± 5)		Greywackes (18 ± 3)	Shales (6 ± 2) Marls (7 ± 2)
	Non-Clastic	Carbonates	Crystalline Limestone (12 ± 3)	Sparitic Limestone (10 ± 2)	Micritic Limestone (9 ± 2)	Dolomites (9 ± 3)
		Evaporites		Gypsum 8 ± 2	Anhydrite 12 ± 2	
		Organic				Chalk 7 ± 2
METAMORPHIC	Non Foliated		Marble 9 ± 3	Hornfels (19 ± 4) Metasandstone (19 ± 3)	Quartzites 20 ± 3	
	Slightly foliated		Migmatite (29 ± 3)	Amphibolites 26 ± 6		
	Foliated**		Gneiss 28 ± 5	Schists 12 ± 3	Phyllites (7 ± 3)	Slates 7 ± 4
IGNEOUS	Plutonic	Light	Granite 32 ± 3 Granodiorite (29 ± 3)	Diorite 25 ± 5		
		Dark	Gabbro 27 ± 3 Norte 20 ± 5	Dolerite (16 ± 5)		
	Hypabyssal		Porphyries (20 ± 5)		Diabase (15 ± 5)	Peridotite (25 ± 5)
	Volcanic	Lava		Rhyolite (25 ± 5) Andesite 25 ± 5	Dacite (25 ± 3) Basalt (25 ± 5)	Obsidian (19 ± 3)
		Pyroclastic	Agglomerate (19 ± 3)	Breccia (19 ± 5)	Tuff (13 ± 5)	

* Conglomerates and breccias may present a wide range of m_i values depending on the nature of the cementing material and the degree of cementation, so they may range from values similar to sandstone to values used for fine grained sediments.

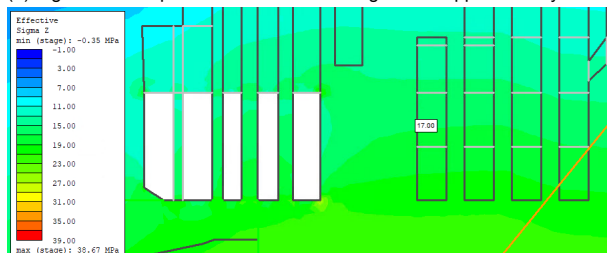
** These values are for intact rock specimens tested normal to bedding or foliation. The value of m_i will be significantly different if failure occurs along a weakness plane.

Figure 13.6: Guidelines for estimating M_i value if laboratory testing is not possible. Hoek 2007

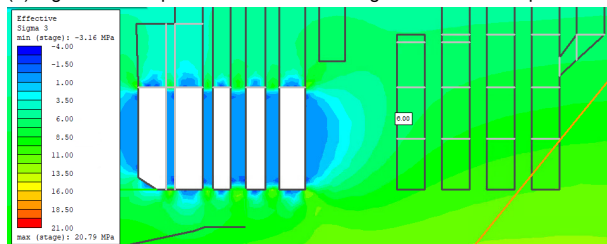
Appendix B



(a) Sigma 1 at the point of measurement. Sigma 1 is approximately the vertical stress at this point.



(b) Sigma Z at the point of measurement. Sigma Z is the out of plane stress at this point.



(c) Sigma 3 at the point of measurement. Sigma 3 is the horizontal in plane stress at this point.

Figure 14.1: Stresses at the point that was measured by SYNTEF.

15

Appendix C

In this appendix, the results for the cost model are given from the excel file in which the model has been made. The first part of this appendix is for the cost model of the sublevel open stoping method. The second part is for the Vertical Crater Retreat mining method.

15.1. sublevel open stoping

Stope (footwall)			Stope (hangingwall)		
width	m	27.5	width	m	27.5
height	m	45	height	m	45
length	m	60	length	m	50
BCM	m3	73980	BCM	m3	61605
LCM	m3	96174	LCM	m3	80087
weight	tonnes	196047	weight	tonnes	163253
Production Drilling Per stope			Production Drilling Per stope		
borehole diameter	mm	76	borehole diameter	mm	76
borehole length	m	45.0	borehole length	m	45.0
stemming length**	m	1.5	stemming length**	m	1.5
explosive length	m	43.5	explosive length	m	43.5
borehole volume	m3	0.2041	borehole volume	m3	0.2041
stemming volume	m3	0.0069	stemming volume	m3	0.0068
explosive volume	m3	0.1972	explosive volume	m3	0.1973
burden	m	2.70	burden	m	2.70
spacing	m	3.0	spacing	m	3.0
boreholes*	#	195	boreholes*	#	161
total volume holes	m3	38.463	total volume holes	m3	31.771
Blasting			Blasting		
density explosive	kg/m3	840	density explosive	kg/m3	840
weight	kg	32309	weight	kg	26688
powder factor	kg/tonnes	0.165	powder factor	kg/tonne	0.163
Detonator	#/hole	2	Detonator	#/hole	2
	#	390		#	322
bottom charge	#/hole	2	bottom charge	#/hole	2
	#	390		#	322
shocktube	m/hole	45	shocktube	m/hole	45
	#	8775		#	7245

Figure 15.1: Stope calculations

Drift			Vertical slot		
width	m	10	width	m	3
height	m	6.5	height	m	45
length	m	5	length	m	2
BCM	m3	325	BCM	m3	270
LCM	m3	422.5	LCM	m3	351
weight	tonnes	861.25	weight	tonnes	715.5
drift drilling			Vertical slot drilling		
borehole diameter	mm	51	borehole diameter	mm	76
borehole length	m	5.0	borehole length	m	45.0
stemming length**	m	0.5	stemming length**	m	1.5
explosive length	m	4.5	explosive length	m	43.5
borehole volume	m3	0.0102	borehole volume	m3	0.2041
stemming volume	m3	0.0010	stemming volume	m3	0.0069
explosive volume	m3	0.0092	explosive volume	m3	0.1972
burden	m	0.9	burden	m	1.0
spacing	m	0.9	spacing	m	1.0
boreholes	#	100	boreholes	#	12
total volume holes	m3	1.021	total volume holes	m3	2.450
Blasting			Blasting		
density explosive	kg/m3	840	density explosive	kg/m3	840
weight	kg	858	weight	kg	2058
powder factor	kg/tonne	0.996	powder factor	kg/tonne	2.876
Detonator	#/hole	1	Detonator	#/hole	5
	#	100		#	60
bottom charge	#/hole	1	bottom charge	#/hole	5
	#	100		#	60
shocktube	m/hole	5	shocktube	m/hole	35
	#	500		#	420

Figure 15.2: drift and vertical slot calculations

Stope top slice development (footwall)			Stope top slice Development (hangingwall)		
width	m	27.5	width	m	27.5
height	m	6.5	height	m	6.5
length	m	60	length	m	50
BCM	m3	10725	BCM	m3	8938
LCM	m3	13943	LCM	m3	11619
weight	tonnes	28421	weight	tonnes	23684
development Dri per 5x10x6.5m block			Development Dri per 5x10x6.5m block		
borehole diameter	mm	51	borehole diameter	mm	51
borehole length	m	5.0	borehole length	m	5.0
stemming length**	m	0.5	stemming length**	m	0.5
explosive length	m	4.5	explosive length	m	4.5
borehole volume	m3	0.0102	borehole volume	m3	0.0102
stemming volume	m3	0.0010	stemming volume	m3	0.0010
explosive volume	m3	0.0092	explosive volume	m3	0.0092
burden	m	1.00	burden	m	1.00
spacing	m	1.0	spacing	m	1.0
boreholes	#	100	boreholes	#	100
total volume holes	m3	0.919	total volume holes	m3	0.919
development drill whole slice			development drill whole slice		
blocks	#	26	blocks	#	22
boreholes	#	2600	boreholes	#	2200
total volume holes	m3	23.90	total volume holes	m3	20.22
Blasting			Blasting		
density explosive	kg/m3	840	density explosive	kg/m3	840
weight	kg	20077	weight	kg	16988
powder factor	kg/tonne	0.706	powder factor	kg/tonnes	0.717
Detonator	#/hole	1	Detonator	#/hole	1
	#	100		#	100
bottom charge	#/hole	1	bottom charge	#/hole	1
	#	100		#	100
shocktube	m/hole	5	shocktube	m/hole	5
	#	500		#	500

Figure 15.3: top slices calculations

Amount of explosives		
ANFO	kg	98977
	m3	117.83
Detonator	#	1072
Booster	#	1072
shocktube	m	17940

Figure 15.4: Amount of explosives

drilling time			Mucking		
Longhole			volume muckpile drift 5m block		
holes per shift	#	2.5	width	m	10
time per hole	hour	2.2	height	m	6.5
holes per stope	#	195	length	m	5
holes per slice	#	49	BCM	m3	325
shifts for drilling	#	19.6	LCM	m3	422.5
2 shift days	#	9.8	weight	tonnes	861.25
drift holes			mucking of drift		
drill speed	m/min	2.5	bucket size	m3	6.5
length holes	m	5	weight loose material	tonn	1.6
time per hole	min	2	weight bucket	tonnes	10.4
booms of drifter	#	2	scoops	#	83
holes per drift block* #		102	cycle time mucking		
holes per boom	#	51	loading	sec	15
set up time	min/hole	1	dumping	sec	15
time per drift	min	153	speed*	km/h	12
				m/s	3.33
Loading			distance	m	50
longhole			cycle time	sec	60.00
holes	#	10	cycle time	min	1
loading holes	hour	1.5	time needed for drift	min	83
loading of 1 hole	min	9			
loading of slice	hour	7.35			
set up time**	hour	5.5			
total time	hour	12.85			
total per hole	min	16.00			
drift					
holes	#	100			
loading time	hours	2.5			
loading of 1 hole	min	1.5			
loading of block	min	153			
set up time**	min	0.9			
total time	min	244.8			
total time	hour	4.08			
total per hole	min	2.4			

Figure 15.5: Operations calculations

shift times		shift length	effective length
shifts		hours	hours
miners	monday - Thursday	13	12
	Friday	6.58	5.5
mechanics	Monday - Friday	12.58	11.5
wages			
Operator	NOK/year	577200	
foreman	NOK/year	613800	
	NOK/month	48100	
average working days	per month	9	
average working hours*	hour/month	104.16	
effective working hours*	hour/month	95	
average salary	NOK/hour	462	
	NOK/shift	2540	

Figure 15.6: Personnel calculations

Drilling rig	per unit	per hour	per hole
gasoline	liter	0	0
lubricants	liter	0.894667	1.97
track	#	0.002	0.0044
drilling bits	#	0	0.1125
drilling rod	#	0	0.05
electric power	kWH	100.5556	221.22
maintenance	time	0.429782	0.95
Explosive truck		per hour	
diesel	liter	15.13	
lubricants	liter	0.49	
tires	#	0.017	
maintenance	time	0.276513	
drifter	per unit	per hour	
gasoline	liter	0	
electricity	kWh	77	
lubricants	liter	0.626667	
tires	#	0.000533	
drilling bits	#	0.1125	
Drilling rod	#	0.05	
maintenance	time	0.345278	
Loaders		per hour	
gasoline	liter	45.62	
lubricants	liter	1.05	
tires	#	0.002	
bucket teeth	#	0.01	
maintenance	time	0.334867	
Support vehicles	per unit	per hour	
gasoline	liter	15.13462	
lubricants	liter	0.313333	
tires	#	0.01865	
maintenance	time	0.132688	

Figure 15.7: Equipment calculations

longhole drilling cost		
per hole		
operator	NOK	1015.94
drill bit	NOK	152.62
drill rod	NOK	183.43
electricity	NOK	12.509
track	NOK	44
lubricants	NOK	133.94
Maintenance	NOK	497.91
total	NOK	2040.33
total	NOK/m	45.34
Longhole Blasting costs		
per hole		
Operator	NOK	246.29
ANFO	NOK	2240.96
bottom charge	NOK	138.13
Shocktube	NOK	34.81
loading truck	NOK	64.24
Maintenance	NOK	188.96
Total	NOK	2913.39
Longhole cost total	footwall stope	hangingwall stope
NOK	965976	797549
NOK/m3	13.06	12.95
NOK/tonne	4.93	4.89

Figure 15.8: Finances calculations part 1

drifting cost per 5m block		
Maintenance	NOK	220.72
operator	NOK	1295.32
drill bit	NOK	83.80
drill rod	NOK	196.88
electricity	NOK	4.79
lubricants	NOK	46.91
tires	NOK	2.93
Total	NOK	1851.35
drift loading per 5m block		
ANFO	NOK	11604.55
detonators	NOK	100
bottom charge	NOK	6906.38
shocktube	NOK	386.75
operator	NOK	1884.10
loading truck	NOK	982.83
Maintenance	NOK	188.96
Total	NOK	22053.57
drift mucking		
Operator	NOK	638.81
front loader	NOK	761.76
Maintenance	NOK	215.91
Total	NOK	1616.49
Drifting total	NOK	25521.41
costs	NOK/m3	78.53
	nok/tonne	29.63298173

Figure 15.9: Finances calculations part 2

Costs	Unit	Price
		NOK
Diesel	liter	8.118
Electricity	kWH	0.05654
lubricants	liter	68.05
drill bit 51 mm	1	677.16
drill bit 76mm	1	1356.6
drifting rod	1	3579.6
longhole rod	1	3668.52
Track	1	10000.00
tires	1	5000.00
bucket teeth	1	10000.00

Figure 15.10: Costs for certain spare parts

15.2. Vertical Crater Retreat

The table for personnel and for costs of certain consumables is the same for sublevel open stoping and vertical crater retreat.

Stope (northern)			Stope (Southern)		
width	m	27	width	m	27
height	m	45	height	m	45
length	m	60	length	m	50
BCM	m3	72630	BCM	m3	60480
LCM	m3	94419	LCM	m3	78624
weight	tonnes	192469.5	weight	tonnes	160272
Production Drilling			Production Drilling		
Per stope			Per stope		
borehole diameter	mm	152	borehole diameter	mm	152
explosive length	mm	912	explosive length	mm	912
explosive length	m	0.912	explosive length	m	0.912
explosive volume	m3	0.017	explosive volume	m3	0.017
explosive weight	kg	13.90	explosive weight	kg	13.90
thickness slice	m	4.572	thickness slice	m	4.572
slices	#	10	slices	#	10
total explosive volume	m3/hole	0.165	total explosive volume	m3/hole	0.165
burden	m	2.70	burden	m	2.70
spacing	m	3.0	spacing	m	3.0
boreholes*	#	191	boreholes*	#	158
total volume holes	m3	31.609	total volume holes	m3	26.147
Blasting			Blasting		
density explosive	kg/m3	840	density explosive	kg/m3	840
weight	kg	26551	weight	kg	21964
powder factor	kg/tonnes	0.138	powder factor	kg/tonnes	0.137
Detonator	#/hole	10	Detonator	#/hole	10
	#	1910		#	1580
bottom charge	#/hole	10	bottom charge	#/hole	10
	#	1910		#	1580
shocktube	m/hole	150	shocktube	m/hole	150
	#	28650		#	23700

Figure 15.11: Stope calculations for VCR

Drift			Vertical slot		
width	m	10	width	m	3
height	m	6.5	height	m	45
length	m	5	length	m	2
BCM	m3	325	BCM	m3	270
LCM	m3	422.5	LCM	m3	351
weight	tonnes	861.25	weight	tonnes	715.5
drift drilling			Vertical slot drilling		
borehole diameter	mm	51	borehole diameter	mm	76
borehole length	m	5.0	borehole length	m	45.0
stemming length**	m	0.5	stemming length**	m	1.5
explosive length	m	4.5	explosive length	m	43.5
borehole volume	m3	0.0102	borehole volume	m3	0.2041
stemming volume	m3	0.0010	stemming volume	m3	0.0069
explosive volume	m3	0.0092	explosive volume	m3	0.1972
burden	m	0.9	burden	m	1.0
spacing	m	0.9	spacing	m	1.0
boreholes	#	100	boreholes	#	12
total volume holes	m3	1.021	total volume holes	m3	2.450
Blasting			Blasting		
density explosive	kg/m3	840	density explosive	kg/m3	840
weight	kg	858	weight	kg	2058
powder factor	kg/tonne	0.996	powder factor	kg/tonne	2.876
Detonator	#/hole	1	Detonator	#/hole	1
	#	100		#	12
bottom charge	#/hole	1	bottom charge	#/hole	2
	#	100		#	24
shocktube	m/hole	5	shocktube	m/hole	5
	#	500		#	60

Figure 15.12: drift and vertical slot calculations for VCR

Stope top slice development (northern)			Stope top slice Development (Southern)		
width	m	27	width	m	27
height	m	6.5	height	m	6.5
length	m	60	length	m	50
BCM	m3	10530	BCM	m3	8775
LCM	m3	13689	LCM	m3	11408
weight	tonnes	27905	weight	tonnes	23254
development Drilling per 5x10x6.5m block			Development Drilling per 5x10x6.5m block		
borehole diameter	mm	51	borehole diameter	mm	51
borehole length	m	5.0	borehole length	m	5.0
stemming length**	m	0.5	stemming length**	m	0.5
explosive length	m	4.5	explosive length	m	4.5
borehole volume	m3	0.0102	borehole volume	m3	0.0102
stemming volume	m3	0.0010	stemming volume	m3	0.0010
explosive volume	m3	0.0092	explosive volume	m3	0.0092
burden	m	1.00	burden	m	1.00
spacing	m	1.0	spacing	m	1.0
boreholes	#	100	boreholes	#	100
total volume holes	m3	0.919	total volume holes	m3	0.919
development drilling whole slice			development drilling whole slice		
blocks	#	26	blocks	#	22
boreholes	#	2600	boreholes	#	2200
total volume holes	m3	23.90	total volume holes	m3	20.22
Blasting			Blasting		
density explosive	kg/m3	840	density explosive	kg/m3	840
weight	kg	20077	weight	kg	16988
powder factor	kg/tonne	0.719	powder factor	kg/tonnes	0.731
Detonator	#/hole	1	Detonator	#/hole	1
	#	100		#	100
bottom charge	#/hole	1	bottom charge	#/hole	1
	#	100		#	100
shocktube	m/hole	5	shocktube	m/hole	5
	#	500		#	500

Figure 15.13: top slices calculations for VCR

Amount of explosives		
ANFO	kg	88496
	m3	105.35
Detonator	#	3802
Booster	#	3814
shocktube	m	53910

Figure 15.14: Amount of explosives for VCR

drilling time			Mucking		
Longhole			volume muckpile drift 5m block		
holes per shift	#	2	width	m	10
time per hole	hour	2.75	height	m	6.5
holes per stope	#	191	length	m	5
holes per slice	#	48	BCM	m3	325
shifts for drilling	#	24	LCM	m3	422.5
2 shift days	#	12	weight	tonnes	861.25
drift holes			mucking of drift		
drill speed	m/min	2.5	bucket size	m3	6.5
length holes	m	5	weight loose material	tonn	1.6
time per hole	min	2	weight bucket	tonnes	10.4
booms of drifter	#	2	scoops	#	83
holes per drift block*	#	102	cycle time mucking		
holes per boom	#	51	loading	sec	15
set up time	min/hole	1	dumping	sec	15
time per drift	min	153	speed*	km/h	12
				m/s	3.33
Loading			distance	m	50
longhole			cycle time	sec	60.00
holes	#	10	cycle time	min	1
loading holes	hour	1.5	time needed for drift	min	83
loading of 1 hole	min	9			
loading of slice	hour	28.65			
set up time**	hour	5.5			
total time	hour	34.15			
total per hole	min	11.00			
drift					
holes	#	100			
loading time	hours	2.5			
loading of 1 hole	min	1.5			
loading of block	min	153			
set up time**	min	0.9			
total time	min	244.8			
total time	hour	4.08			
total per hole	min	2.4			

Figure 15.15: Operations calculations for VCR

longhole drilling cost		
per hole		
operator	NOK	1269.92
drill bit	NOK	152.62
drill rod	NOK	183.43
electricity	NOK	15.636
track	NOK	55
lubricants	NOK	167.43
Maintenance	NOK	607.06
total	NOK	2451.09
total	NOK/m	54.47

Longhole Blasting costs		
per hole		
Operator	NOK	169.32
ANFO	NOK	1880.18
bottom charge	NOK	690.64
Shocktube	NOK	116.03
loading truck	NOK	44.16
Maintenance	NOK	188.96
Total	NOK	3089.29

Longhole cost total	Footwall stope	Hanging wall stope
NOK	1058213	875381
NOK/m3	14.57	14.47
NOK/tonne	5.50	5.46

Figure 15.16: Finances calculations part 1 for VCR

drifting cost per 5m block		
Maintenance	NOK	220.72
operator	NOK	1295.32
drill bit	NOK	83.80
drill rod	NOK	196.88
electricity	NOK	4.79
lubricants	NOK	46.91
tires	NOK	2.93
Total	NOK	1851.35

drift loading per 5m block		
ANFO	NOK	11604.55
detonators	NOK	100
bottom charge	NOK	6906.38
shocktube	NOK	386.75
operator	NOK	1884.10
loading truck	NOK	982.83
Maintenance	NOK	188.96
Total	NOK	22053.57

drift mucking		
Operator	NOK	638.81
front loader	NOK	761.76
Maintenance	NOK	220.7197532
Total	NOK	1621.29

Drifting total	NOK	25526.21
costs	NOK/m3	78.53
	NOK/tonne	29.63

Figure 15.17: Finances calculations part 2 for VCR